

THESIS FOR THE DEGREE OF DOCTOR OF PHILOSOPHY

Frequency Transfer Techniques and Applications in  
Fiber Optic Communication Systems

SVEN-CHRISTIAN EBENHAG



Photonics Laboratory  
Department of Microtechnology and Nanoscience – MC2  
CHALMERS UNIVERSITY OF TECHNOLOGY  
Göteborg, Sweden, 2013

# Frequency Transfer Techniques and Applications in Fiber Optic Communication Systems

SVEN-CHRISTIAN EBENHAG

Göteborg, May 2013

© SVEN-CHRISTIAN EBENHAG, 2013

ISBN 978-91-7385-825-0

Doktorsavhandlingar vid Chalmers Tekniska Högskola

Ny serie nr 3506

ISSN 0346-718X

Technical report MC2-245

ISSN 1652-0769

Photonics Laboratory

Department of Microtechnology and Nanoscience - MC2

Chalmers University of Technology, SE-412 96 Göteborg, Sweden

Phone: +46 (0) 31 772 1000

**Front cover illustration:** Frequency stability presented as a Modified Allan Deviation graph of four types of oscillators/clocks, Quartz (QZ\_A), Rubidium (RB\_A), Cesium beam frequency standard (CS\_A and CS\_B) and Hydrogen-MASER (HM\_A and HM\_B).

Printed by Bibliotekets reproservice, Chalmers University of Technology  
Göteborg, Sweden, May 2013

# Abstract

Modern society is dependent on communications and the developments of these increases constantly through a seemingly endless demand for communication services and thereby synchronization and time. This is confirmed by a vast range of research on communications, irrespective of technology and protocol.

Historically, the national metrology institutes are the distributors of stable accurate time and frequency through national timescales, but that situation has changed with the arrival of Global Navigation Satellite Systems (GNSS) such as GPS (Global Positioning System). The introduction of GNSS-based solutions has resulted in improvement for system users and owners in need of time and frequency. When using a GNSS receiver, sufficient accuracy and precision is often achieved. However, a disadvantage of this development is that GNSS-solutions are based on weak radio signals that can be interfered with.

The main objective of the research that forms the groundwork for this thesis is the development of new fiber based methods for time and frequency. The aim is to complement GNSS-based methods for redundancy, with the intention of strengthening the robustness of the Swedish infrastructure. The research has resulted in two unique and innovative transmission technologies, one of which has been patented (two-color, one-way).

The first method is based on a non-insertion technology that utilizes passive listening to existing data frames in a fiber optical network and does not require any particular bandwidth. This technology only uses a fraction of the optical signal for time and frequency measurement from an indirect connection to the network. This method has resulted in a precision relative to the GPS carrier phase of less than 1 ns root mean square for distances exceeding 1,100 km. This precision has been achieved for all of the included experiments, conducted within the framework of the thesis, regardless of configuration.

The other fiber based technology is a one-way method that uses two wavelengths (colors) for the realization of a correction algorithm and signals thereto. It was developed because the symmetry required for performing two-way time and frequency transfer is rarely precise enough.

This optical fiber technique was evaluated with respect to a GPS precise point positioning technique in an urban fiber optical network. The difference in frequency stability between the two systems has been shown to be about  $3 \times 10^{-15}$  over an averaging interval of 10,000 s for a distance of 3 km. The method has also been evaluated in several laboratory experiments with fiber distances up to 160 km. The best performing result is presented as time resolved transit time variations compared with arrival time difference. The standard deviation of the difference between the reference measurement and the one-way, two-color technique result is 3.12 ns and the data showed temperature dependence in transit time of 6 ns / °C.

**Keywords:** Time transfer, synchronization, UTC, optical fiber network, GPS carrier phase, synchronous optical networking (SONET), synchronous digital hierarchy (SDH), global positioning system (GPS), optical fiber.



# List of Publications

## Appended Publications

This thesis is based on work in Papers A to K.

- [A] R. Emardson, P.O. Hedekvist, M. Nilsson, **S.C. Ebenhag**, K. Jaldehag, P. Jarlemark, C. Rieck, J. Johansson, L. Pendrill, P. Löthberg and H. Nilsson, “Time Transfer by Passive Listening over a 10 Gb/s Optical Fiber”, *IEEE Trans. Instr. Meas.*, vol. 57, pp. 2495–2501, 2008.
- [B] **S.C. Ebenhag**, K. Jaldehag, P. Jarlemark, P.O. Hedekvist, R. Emardson and P. Löthberg, “Time Transfer Using an Asynchronous Computer Network: Results from a 500 km Baseline Experiment”, *Precise Time and Time Interval (PTTI) Systems and Applications Meeting*, pp. 477–488, 2007.
- [C] **S.C. Ebenhag**, P. Jarlemark, R. Emardson, P.O. Hedekvist, K. Jaldehag and P. Löthberg, “Time Transfer over a 560 km Fiber Link”, *European Frequency and Time Forum (EFTF)*, 2008.
- [D] **S.C. Ebenhag**, P.O. Hedekvist, P. Jarlemark, R. Emardson, K. Jaldehag, C. Rieck and P. Löthberg, “Measurements and Error Sources in Time Transfer Using Asynchronous Fiber Network”, *IEEE Trans. Instr. Meas.*, vol. 59, pp. 1918–1924, 2010.
- [E] **S.C. Ebenhag**, K. Jaldehag, C. Rieck, P. Jarlemark, P.O. Hedekvist, P. Löthberg, T. Fordell and M. Merimaa, “Time Transfer between UTC(SP) and UTC(MIKE) Using Frame Detection in Fiber-Optical Communication networks”, *Precise Time and Time Interval (PTTI) Systems and Applications Meeting*, pp. 431–441, 2011.
- [F] **S.C. Ebenhag**, P.O. Hedekvist, C. Rieck, H. Skoogh, P. Jarlemark and K. Jaldehag, “A Fiber Based Frequency Distribution System with Enhanced Output Phase Stability”, *Frequency Control Symposium (FCS) joint with the European Frequency and Time forum (EFTF). IEEE International*, pp. 1061–1064, 2009.
- [G] **S.C. Ebenhag**, P.O. Hedekvist and J. Johansson, “Fiber Based One-Way Time Transfer with Enhanced Accuracy”, *European Frequency and Time Forum (EFTF)*, 2010.
- [H] **S.C. Ebenhag**, P.O. Hedekvist and K. Jaldehag, “Active Detection of Propagation Delay Variations in Single Way Time Transfer Utilizing Dual Wavelengths in an Optical Fiber Network”, *Frequency Control Symposium (FCS) and the European Frequency and Time Forum (EFTF) joint Conference of the IEEE International*, pp. 933–938, 2011.
- [I] **S.C. Ebenhag**, P.O. Hedekvist and K. Jaldehag, “One-Way Time Transfer Utilizing Active Detection of Propagation Delay Variations of Dual Wavelengths in an Optical Fiber Network”, *Precise Time and Time Interval (PTTI) Systems and Applications Meeting*, pp. 9–16, 2011.

- [J] **S.C. Ebenhag** and P.O. Hedekvist, “Real-time Phase Stabilization Utilizing Two Color One-way Frequency Transfer”, *Frequency Control Symposium (FCS), IEEE International IEEE*, pp. 672-677, 2012.
- [K] **S.C. Ebenhag**, P.O. Hedekvist and K. Jaldehag, “Two-Color One-Way Frequency Transfer in a Metropolitan Optical Fiber Data Network”, *NCSLI Measure J. Meas. Sci.*, vol. 8, no. 2, 2013.

## Additional Publications, not Included in this Thesis

The following Papers have been published but are not included in the Thesis. Their content partially overlaps the appended Papers or is outside the scope of this Thesis.

- [L] **S.C. Ebenhag**, P. Jarlemark, P.O. Hedekvist and R. Emardson, “Time Transfer Using an Asynchronous Computer Network: an Analysis of Error Sources”, *Frequency Control Symposium (FCS) joint with the European Frequency and Time Forum (EFTF). IEEE International*, pp. 827–831, 2007.
- [M] **S.C. Ebenhag**, K. Jaldehag, P.O. Hedekvist, R. Emardson, P. Jarlemark, C. Rieck, M. Nilsson, J. Johansson, L. Pendrill, P. Löthberg and H. Nilsson, “Time Transfer Using an Asynchronous Computer Network: Results from Three Weeks of Measurements”, *Frequency Control Symposium (FCS) joint with the European Frequency and Time Forum (EFTF). IEEE International*, pp. 323–326, 2007.
- [N] P.O. Hedekvist, R. Emardson, **S.C. Ebenhag** and K. Jaldehag, “Utilizing an Active Fiber Optic Communication Network for Accurate Time Distribution”, *ICTON '07. International Conference on Transparent Optical Networks*, vol 1, pp. 50–53, 2007.
- [O] **S.C. Ebenhag**, P.O. Hedekvist, C. Rieck, H. Skoogh, P. Jarlemark and K. Jaldehag, “Evaluation of Output Phase Stability in a Fiber Optic Two-Way Frequency Distribution System”, *Precise Time and Time Interval (PTTI) Systems and Applications Meeting*, pp. 117–124, 2008.
- [P] A. Andersson, H. Skoogh, **S.C. Ebenhag** and P.O. Hedekvist, “Evaluation of Temperature Dependent Transit-Time in Dispersion Compensating Fibers”, *OFMC Measurement Of Optical Fibers and Optoelectronics*, 2009.
- [Q] **S.C. Ebenhag**, P.O. Hedekvist and K. Jaldehag, “Fiber Based Frequency Distribution Based on Long Haul Communication Lasers”, *Precise Time and Time Interval (PTTI) Systems and Applications Meeting*, pp. 57–66, 2009.
- [R] K. Jaldehag, C. Rieck and **S.C. Ebenhag**, “Time and Frequency Activities at SP in Sweden”, *Precise Time and Time Interval (PTTI) Systems and Applications Meeting*, pp. 231–252, 2009.
- [S] K. Jaldehag, **S.C. Ebenhag**, P.O. Hedekvist and C. Rieck, “Time and Frequency Transfer using Asynchronous Fiber Optical Networks: Progress Report”, *Precise Time and Time Interval (PTTI) Systems and Applications Meeting*, pp. 383–396, 2009.
- [T] **S.C. Ebenhag**, “Time and Frequency Transfer using Passive Techniques in Active Fiber Optic Networks”, Thesis for the degree of Licentiate of Engineering, Chalmers University of Technology, 2010.

- [U] **S.C. Ebenhag**, P.O. Hedekvist and K. Jaldehag, “Single Way Fiber Based Time Transfer with Active Detection of Time Transfer Variations”, *Precise Time and Time Interval (PTTI) Systems and Applications Meeting*, pp. 413-426, 2010.
- [V] P.O. Hedekvist, **S.C. Ebenhag** and K. Jaldehag, “Active Optical Pre-Compensation in Short Range Frequency Transfer in Optical Single-Mode Fiber”, *Frequency Control Symposium (FCS) and the European Frequency and Time Forum (EFTF) joint Conference of the IEEE International*, pp. 315-316, 2011.
- [W] K. Jaldehag, **S.C. Ebenhag**, C. Rieck and P.O. Hedekvist, “Time Transfer Using Frame Detection in Fiber-Optical Communication Networks: New Hardware”, *Frequency Control Symposium (FCS) and the European Frequency and Time Forum (EFTF) joint Conference of the IEEE International*, pp. 300-303, 2011.
- [X] P.O. Hedekvist and **S.C. Ebenhag**, “Enkelriktad Tidsöverföring med Förhöjd Noggrannhet”, Patent accepted by Swedish Patent and Registration Office, Sweden, 2011.
- [Y] P.O. Hedekvist and **S.C. Ebenhag**, “Time and Frequency Transfer in Optical Fibers”, “Recent Progress in Optical Fiber Research”, ISBN 978-953-307-823-6, *InTech - Open Access Publisher*, pp. 371-386, 2012.
- [Z] **S.C. Ebenhag**, C. Wingqvist and P.O. Hedekvist, “Real-time Phase Stable One-way Frequency Transfer over Optical Fiber”, *European Frequency and Time Forum (EFTF)*, pp. 206-210, 2012.
- [AA] J. Hanssen, C. Ekstrom, **S.C. Ebenhag** and K. Jaldehag, “Evaluation of Time Transfer Units for Time and Frequency Transfer in Optical Fibers Utilizing a Passive Technique based on SONET/SDH”, *Precise Time and Time Interval (PTTI) Systems and Applications Meeting*, pp. 371-376, 2012.

Paper [B] was published in conference proceedings with a less stringent review process. Nevertheless, it has, after publication, been recognized by National aeronautics and space administration (NASA) and referred to in Scientific and Technical Aerospace Reports (STAR), number 24, volume 46, December 8, 2008.

Paper [O] was published in conference proceedings with a less stringent review process. Nevertheless, it has, after publication, been recognized by NASA and referred to in Scientific and Technical Aerospace Reports (STAR), number 19, volume 47, September 28, 2009.

Paper [Q] was published in conference proceedings with a less stringent review process. Nevertheless, it has, after publication, been recognized by NASA and referred to in Scientific and Technical Aerospace Reports (STAR), number 11, volume 48, June 7, 2010.

Paper [S] was published in conference proceedings with a less stringent review process. Nevertheless, it has, after publication, been recognized by NASA and referred to in Scientific and Technical Aerospace Reports (STAR), number 11, volume 48, June 7, 2010.

## Acknowledgements

This thesis is the result of hard persistent work. I would like to thank my wonderful family Anna, Timothy and Edison for giving me the opportunity and their support to finalize this project. Most of all, I want to thank Anna for her patience and understanding during this period.

I wish to thank the Time and Frequency group at SP for their collaboration, support and the opportunity to carry out this work. Special thanks are dedicated to my supervisor, Per Olof Hedekvist, for his supervision and other efforts such as brainstorming and discussions.

There are a couple of people in the time and frequency community that I especially would like to recognize. The first person is Bryan Owings (Symmetricom), for instilling confidence and rewarding discussions. Peter Löthberg (STUPI LLC) deserves many thanks and large recognition for his innovative ideas and support in the form of both discussions and hardware.

My gratitude also goes to the rest of the community for the valuable discussions and information that I have received from you all.

There are many people who have helped me, and I apologize for not mentioning all of them individually here.

*Borås*  
*May 2013*



*Sven-Christian Ebenhag*

This research is supported by the Swedish Post and Telecom Authority (PTS), the Swedish Defense Material Administration (FMV), and departmental funding from Research Institutes in Sweden (RISE). I would like to thank Swedish University computer network (SUNET) for their support in this project by granting access to OptoSUNET.



## Abbreviations in the Text

ADEV	Allan deviation
ANSI	American national standards institute
APD	Avalanche photodiode
AS	Anti-spoofing
ATM	Asynchronous transfer mode
AVAR	Allan variance
AWG	Amplified waveguide grating
A1	Following byte 11110110
A2	Following byte 00101000
BIPM	International bureau of weights and measures
BPSK	Binary phase-shifted key
C/A	Coarse/acquisition
C-band	Conventional band
Cs	Cesium clock
CS	Control segment
CDM	Code-division multiplex
CDMA	Code division multiple access
COADM	Compact Optical Add Drop Module
CV	Common view
CW	Continuous wave
CWDM	Coarse Wavelength Division Multiplexing
DBS	Direct broadcast satellite
D <sub>c</sub>	Chromatic dispersion
DCF	Dispersion compensating fiber
DCM	Dispersion compensation module
DCF77	Deutschland long wave signal Frankfurt frequency 77
DFB	Distributed feedback laser
DGD	Differential group delay
D <sub>M</sub>	Material dispersion
DMUX	Demultiplexer
DoD	Department of defense
D <sub>w</sub>	Waveguide dispersion
DWDM	Dense Wavelength Division Multiplexing
DS1	Digital system 1
E1	European format for digital transmission
EDFA	Erbium doped fiber amplifier
EGNOS	European geostationary navigation overlay service
ESA	European space agency
ET	Ephemeris time
FDM	Frequency division multiplexing
FMV	Swedish defense material administration
FWM	Four way multiplexing

FPGA	Field programmable gate array
Galileo	European global navigation satellite system
GIOVE	Galileo in-orbit validation element
GLONASS	Global'naya navigatsionnaya sputnikovaya sistema (Global navigation satellite system)
GMT	Greenwich Mean Time
GNSS	Global navigation satellite system
GPS	Global positioning system
GPSCP	Global positioning system carrier phase
HF	High frequency
H <sub>m</sub>	Hydrogen-MASER
HR	Header recognizer
IEEE	Institute of electrical and electronics engineers
IGS	International GNSS service
INSAT	Indian satellite
ITU	International telecommunication union
IP	Internet protocol
L-band	Long wavelengths band
LD	Laser diode
LORAN	Long range navigation
LF	Low frequency
MASER	Microwave amplification by stimulated emission of radiation
MDEV	Modified Allan deviation
MEO	Medium Earth orbit
MIKES	National metrology institute of Finland
MMF	Multi-mode fiber
MSAS	MTSAT space-based augmentation system
MTSAT	Multifunctional transport satellite
MUX	Multiplexer
MVAR	Modified Allan variance
NA	Numerical aperture
NASA	National aeronautics and space administration
NGA	National geospatial intelligence agency
NMI	National metrology institute
NTP	Network time protocol
O <sub>c</sub>	Optical clock
OC	Optical carrier
OCXO	Oven controlled crystal oscillator
OLA	Optical limiting amplifier
OptoSUNET	Fiber network operated by the Swedish University Computer Network
OTDR	Optical time-domain reflectometer
PDH	Plesiochronous digital hierarchy
PM	Phase modulation
PMD	Polarization-mode dispersion
POS	Packet over SONET/SDH
PPP	Precise point positioning

pps	Pulse per second
PRN	Pseudo random noise
PSK	Phase shift keying
PTS	Swedish Post and Telecom Authority
P(Y)	Encrypted precision code
Q-factor	Quality factor
Rb	Rubidium
Rec.	Recommendation
RF	Radio frequency
RISE	Research institutes of Sweden
RMS	Root mean square
SA	Selective availability
SBAS	Satellite based augmentation system
SDH	Synchronous digital hierarchy
SI	International System of Units
SMF	Single mode fiber
SNR	Signal to noise ratio
SOH	Section overhead
SONET	Synchronous optical network
SP	Technical Research Institute of Sweden
SRS	Stimulated Raman scattering
SS	Space segment
STAR	Scientific and technical aerospace reports
STS	Synchronous transport signal
STM	Synchronous transport module, synchronous transfer model
STUPI	Svensk Tele Utveckling & Produkt Innovation AB
SUNET	Swedish University computer network
TAI	International atomic time
TCP/IP	Transmission control protocol / internet protocol
TEM	Transverse electro magnetic
TDEV	Time Allan deviation
TIA	Trans-impedance amplifier
TIC	Time interval counter
TOD	Time of day
TTU	Time transfer unit
TVAR	Time Allan variance
TW	Two-way
TWSTFT	Two-way satellite time and frequency transfer
UT	Universal time
UT0	Universal time zero
UT1	Universal time one
UTC	Universal time coordinated
UTC(SP)	Swedish national timescale
UTC(MIKE)	Finnish national timescale
US	User segment

U.S	United States
USA	United States of America
USAF	US Air Force
VLBI	Very long baseline interferometer
VLF	Very low frequency
WAAS	Wide area augmentation system
WDM	Wavelength division multiplexing
XPM	Cross phase modulation

# Table of Contents

<b>Abstract</b>	<b>i</b>
<b>List of Publications</b>	<b>iii</b>
<b>Additional Publications, not Included in this Thesis</b>	<b>v</b>
<b>Acknowledgements</b>	<b>vii</b>
<b>Abbreviations in the Text</b>	<b>ix</b>
<b>Introduction</b>	<b>1</b>
1.1    Organization of the Thesis	3
<b>Time and Frequency</b>	<b>5</b>
2.1    Definition of the SI Unit “Second”	5
2.2    Time Scale	6
2.2.1    Universal Time (UT)	6
2.2.2    Ephemeris Time (ET)	6
2.2.3    International Atomic Time (TAI)	6
2.2.4    Coordinated Universal Time (UTC)	7
2.2.5    Local Time Scales	8
2.3    Frequency	9
2.4    Clocks and Oscillators	10
2.4.1    Cesium Beam Frequency Standard	11
2.4.2    Hydrogen-MASER	12
2.4.3    Rubidium Resonator	13
2.4.4    Optical Frequency Standard	14
2.4.4.1    Optical Clock	15
<b>Optical Fiber and Associated Components</b>	<b>17</b>
3.1    Optical Fiber	17
3.1.1    Dispersion Compensation Fiber (DCF)	18
3.2    Wavelength-Division Multiplexing (WDM)	18
3.2.1    Transmitter and Receivers	18
3.2.2    Loss Compensation	19
<b>Time and Frequency Transfer</b>	<b>21</b>
4.1    One-Way Time and Frequency Transfer	21
4.2    Two-Way Time and Frequency Transfer	23
4.3    Time and Frequency Transfer Utilizing GNSS	24
4.3.1    Positioning Techniques	24
4.3.2    Code Measurements	25
4.3.3    Carrier Phase Measurements	25
4.3.4    Sources of Error	26
4.3.5    Time and Frequency Measurement Using Code-Receivers	27

4.3.6	Time and Frequency Measurement Using Carrier Phase-Receivers	28
4.4	Time and Frequency Transfer Utilizing Optical Fiber	28
4.4.1	Transfer of Microwave Frequency in an Optical Fiber	28
4.4.2	Time Transfer Using Insertion Technique	29
4.4.3	Optical Comb	30
4.4.4	Optical Frequency Transfer	31
<b>Evaluated Techniques for Time and Frequency Transfers</b>		<b>33</b>
5.1	Applied Two-Way Time and Frequency Transfer	33
5.1.1	Non-Insertion Technique	33
5.1.1.1	Backbone Fiber Network used for Non-Insertion Two-Way Technique	34
5.1.1.1.1	SONET	34
5.1.1.1.2	SDH	35
5.1.1.2	Proposed Procedure for Non-Insertion Technique	37
5.1.1.3	Experimental Implementation	38
5.1.1.4	Error and Degradation Modeling	39
5.1.1.4.1	The Router Oscillator and its Influence on the Non-Insertion Technique	41
5.1.1.4.2	Influence of Fiber Nonlinearities	41
5.1.2	Results and Conclusions of the Two-Way Non-Insertion Technique	42
5.2	Applied One-Way Fiber Based Frequency Transfer	43
5.2.1	Dispersion Theory	43
5.2.1.1	Chromatic Dispersion	44
5.2.1.1.1	Material Dispersion	44
5.2.1.1.2	Waveguide Dispersion	45
5.2.1.2	Polarization Mode Dispersion	45
5.2.2	Theory Evaluation	46
5.2.2.1	Experimental Setup for Theory Evaluation	46
5.2.3	Two-Color One-Way Limitation	49
5.2.4	Results and Conclusions of the Two-Color One-Way Technique	49
<b>Summary of Appended Papers</b>		<b>51</b>
<b>References</b>		<b>55</b>
<b>Appendix A Optics</b>		<b>59</b>
A1	Optical Fiber	59
A1.1	Fiber Modes	59
A1.2	Refractive Index Profiles	61
A1.3	Propagation Losses	62
A1.4	Dispersion Properties	62
A1.4.1	Dispersion Compensation Fiber (DCF)	62
A1.5	Polarization Properties	62
A1.6	Transmission Capacity of Optical Fibers	63
A1.6.1	Wavelength-Division Multiplexing (WDM)	63
A1.6.1.1	Basic WDM Scheme	63
A1.6.1.2	Capacity and Spectral Efficiency of WDM	64
A1.6.1.3	Telecom Windows	66
A1.6.1.4	WDM Transmitter and Receivers	67
A1.7	Fiber Applications	67

A2	Loss Compensation	68
A2.1	Erbium-Doped Fiber Amplifier	69
A2.1.1	Operation Principle and Setup	69
A2.1.2	Erbium-Doped Amplifiers in Telecom Systems	70
<b>Appendix B Sources for Precise Time and Frequency Transfer</b>		<b>73</b>
<b>Appendix C Variance</b>		<b>75</b>
C1.1	Standard Variance	76
C1.2	Allan Variance	76
C1.3	Overlapping Allan Variance	77
C1.4	Modified Allan Variance	77
C1.5	Time Allan Variance	78
<b>Appendix D OptoSUNET</b>		<b>79</b>
<b>Appendix E GPS, GLONASS and Galileo</b>		<b>81</b>
E1	GPS	81
E1.2	GPS Structure and Operation	81
E1.2.1	Space Segment	81
E1.2.2	Control Segment	82
E1.2.3	User Segment	82
E1.3	GPS Signals	82
E1.3.1	Navigation Message	83
E1.4	Time Keeping in GPS	83
E1.5	Sources of Degradation in GPS	84
E1.5.1	Satellite Orbits	84
E1.5.2	Atmospheric Effects	84
E1.5.2.1	Multipath Effects	85
E1.5.3	Disturbance	85
E2	GLONASS	86
E2.1	GPS/GLONASS Comparison	86
E3	Galileo	86
<b>Papers A–K</b>		



# Chapter 1

## Introduction

**T**ime is a man-made concept we use to keep track of changes. Time also has a definition and various redundant realizations. Since there are several realizations around the globe, we need methods to compare them to each other. These methods are referred to as time transfer, often using GNSS (Global Navigation Satellite System) as a transfer catalyst. A large number of systems, such as telecommunication systems, require a precision in synchronization better than 0.1  $\mu\text{s}$ , and for some systems that use GNSS, fractions of 1 ns are important. This underscores that high-precision time and frequency transfer is crucial for other users than timing facilities. Electric power companies use synchronized systems when measuring stability and searching for faults in their networks. For scientists working with radio astronomy with very long baseline interferometer (VLBI) measurements, synchronization and timing are important factors and many laboratories operate their own time scales with atomic clock references. Scientists who navigate spacecraft are heavily dependent on synchronized control stations. Furthermore, the financial markets are dependent on time and date stamps for identification of transactions in order to organize them in chronological order. There are many more areas that rely on time and frequency synchronization with varying accuracy and precision.

A summary table of common time and frequency transfer techniques and their specifications is included in Appendix B.

This thesis focuses on high-performance time and frequency transfer in the sense of precision better than 1 ns over a substantial amount of time, as well as a frequency comparison that exceeds the frequency performance of commercial atomic clocks. It might be difficult to believe that these specifications could affect someone on a daily basis, but they do, since most of the technologies used for everyday things such as cellphones, internet, television and so on must all be synchronized in order to work properly.

Some of these systems use GPS, which is an abbreviation for Global Positioning System, and is operated by the DoD (Department of Defense) in the United States of America. Satellites (30 per April, 2013) are used in order to provide a receiver with the ability to determine its position (longitude, latitude and altitude), as well as time all around the globe, independent of weather and time of day. Since GPS is free of charge for public use, this technique is commonly used for synchronization, timing and positioning in different applications. In many applications, the satellites' built-in atomic standard is used as a time reference. GPS is crucial for modern navigation in the air, on land, sea, as well as for land-surveying and mapping operations.

Although GPS supports accurate synchronization of clocks and oscillators at different locations, it relies on transmission over weak radio signals (less than  $6.31 \times 10^{-16}$  W) [1]. This weak radio signal is a disadvantage of GPS, since it is fairly easy to tamper with [2]. As requirements for accurate time and frequency synchronization have increased, the need for a complementary time and frequency transfer technique has been identified. This technique must be independent of GPS and allow synchronization even in cases when GPS or other GNSS signals are unavailable.

The Swedish Post and Telecom Authority (PTS) monitor the electronic communication and postal sectors in Sweden. The Authority works with consumer and competition issues, efficient utilization of resources and secure communications. In order to realize the National Swedish time scale UTC (SP) (Universal Time Coordinated (SP Technical Research Institute

of Sweden)) [3], comparisons of high-performance clocks within Sweden are utilized. A PTS objective is to ensure redundancy of these comparisons.

SP was commissioned to develop a supplementary system to the existing and well-established satellite-based time transfer methods (GPS and two-way satellite time and frequency transfer (TWSTFT)). That is also the objective of the research upon which this thesis is based, i.e. to develop new optical fiber based methods for time and frequency transfer, with the intention of strengthening the robustness of the Swedish infrastructure. This infrastructure has been partly strengthened as a result of this research, since a complementary, permanent fiber connection for comparisons between some clocks associated with UTC(SP) is in service.

The technologies that were developed in association with this thesis can at present not be used for comparisons between optical frequency standards. In order to achieve that, continuous wave (CW) based methods should be used. The fiber based techniques presented in this forum are designated for comparison of Hydrogen-MASER and Cesium beam frequency standards utilizing existing optical networks, since those were the only standards available when this work was carried out.

This research has resulted in two unique and innovative transmission methods, one of which has been patented.

The first 5 appended Papers of this thesis are a presentation of the non-insertion technology that utilizes passive listening for time and frequency transfer that was developed, along with its benefits, such as precision relative to the GPS carrier phase of less than one nanosecond root mean square (RMS).

The technique utilizes two-way time and frequency transfer over an asynchronous fiber optical transmission protocol network. The non-insertion method is based on passive listening to existing data frames in a network.

Paper 6 acts as a link between the first five Papers of post-processed timing information, to the last Papers aiming for real-time adjustments and describes a selected work on real-time stabilized phase over optical fiber.

The final 5 appended Papers of this Thesis are a presentation of the research behind the patented fiber based one-way technique that utilizes two wavelengths for realization of a correction algorithm and correction signals. The fundamental background for the one-way technique is the noted interest in alternative solutions to two-way transfer, such as broadcasting and integrity issues, as well as the observation that the symmetry required for high performance two-way solutions is rarely accurate enough.

## 1.1 Organization of the Thesis

The introductory part of this thesis is intended to give an introduction to and comprehension of selected parts of optical time and frequency transfer as a bridge between traditional time transfer and optical communications.

The thesis is organized to provide essential information for understanding the proposed non-insertion technique that is used for time and frequency transfer in fiber optical networks as well as one-way, two-color time and frequency transfer.

The next section, Chapter 2 contains an introduction to the basics of time and frequency, time scales and oscillators for an understanding of the high-performance reference clocks used in time and frequency transfer. Chapter 3 covers some of the optical fiber components that are utilized. After that, chapter 4 presents selected facts upon which time and frequency transfer techniques are based. Chapter 5 presents the evaluated techniques for time and frequency transfers utilized within the research of this thesis, including selected results and conclusions from the appended Papers [A-K]. Chapter 6 provides a summary of the appended Papers [A-K] followed by references and the appendices.

The appendices contain more detailed information about fiber optic components, various sources for precise time and frequency transfer, different kinds of commonly used mathematical models of variance, OptoSUNET, which was utilized as a test bed and GNSS. These have been appended to the thesis to provide readers who to some extent desire a deeper understanding of this field of research access to it.



## Chapter 2

### Time and Frequency

This chapter gives a brief introduction to time and frequency from a national metrology institute (NMI) point of view and the intention is also to provide a comprehension of the fiber optic time and frequency transfer methods in chapter 5 which are the foundation of this thesis.

The method used by mankind to measure time has changed through history. Industrialization and the arrival of railways made it easier to travel and transport goods long distances. Consequently, the expansion of local time scales to larger areas became necessary, due to the fact of passing through several local time scales. This resulted in travelers needing to adjust their clocks repeatedly to local time. In Sweden, the solution to this problem was to introduce one common time zone for the entire country.

One of the earliest methods for measuring time was the Earth's rotation. This was not a very accurate way of measuring, due to the variation in rotational velocity. These variations are evident in the different lengths of a day from day to day, and year to year. Due to these variations, this method was abandoned for better methods with less fluctuation.

The twentieth century saw a major increase in the need for stable and well-defined time, due to the development of radio and data communication. Communication systems are often interconnected and are therefore dependent on reliable and synchronized clocks. Synchronization potentially increases the communication speed.

#### 2.1 Definition of the SI Unit “Second”

The definition of the SI (International System of Units) unit “second” has changed several times during the 20<sup>th</sup> century. Until 1960, it was based on 1/86,400<sup>th</sup> of the mean solar day for universal time one (UT1) at the Greenwich meridian. The initial phase was chosen such that 00:00:00 UT1 would, on average, coincide with midnight at Greenwich and was thus named GMT (Greenwich Mean Time). In the years between 1960 and 1967, it was based on 1/315,569,259,747<sup>th</sup> of the tropical year. A tropical year is calculated from observations of the sun in the year 1900 ephemeris time (ET). This means that one second was equal to one mean second at year 1900 based on the Earth's rotation. The initial phase was chosen so that UT1 and ET approximately agreed in the year 1900. In 1988, the difference between the two time scales was 56 seconds, due to variations in the Earth's rotation relative to its own axis as well as other Earthly variations. The most recent change in the SI unit second was made in 1967. Since then, it has been defined to be the duration of 9,192,631,770 periods of the radiation corresponding to the transition between the two hyperfine levels of the ground state of the Cesium 133 atom. All of these definition changes have been the result of society's ever increasing need for stable time and synchronization [4].

## **2.2 Time Scale**

A time scale is defined by a starting point and is thereafter continuously accumulated in time units. These time units are defined as time intervals. A good example of a time interval is a second, which accumulates and then transforms into minutes, hours, days, weeks, months, years, etc. The difference between different time scales is their starting points and the length of their time units, or both. As described in previous section, the definition of a second has changed several times throughout the history of timekeeping. This has resulted in the use of several different time scales for setting the official world time. The following section will describe some of these timescales.

### **2.2.1 Universal Time (UT)**

Universal time is based on the Earth's rotation around its own axis. "True" solar time is the time interval between two occurrences of the highest possible observation of the sun above the horizon. This time is dependent upon the location where these measurements are made and during which season of the year. The largest contributing factor to these variations is the difference in the Earth's inclination relative to its plane during its rotation around the Sun. One important factor is the fact that the Earth's rotation around the Sun follows a path that is not circular, but slightly elliptic and these variations can be several tens of minutes. The corrections of these variations are called time equations and they are used to derive a mean solar day. There is one time scale based on this and it is called universal time zero (UT0), which is equal to mean solar time with correction at the Zero Meridian, located at Greenwich, England.

One important factor in UT0 variations is the wandering of the Earth's poles. This is caused by shifts between the Earth's rotation axis relative to its surface. Correction for these phenomena can reach values in the order of 30 m [4]. The time scale UT1 is obtained by using these corrections. Despite this correction for dynamic Earth variations, the stability of UT1 was not deemed good enough to be used as a base for the SI unit of second. Society required a better and more stable definition in the long term [4].

### **2.2.2 Ephemeris Time (ET)**

An ephemeris is a table of values that gives the positions of astronomical objects in the sky at any given time. The ephemeris time scale is based on the Earth's rotation around the Sun, which is much more stable than the Earth's rotation around its own axis. Even though ET is more precise than UT1, its stability is still not sufficient for our modern society.

### **2.2.3 International Atomic Time (TAI)**

The dynamic time scales of UT and ET are based on counting periods of the Earth's rotation. An atomic time scale is achieved by counting the cycles of an atomic resonant frequency. The first atomic clocks started to appear in the 1940's, resulting in the atomic time scales. These time scales were first used to evaluate variations in the UT and ET time scales. Because of these studies, this work laid the foundation for a change in the SI definition of the unit 1 second, from Earth-based to atomic-based, that resulted in a change 1967.

TAI is the coordinated reference time established by the International Bureau of Weights and Measures (BIPM) and is based on time from atomic clocks maintained according to the agreed definition of one second, the time unit in SI.

The initial phase of TAI coincides with UT1 on January 1, 1958 at 00:00:00 at the Greenwich Meridian.

A coordinated time scale means that time is one of the coordinates in a system of three space coordinates ( $x$ ,  $y$ ,  $z$ ) and a time coordinate. This means that TAI is a coordinated time scale defined within a geocentric reference frame. The frame origin is in the Earth's center, with the SI second realized on the rotating geoid as a unit. Therefore, clocks that are a part of TAI must be located at sea level or be corrected for any difference in altitude. The reason for this is the gravitational effects in the theory of relativity [4]. A clock that is less affected by gravity will run faster than one with higher gravitational pull. For two clocks located one kilometer apart, one at sea level and one further out in space, this rate difference will be approximately 10 ns a day.

Compared to UT and ET, TAI is not a physical clock. It is a system time or a "paper clock", calculated using more than 450 clocks in approximately 70 laboratories (2013) around the globe as a weighted mean value. Information from primary frequency standards are applied on the weighted mean value which results in TAI. A major advantage with TAI is that it can be realized in any laboratory with access to an atomic clock and its achievable precision is better than a few nanoseconds when measuring more than one minute.

Earth variations, such as rotation speed, sunrise and sunset do not affect TAI. The length of the time interval one second in TAI was set using the definition of one second in ET, and that second was in the same way based on the UT1 second in 1900. The effect of these relationships is that one mean solar day will historically be a couple of milliseconds longer 100 years from now, due to the Earth's deceleration. This increase causes UT1 and TAI to drift apart [4].

## 2.2.4 Coordinated Universal Time (UTC)

Even though the SI definition of one second was changed in 1967, official world time was based on UT1 until 1972. The world had then come to need a stable official time scale with the characteristics of an atomic time scale. Simultaneously, astronomers, physicists, navigators and the general public were in need of a time scale that followed the Earth's rotation. UTC (Universal Time Coordinated), a new time scale, became the solution to this problem. UTC was first derived in 1961 and was based on atomic clocks, but its frequency was adjusted a few times a year to keep it in phase with UT1 and the mean solar day. The advantage with this time scale was that it had the characteristics of an atomic time scale, such as TAI. A major problem was the frequent clock adjustments that were required due to the difficulty of predicting UT1. A better method of defining UTC was needed.

Since UTC was to become the official world time, 00:00:00 UTC would coincide with midnight at the Zero Meridian (Greenwich). The difference between UTC and TAI is always an integer number of seconds. When the difference between UTC and UT1 is larger than 0.9 seconds, a second is inserted or subtracted relative to TAI. This is done instead of using the previous method of continuous alignment. The inserted or subtracted seconds are called leap seconds. Leap seconds are usually timed to be introduced at midnight on June 30<sup>th</sup> or December 31<sup>st</sup>. This means that UTC encompasses the good characteristics of TAI, since it uses the same definition of one second, but the difference is that UTC follows the speed of the Earth's rotation [4]. The difference between UTC and TAI is illustrated in Fig. 2.1.

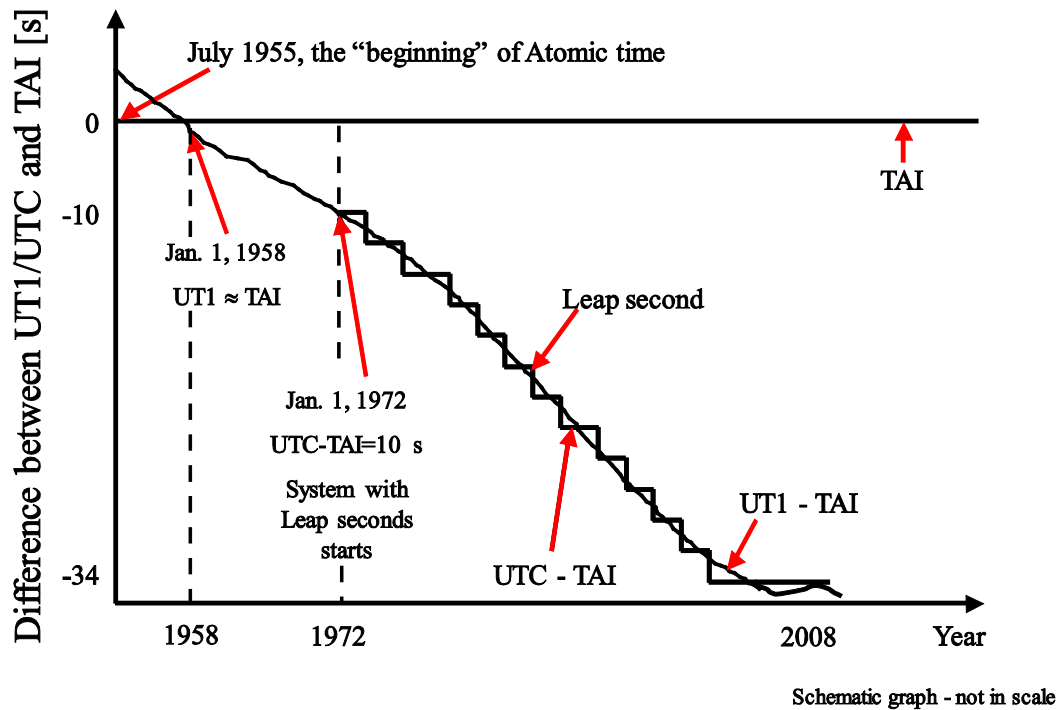


Figure 2.1: Relationship between the timescales UT1, TAI and UTC. The y-axis represents their difference in seconds and the x-axis represents years.

### 2.2.5 Local Time Scales

Local time scales can be calculated from UTC by either adding or subtracting an integer number of half hours, depending on time zone. This is also dependent on daylight saving time decisions. Official distribution and broadcasting of timing signals through the telecommunication network, television, the internet, earthbound or satellite-based radio transmissions are often traceable to UTC [4]. Official time in Sweden is UTC+1 hour during wintertime and UTC+2 hours during summertime [3].

## 2.3 Frequency

Frequency is the number of occurrences of a repetitive event per unit of time. The unit of time must be fixed to enable the counting of the repetitive event, and the numbers of counts is then divided by the unit of time to receive the frequency. The unit for frequency is Hertz, after the physicist Heinrich Rudolf Hertz, and it defines one occurrence per second.

Anything that swings in some kind of way can be used to measure a time interval by counting and keeping track of the number of swings or ticks as is illustrated in Fig. 2.2.

A condition for the determination of a time interval is that the number of swings that take place in a recognized unit of time, such as a day, an hour, a minute or a second, are known. A time interval can be measured if the frequency is known [5].

Propagation is achieved in time and space hence there is a delay between the transmitted and received.

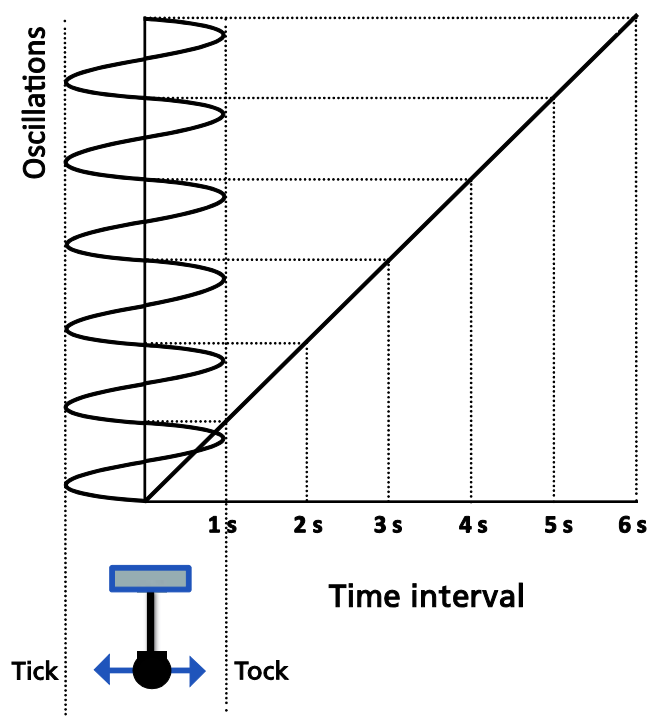


Figure 2.2: A simple illustration of the relationship between time interval and frequency. A time scale is created by counting time events [5]. The x axis represents how the time interval is related to the oscillations on the y axis.

The preferred way of analyzing frequency stability is to calculate its variance. Variance is further explained in Appendix C.

## 2.4 Clocks and Oscillators

Some of the earliest clocks were built in ancient Egypt [5]. The Egyptians constructed both sundials and water clocks. The simplest form of water clocks consisted of an alabaster bowl, wide at the top and narrow at the bottom, marked on the inside with horizontal “hour” marks. The bowl was filled with water that leaked out through a small hole in the bottom. Later, the Greeks and Romans continued to rely on these clocks, but with the addition of sand clocks.

Sometime between the 8<sup>th</sup> and 11<sup>th</sup> centuries A.D., the Chinese constructed a clock that possessed some of the characteristics of a mechanical clock. This new type of clock was still a water clock, since it was powered by water falling onto a turn wheel. Sand was introduced to these “turn wheel clocks” in the 14<sup>th</sup> century to avoid the problem of the water in water clocks freezing. The mechanical clock was developed sometime in the 14<sup>th</sup> century and was powered by a weight attached to a cord wrapped around a cylinder. That type of clock kept the time accurately, within 15 minutes a day. Due to internal components and friction, it was hard to manufacture duplicates that kept the exact same time. The quality and production of these clocks was entirely dependent upon the craftsmen involved. In order to keep more accurate time, some kind of periodic device, whose frequency was essentially a property of the device itself and not primarily dependent on a number of external factors, was needed. A pendulum is such a device. The Dutch scientist Christian Huygens built his first clock in 1656, and that clock was accurate to within 10 seconds a day.

At the same time, an English scientist was experimenting with clocks using straight metal springs to regulate the clock frequency. However, the first pocket watch was patented by Huygens in 1675 [5].

There are three main features that define a clock, and these are described in Table 2.1.

Table 2.1: Three main features that define a clock

<b>Main features that defines a clock</b>
<ul style="list-style-type: none"><li>• A device that produces “periodic phenomena” (resonator).</li><li>• A device that sustains periodic motion by feeding energy to the resonator (oscillator).</li><li>• A device for counting, accumulating and displaying the ticks or swings of the oscillator.</li></ul>

An ideal resonator only has an initial phase and then continues to resonate without further maintenance. There is a measure of oscillators that is known as the Q-factor. The Q-factor is the number of swings a resonator will make before its energy has diminished to half of the energy imparted with the initial push. A high-Q resonator will not resonate at all unless it resonates at its natural frequency. This feature is closely related to the accuracy and stability of a resonator, which means that a single-frequency resonator is more accurate than a resonator that can resonate at a range of frequencies. A resonator with a range of frequencies will most likely wander and therefore be more unstable than a single-frequency resonator. The work presented in this thesis focuses on time transfer between single-frequency resonators such as Cesium, Hydrogen and Rubidium oscillators [5].

The Q-factor can mathematically be explained according to Eq. (2.1) in which  $\nu_o$  is the resonant frequency and  $\Delta\nu$  is the width of the range of frequencies for which the energy is at least half its peak value.

$$Q \equiv \frac{\nu_o}{\Delta\nu} \quad (2.1)$$

Table 2.2 presents typical Q-factors and accuracies for different types of resonators. The values state that higher Q-factor increase the stability and to some extent the accuracy. The increase in Q-factor can be found out by Eq. (2.1) since a higher resonant frequency and narrower bandwidth will increase the Q-factor.

Table 2.2: Typical Q-factor and accuracy for resonators

Type of standard	Q-factor	Accuracy [4, 6]
• Inexpensive balance wheel watch	1000	Calibration required
• Tuning fork watch	2000	Calibration required
• Quartz clock	$10^5$ – $10^6$	Calibration required
• Rubidium clock (Rb)	$10^6$	Calibration required
• Cesium clock (Cs) (commercial)	$10^7$ – $10^8$	$1 \times 10^{-13}$ – $5 \times 10^{-12}$
• Hydrogen-MASER clock (Hm)	$10^9$	$1 - 5 \times 10^{-12}$
• Optical clock (Oc)	$\sim 10^{15}$	$< 1 \times 10^{-17}$

### 2.4.1 Cesium Beam Frequency Standard

Cesium beam frequency standards are the most common oscillators used for realization of the SI-unit second. They are commercially available and installed both in NMIs and network operators etc.

Cesium atoms are heated into a gas which is propagated through a small opening. The atoms are then channeled through a magnetic field that separates the atoms into two streams, where only the atoms in the correct state are allowed to proceed down the tube. The selected beam, see Fig. 2.3, passes through a microwave cavity and is exposed to a radio frequency near 9,192,631,770 Hz that places the atoms in a superposition between the two hyperfine states. The atoms then proceed over a certain distance/time where their superposition state is free to evolve before passing through a second microwave cavity that is identical to the first. If the microwave radiation is completely in resonance with the atom, the transition is completed. At the end of the tube, another magnetic gate only allows those atoms that have completed the transition to pass through to a detector. The signal from the detector is feedback-coupled to the radio signal through a crystal oscillator to maximize the number of resonant atoms [5, 7].

Carefully constructed Cesium-beam tube resonators in laboratories have Q-factors of over 100 million. Laboratory oscillators keep time with an accuracy of less than one second in 10 million years [5].

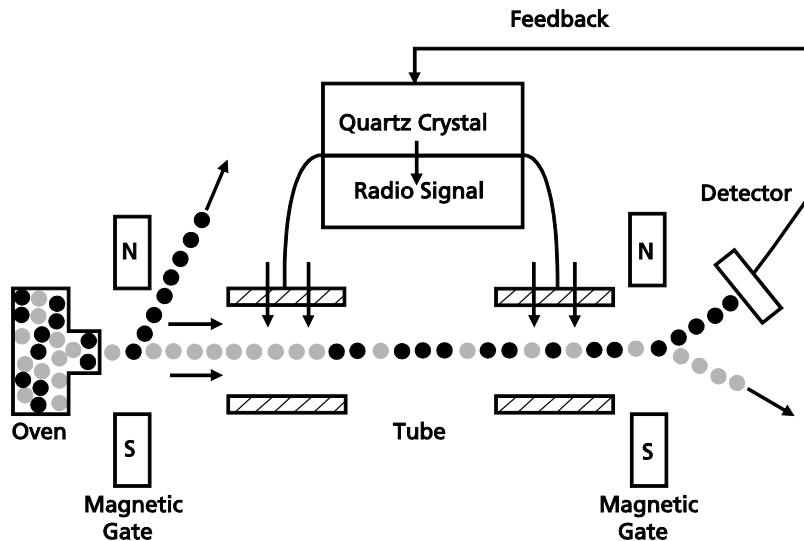


Figure 2.3: Simple schematic diagram of a Cesium Beam Frequency Standard [5, 7]. The Cesium atoms are propagated through a small opening to be further channeled through a magnetic field that separates the atoms into two streams, where only the atoms in the correct state are allowed to proceed down the tube. The selected beam passes through a microwave cavity and is exposed to a radio frequency that places the atoms in a superposition between the two hyperfine states. The atoms are then passed through a second microwave cavity, and if the microwave radiation is completely in resonance with the atom, the transition is completed. At the end of the tube, another magnetic gate only allows those atoms that have completed the transition to pass through to a detector. The signal from the detector is feedback-coupled to the radio signal to maximize the number of resonant atoms.

## 2.4.2 Hydrogen-MASER

MASER is an acronym for Microwave Amplification by Stimulated Emission of Radiation. A feature of the Hydrogen-MASER is that it is based on the direct observation of the atomic radio signal. The Hydrogen atom is used as the resonator in the MASER, and this atom has a particular resonant frequency of 1,420,405,752 Hz. As in the Cesium-beam tube, Hydrogen gas is channeled through a magnetic gate that only allows atoms in the certain state to pass. The atoms that make it through this gate enter a quartz glass storage bulb several centimeters in diameter. The inside of the storage bulb is coated with a Teflon material. This coating reduces the frequency-perturbing effects that are caused by collisions of the Hydrogen atoms with the inside wall of the bulb. The Q-factor for a Hydrogen-MASER is about 10 times higher than that of a Cesium-beam oscillator. If the bulb contains enough Hydrogen atoms in the correct state, “self-oscillations” will occur in the bulb. Eventually, one atom will spontaneously emit a photon at the resonant frequency. Under the right conditions, this will trigger a stimulated process. This stimulated emission is in phase with the radiation that produced it, and the signal it generates keeps a crystal oscillator in phase with the resonant frequency of the Hydrogen atoms [5, 8]. Figure 2.4 shows a simple schematic diagram of a Hydrogen resonator.

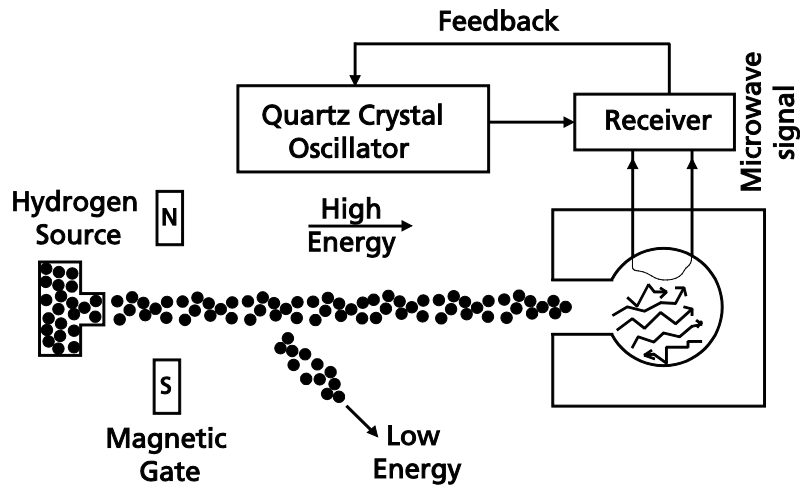


Figure 2.4: Simple schematic diagram of a Hydrogen resonator. Hydrogen gas is channeled through a magnetic gate that only allows atoms in a correct state to pass. The atoms that make it through this gate enter a quartz-glass storage bulb. If the bulb contains enough Hydrogen atoms in the correct state, “self-oscillations” will occur in the bulb. Eventually, one atom will spontaneously emit a photon at the resonant frequency. Under the right conditions, this will trigger a stimulated process. This stimulated emission is in phase with the radiation that produced it, and the signal it generates keeps a crystal oscillator in phase with the resonant frequency of the Hydrogen atoms [5, 8].

### 2.4.3 Rubidium Resonator

The quality of a Rubidium oscillator is usually lower than that of a Cesium resonator, but the price for the user is also lower.

This device is based on the resonant frequency of Rubidium atoms in a gaseous state that are held at very low pressure in a chamber. One resonant frequency of Rubidium is excited by an intense beam of light, and another resonant frequency is excited by a radio wave in the microwave region. As the light shines through the glass bulb containing Rubidium gas, atoms in the susceptible energy state will absorb energy. A radio signal at the correct frequency will convert the maximum number of atoms possible into the correct energy state to absorb energy from the light beam. The intensity of the light beam that shines through is detected and used to generate a signal that controls the microwave frequency in order to make the light beam reach a minimum value. Figure 2.5 shows a simple schematic diagram of a Rubidium resonator.

Some of the best Rubidium oscillators have Q-factors around 100 million and are stray less than one millisecond in a few months. They have a slow drift and need to be reset or steered occasionally. This drift is due to the drift in the light source and the absorption of Rubidium in the walls of the storage bottle [5].

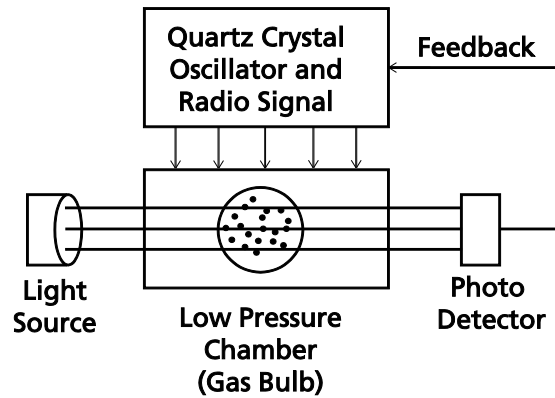


Figure 2.5: Simple schematic diagram of a Rubidium resonator. The device is based on the resonant frequency of Rubidium atoms in a gaseous state that are held at low pressure in a chamber. One resonant frequency of Rubidium is excited by an intense beam of light, and another resonant frequency is excited by a radio wave in the microwave region. As the light shines through the glass bulb containing Rubidium gas, atoms in the susceptible energy state will absorb energy. A radio signal at the correct frequency will convert the maximum number of atoms possible into the correct energy state to absorb energy from the light beam. The intensity of the light beam that shines through is detected and used to generate a signal that controls the microwave frequency in order to make the light beam reach a minimum value [5].

#### 2.4.4 Optical Frequency Standard

Oscillators based on atomic microwave transitions will eventually be replaced by equipment based on optical transitions, which will likely result in a change of the SI second. Several laboratories around the world are currently working on these frequency standards [9].

Optical frequency standards are used for producing or probing optical frequency signals, and the measurement of these can be performed with far higher precision than other types of frequency standards. An optical frequency standard is in a sense a laser, emitting light with a well-defined and known optical frequency. When combined with optical clockwork, such a frequency standard can form the basis of an optical clock.

An optical frequency standard is usually based on an optical transition within an ultra-narrow bandwidth of certain atoms. This transition is used to stabilize the frequency of a single-frequency laser to the transition frequency. In order to reduce inhomogeneous broadening by thermal movement and collisions, the particles' density and relative velocities need to be minimized. One possibility is to keep the particles in a trap within a vacuum chamber and to apply laser cooling in order to strongly reduce the temperature [10].

### 2.4.4.1 Optical Clock

Optical clocks can offer an extremely high frequency precision and stability, exceeding the performance of the best Cesium atomic clocks.

One challenge in the early years of optical clocks was to measure and relate the stable optical frequency to a microwave frequency standard, such as a Cesium atomic clock. This was solved with the realization of frequency combs from femtosecond mode-locked lasers [10]. Figure 2.6 shows a schematic illustration of an optical clock.

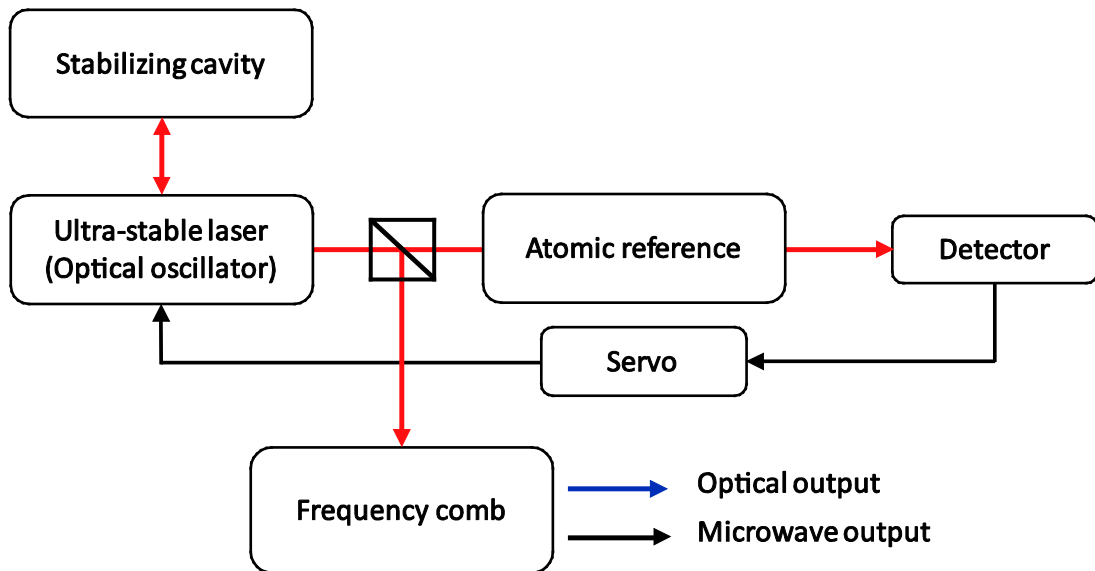


Figure 2.6: A schematic illustration of an optical clock. An ultra-stable clock laser, stabilized to an external cavity, acts as the optical oscillator. By preparing an atomic sample (usually in an ion trap or a lattice trap) the laser can be used to probe an ultra-narrow atomic transition. Using a detector and servo-electronics, the ultra-stable laser can then be locked to the transition, and hence inherit the absolute frequency stability of the atomic reference. Finally, by locking one of the comb teeth of a frequency comb to the ultra-stable laser output, the clock laser's frequency stability is transferred to an optical or microwave (or both) frequency/wavelength of choice, e.g. commonly used optical 1550 nm wavelength or a 10 MHz microwave signal.

Compared to microwave standards such as Cesium atomic clocks, optical clocks have some of the key advantages that are summarized in Table 2.3.

Table 2.3: Optical Clock Advantages

---

**Key Advantages of an Optical Clock**

---

- There are certain atoms and ions with extremely well-defined clock transitions that promise higher accuracy and stability than the best microwave atomic clocks. The anticipated relative frequency uncertainty of atomic optical clocks for long enough averaging times is in the order of  $10^{-18}$  [6].
  - The high optical frequencies themselves are of great importance, since they allow precise clock comparisons within much shorter time periods. For example, a  $10^{-15}$  precision can be achieved in a few seconds if the compared frequencies are in the optical range, whereas a full day would be required for microwave clocks.[6]
  - Optical signals can easily be transported over long distances using fiber, whereas microwave incur much higher losses.
- 
- 

Therefore, it is to be expected that in the near future the use of the Cesium clock as the fundamental timing reference will be replaced with an optical clock, although at the moment it is not clear which type of optical clock would be used for such a standard. The definition of the second will then be changed to refer to an optical frequency rather than a microwave frequency. However, even after that profound change, Cesium clocks (and other non-optical atomic clocks, such as Rubidium clocks) will continue to play an important role in technological applications as they can be simpler and more compact than optical clocks [10].

## Chapter 3

# Optical Fiber and Associated Components

This optics section gives a short introduction to optical fiber and some of the optical components used in this research, with the intention of providing an understanding of the fiber optic time and frequency transfer methods in Chapter 5. A more elaborated description of some optic components can be found in Appendix A.

The length and characteristics of optical single-mode fibers (SMF) are not limiting factors when it comes to the choice of using fiber for time and frequency transmissions. The real limitations lie in the electrical equipment that is needed and also depends on the choice of transmission technology. That choice is also a matter of cost, since maintaining dedicated fiber networks is expensive, although in return they offer the best performance in terms of time and frequency transfer.

### 3.1 Optical Fiber

An optical fiber is a dielectric waveguide made of a low-loss material, such as silica glass. It has a central core through which the light is guided, surrounded by a cladding with a lower refractive index. Light rays inside the fiber that incident on the core-cladding boundary at angles larger than the critical angle undergo total internal reflection and are continuously guided through the core without being refracted into the cladding [11].

Optical fiber as a waveguide propagates the signal in forms of different modes. Each mode travels along the axis of the waveguide with a distinct propagation constant and group velocity, maintaining its transverse spatial distribution and a varying polarization. Each mode is described as the sum of the multiple reflections of a transverse electromagnetic (TEM) wave bouncing within the core. If the core is small, only a single mode is supported and the fiber is said to be a single-mode fiber [12].

The parameters for a standard single-mode fiber used for communication purposes are defined in the International Telecommunication Union T standard G.652 (ITU-T G.652) [13]. In the appended Papers, it also appears under the name SMF-28, which is a registered trademark for the G.652 fiber made by Corning Inc. The G.652 standard describes a single-mode optical fiber and cable which has zero-dispersion wavelength around 1310 nm and typical value of 17 ps / (nm × km) for 1550 nm. Both analogue and digital transmission can be used with this fiber.

The linear effect that describes how the different parts of a signal travel at different speeds and thereby cause the data bits or amplitude modulation to smear out is called dispersion. Dispersion is a major limiting factor for any long-haul lightwave system with high data rates. The parameter  $\beta_2$  is known as the second order dispersion parameter, and it is a measure of the pulse broadening in a fiber. For normal dispersion fiber, the  $\beta_2$  constant is highly negative [12].

### **3.1.1 Dispersion Compensation Fiber (DCF)**

There is a solution for minimizing the total dispersion and the basic idea consists of periodically compensating dispersion along the fiber link. This is performed using fibers or devices with inverse dispersion characteristics. The use of dispersion compensating fibers (DCF) provides an all-optic technique that is capable of overcoming the detrimental effects of chromatic dispersion in optical fibers. A prerequisite for this is that the average signal power is low enough for the nonlinear effects to remain negligible [12].

## **3.2 Wavelength-Division Multiplexing (WDM)**

Signals can be multiplexed in the spectral domain through frequency-division multiplexing (FDM). This technology is routinely used for radio waves and microwaves. Its extension to the optical domain enables high bit-rate capacity in lightwave systems through the large frequency associated with the optical carrier. Wavelength-division multiplexing (WDM) is a technology that multiplexes multiple optical carrier signals in a single optical fiber by using different wavelengths (colors) of laser light to carry different signals. This allows for a multiplication of capacity, in addition to enabling bidirectional communication over a single strand of fiber. This is a form of FDM, but is commonly called WDM.

WDM increases system capacity through the simultaneous transmission of multiple bit streams in the same fiber.

For any given system bandwidth, a link's capacity depends on how closely the channels can be compressed in the wavelength domain. The minimum channel spacing is limited by interchannel crosstalk. The channel frequencies or wavelengths in fixed grid WDM systems have been standardized by the recommendation from ITU with a span of 12.5 GHz [14-15].

### **3.2.1 Transmitter and Receivers**

The spacing between assigned channels in WDM systems can be narrow and the precision of the emitted wavelength is important. A fully-equipped system can require a high number of lasers.

The transmitters are usually equipped with distributed feedback lasers (DFB) or tunable lasers. A DFB is manufactured for a specific wavelength, but is slightly tunable to operate at the assigned channel. Even though the cost of a DFB is relatively low, the number of spare parts that need to be kept in stock for repairs is high. A tunable laser for communication is usually designed to cover a full communication band (see Appendix A), but is generally a more expensive solution. A tunable laser emits a continuous flow of light and data is modulated onto the light using external modulators. These modulators are sometimes integrated with the laser chip, but are not part of the laser cavity.

Receivers are optimized for high responsivity, low noise and sufficient bandwidth. If the received power level is sufficiently high, a p-i-n detector can be used, which is a less expensive solution than the avalanche photo-diode (APD) with internal optical magnification. In either case, the detector is followed by a matched trans-impedance amplifier, increasing the signal strength and harmonizing it to the succeeding electronics.

### 3.2.2 Loss Compensation

Fiber losses must be compensated in lightwave systems with reaches longer than 100 km, due to the cumulative effects eventually making the signal so weak that the information cannot be recovered at the receiver.

Optical amplifiers that are used for loss compensation can be divided into two categories, known as lumped and distributed amplifiers. Most present systems employ lumped, Erbium-doped fiber amplifiers (EDFAs) in which losses accumulated over fiber lengths of 60 to 80 km are compensated through amplification using short lengths (~10 m) of Erbium-doped fibers. In distributed amplification, the transmission fiber itself is used for signal amplification, e.g. by exploiting the nonlinear phenomena of stimulated Raman scattering (SRS) [16]. Using them for loss compensation requires the periodic injection of optical power from one or more pump lasers through fiber couplers. This amplification method has enjoyed increased interest in the deployment of new systems.

Any loss management technique based on optical amplification degrades the signal-to-noise ratio (SNR) of the optical bit stream, since all optical amplifiers add noise to the signal due to amplified spontaneous emission [11-12, 17-18].



## Chapter 4

# Time and Frequency Transfer

This chapter gives an introduction to basic one-way and two-way time and frequency transfer, regardless of the transmission medium. After an initial overview, GNSS-based transfer is presented since that method has been used as a reference for the fiber based techniques presented in Chapter 5. The subsequent section is an introduction to fiber based time and frequency transfer and is intended as a background for Chapter 5.

Time transfer methods are used to transfer time and/or frequency information from a reference clock at one location to a remote location. Radio-based navigation systems are frequently used for this purpose. Among the users of radio-based navigation systems, such as GPS, for timing and synchronization purposes we find national time laboratories that contribute to UTC at the highest level. Another group with an interest in clock comparison is those who deal with fundamental physics. But also monetary institutions, cellphone service providers and law enforcement organizations require time or frequency information with varying levels of accuracy and precision. Appendix B presents a list of time transfer methods [19].

Time is transferred using satellites with an accuracy of a few ns [20-21]. Accurate time and frequency transfer over existing fiber optic networks, however has attracted increasing interest in recent years, as awareness of the dependence on GPS and vulnerability to satellite transmission interference [2] has risen.

Experimental field trials on two-way time and frequency transfer in existing fiber have been made previously using dedicated transmission capacity [22-24]. These solutions actively transmit a timing signal over the network, and thereby require direct access to the infrastructure. They may therefore be difficult to implement in non-dedicated networks. As an alternative, a technique utilizing the data that is already being transmitted in the network to recover time information has been developed. This section is intended to provide an overview of basic one-way and two-way time and frequency transfer methods, with example applications in GNSS and fiber.

## 4.1 One-Way Time and Frequency Transfer

In a setup for a one-way time and frequency transfer, one side of the communication path transmits its current frequency or time, or both, to the other side. The transmitting side can be simultaneously sending its frequency and time to several receivers and in that sense serve as a hub. The information can be handled in several different ways on the receiving end, but a decoding process must often be performed.

After decoding, the information can be used to either report the time, or for example adjust a local clock that provides hold-over time reports between message receptions. This kind of setup is preferable when the transmitting side is unable to receive information or is prohibited from doing so. One-way systems can be technically simple and serve many receivers.

Figure 4.1 shows an example of a one-way time and frequency transfer between two clocks, *A* and *B*. The clocks are compared to each other using a time interval counter (TIC) located close to clock *B*. A predetermined signal, e.g. a 10 MHz sine wave, is transmitted from clock *A* at time  $t_1(t_A)$ , and when it arrives at clock *B*, the arrival time  $t_1(t_B)$  is measured with respect to the local clock *B*;  $t_2(t_B)$ . Therefore  $TIC_B$  is the measurement of clock *A* relative to clock *B*

including the propagation delay ( $\tau_A + \tau_A(t)$ ) in the transmission path, as described by Eq. (4.1)

$$TIC_B = t_2(t_B) - t_1(t_B) = t_2(t_B) - (t_1(t_A) + \tau_A + \tau_A(t)). \quad (4.1)$$

where  $\tau_A$  is a constant and the most important  $\tau_A(t)$  indicates that the delay varies in time deterministically and randomly.

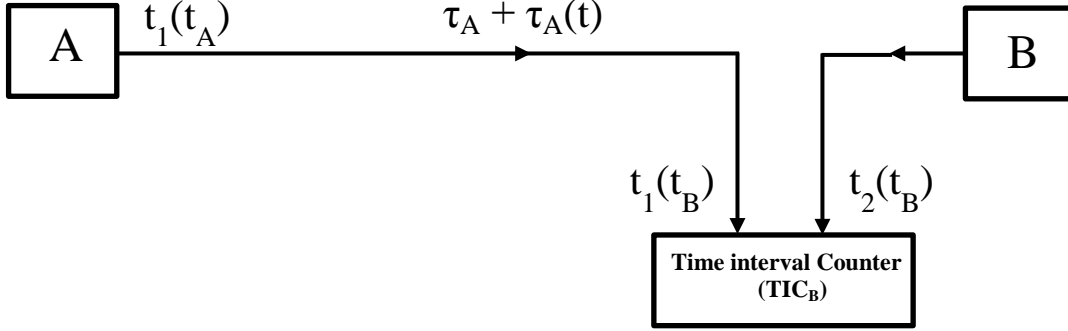


Figure 4.1: Schematic diagram of an uncompensated one-way time and frequency transfer between two clocks, *A* and *B*. The clocks are compared to each other using a time interval counter (TIC) that is located close to clock *B*. A predetermined signal is transmitted from clock *A* at time  $t_1(t_A)$ , and when it arrives at clock *B*, the arrival time  $t_1(t_B)$  is measured with respect to the local clock *B*;  $t_2(t_B)$ . Therefore  $TIC_B$  is the measurement of clock *A* relative to clock *B* including the propagation delay ( $\tau_A + \tau_A(t)$ ) in the transmission path.

Time transfer is performed given that an initial calibration of the transit time over the path is performed.

The final frequency comparison between clocks *A* and *B* is achieved by estimating the slope of a series of time interval measurements as described by Eq. (4.2), which for an uncompensated link is affected by the varying propagation delay,

$$t_2(t_B) - t_1(t_A) = TIC_B + \tau_A + \tau_A(t), \quad (4.2)$$

and accounting for possible ambiguities due to the repetitive signal that is dependent on the transmitted signal's frequency and the relative frequencies of clocks *A* and *B*.

Even though the average transit time delay can be estimated by calibration, variations in transit time will always affect the comparison unless they are continuously measured and compensated.

To perform a time transfer between two points, an initial calibration of the transit time at starting point,  $\tau_A$ , must be carried out, i.e. the time it takes for a given level of an edge of a signal or pulse to propagate between points *A* and *B*. Based on this reference, setting a starting value at the receiver clock, time is achieved by adding periods of a repetitive signal with a known or presumed stability.

Several types of systems are used for one-way time and frequency transfer, including ground-based transmitters such as long range navigation (LORAN) [25] (operational in Europe and Asia), Deutschland long wave signal Frankfurt frequency 77 (DCF77) [26], and satellite-based systems such as GPS. A few of these systems do not compensate for variations in transit delays. In the proceeding analysis, the stability of the frequency, i.e. the operational part of time transfer, is characterized presuming alternative techniques for initialization of a time transfer.

## 4.2 Two-Way Time and Frequency Transfer

The difference between two-way transfers compared to one-way transfers is that all receivers in a communication link both transmit and receive information.

In two-way transfers, two different one-way transfer paths are used to determine the difference between the local clock and the remote clock. The sum of this transit time difference is the round-trip delay between the two locations. A common assumption is that path delays are evenly distributed between the two directions, and if that assumption is valid, then half the round-trip delay in each propagation path should be compensated. However, this not the case and one drawback with two-way time and frequency transfer is that the propagation delay in the two directions may be asymmetric. This will appear as a systematic error in the transfer results. This error is usually handled by calibrating the asymmetry, which also results in a time transfer. Figure 4.2 illustrates an example of two-way time and frequency transfer between two clocks, *A* and *B*. The clocks are compared to each other with two time interval counters.

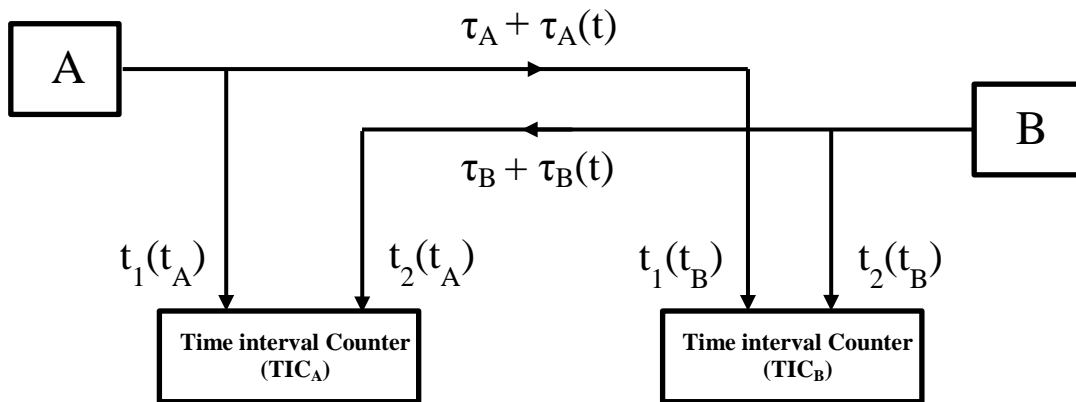


Figure 4.2: Schematic diagram of a two-way time and frequency transfer between two clocks, *A* and *B*. The clocks are compared to each other with two time interval counters. A well-defined signal is transmitted from clock *A*, and the time it leaves the sender is measured at the master clock *A*;  $t_1(t_A)$ . When the signal arrives at clock *B*, the arrival time is measured at the local clock *B*;  $t_1(t_B)$ . In addition, another well-defined signal is transmitted back from *B* to *A*, resulting in the time stamps  $t_2(t_B)$  and  $t_2(t_A)$ . Therefore,  $TIC_A$  measures *A* compared to *B*, including the propagation delay from its transmission path Eq. (4.3), while  $TIC_B$  measures *B* compared to *A*, including the corresponding propagation delay from its transmission path.

A well-defined signal is transmitted from clock  $A$ , and the time it leaves the sender is measured at the master clock  $A$ ;  $t_1(t_A)$ . When the signal arrives at clock  $B$ , the arrival time is measured at the local clock  $B$ ;  $t_1(t_B)$ . In addition, another well-defined signal is transmitted back from  $B$  to  $A$ , resulting in the time stamps  $t_2(t_B)$  and  $t_2(t_A)$ . Therefore,  $TIC_A$  measures  $A$  compared to  $B$ , including the propagation delay from its transmission path Eq. (4.3), while  $TIC_B$  measures  $B$  compared to  $A$ , including the corresponding propagation delay from its transmission path Eq. (4.4).

$$TIC_A = t_1(t_A) - t_2(t_A) = t_1(t_A) - (t_2(t_B) + \tau_B + \tau_B(t)) \quad (4.3)$$

$$TIC_B = t_2(t_B) - t_1(t_B) = t_2(t_B) - (t_1(t_A) + \tau_A + \tau_A(t)) \quad (4.4)$$

The clock comparison Eq. (4.5) is the result of Eqs. (4.3 and 4.4), with the inclusion of an asymmetry factor,  $F(t)$ , that takes potential differential path delays between  $\tau_A + \tau_A(t)$  and  $\tau_B + \tau_B(t)$  into account.

$$t_1(t_A) - t_2(t_B) = \frac{TIC_A - TIC_B - (\tau_A - \tau_B) - (\tau_A(t) - \tau_B(t))}{2} = \frac{TIC_A - TIC_B - F(t)}{2} \quad (4.5)$$

Thus, the relationship between signal emitters  $A$  and  $B$  can be determined from measured data, and the calculations can be made at either end of the link as soon as data is exchanged.

Examples of systems that utilize this technique are TWSTFT [27] and Network Time Protocol (NTP) [28].

TWSTFT is used for timescale comparisons in time laboratories and the technique utilizes a geostationary communication satellite as a common link between the laboratories. NTP uses packet-based messages over an internet protocol (IP) network.

Appendix B contains sources for time and frequency transfer [19].

### 4.3 Time and Frequency Transfer Utilizing GNSS

This section contains an introduction to time and frequency transfer utilizing a GNSS, with the aim of providing a brief understanding of the basics. Additional information about individual GNSS systems, such as GPS, GLONASS (Global'naya navigatsionnaya sputnikovaya sistema (Global navigation satellite system)) and Galileo (European global navigation satellite system), can be found in Appendix E.

#### 4.3.1 Positioning Techniques

The technique requires precise timing, which is provided by several atomic clocks onboard each satellite and the position determination is based on a concept called time of arrival ranging. This method involves transmitting a signal at a known time and measuring the arrival of the signal at a later known time. If the two clocks providing the time of transmission and reception are synchronized, it is possible to calculate the signal's travel time and thereby the distance between the satellite and the receiver. The oscillator used for time measurements must be accurate, otherwise the range measurements will not be accurate and precise positioning will not be possible. Clock bias error leads to incorrect positioning. However, a clock offset in the receiver could be acceptable if it is treated as a "fourth coordinate" ( $x, y, z$

and  $t$  (time)). Each satellite broadcasts almanacs that contain information about satellite positions and clock corrections at any given moment, updated regularly with respect to reference stations on Earth. The information about satellite position is called the ephemeris and is included in the signal transmitted from the GPS satellite. GPS and GLONASS are examples of positioning systems that are in use today. The Galileo system is intended to be fully operational within a few years [29-32].

### 4.3.2 Code Measurements

In present-day GNSS, each satellite transmits pseudo-random noise codes. These coarse codes are called C/A (coarse/acquisition) codes and are available for civilian use, while precision codes with higher chip rates, which allow more accurate positioning, are called P(Y)-codes and are primarily intended for military use. The receiver generates a copy of the code, which is known, and continuously tries to align it with the code received from the satellite. The internal code's time shift is a measure of the signal's travel time from the satellite. Hence, by multiplying the speed of light with the measured time, the distance to the satellite can be obtained. Measuring the distance to three satellites in this fashion yields a 3-dimensional position. However, a clock offset must be resolved in order to match the receiver's internal clock with the satellite system's time. Ranging towards four different satellites simultaneously provides an unambiguous solution [29-32]. The available resolution of the 30 m P(Y)-code is equal to 30 cm and yields a precision of 1 ns, while the resolution of the 300 m C/A-code is equal to 3 m and yields a precision of 10 ns [32].

### 4.3.3 Carrier Phase Measurements

For even higher precision, the phase of the underlying carrier, with its higher frequency (compared to the code rates), is used instead of or sometimes together with the code. Because the carrier's wavelength is much shorter than the code's wavelength (bit length), resolutions using carrier phase measurements are much more precise than those using code measurements.

When using the carrier phase of the GNSS signal, the number of wavelengths between the satellite and the receiver must be estimated, and every integer of wavelengths will cause an ambiguity. Furthermore, the initial phase ambiguity parameter has to be estimated for each satellite. One solution is to make several measurements that can be assumed to have the same unknown initial cycle ambiguity, and then subtract one from the other. If loss-of-lock has not occurred, sequential measurements will be referred to the same initial carrier phase ambiguity. Based on code measurements, the receiver can calculate an initial phase ambiguity parameter that can be iterated after each new measurement. The carrier phase's short wavelength makes it sensitive to sources of error, and a better estimate to solve ambiguity parameters for the phase is through the support of other receivers in the area. The data from these receivers needs to be differenced in order to resolve all parameters, including 3-dimensional positions, time, all phase ambiguity parameters and receiver clock bias. This is done with long observation periods (several minutes or more), where the data from all receivers is gathered and processed at a later stage. In spite of the fact that developments in software and receiver technology now make it possible to resolve all parameters in real-time, the technique is sensitive and requires that data from other stations be disseminated to the user in real-time.

Maintaining an integer cycle count as the satellite-to-receiver range changes with time is something sophisticated receivers can do in most situations. However, in noisy environments or when the antenna is partly blocked, it might be difficult for the receiver to remain locked to

the signal, and so-called cycle slips can occur. Methods to solve the problems related to carrier phase-based navigation are currently under development in many different applications [29-34].

The resolution when using the carrier phase of the 20 cm carrier is equal to 2 mm and yields a precision that is less than 10 ps [34].

#### 4.3.4 Sources of Error

The accuracy of GNSS positioning is limited by two factors, namely range measurement errors and the satellite-to-user geometry. A summary of common range errors is presented in Table 4.1.

Table 4.1: Products of GNSS range errors [29-34].

<b>Range errors are the products of</b>
<ul style="list-style-type: none"><li>• Uncertainties in the satellite clock bias that is broadcast from the satellite.</li><li>• Uncertainties in the satellite ephemeris.</li><li>• For GPS, the intentional degradation (dithering) enforced by the United States Department of Defense, called Selective Availability (SA). It is associated with the satellite ephemeris and clock. Since May 2, 2000, SA has been discontinued by the U.S. authorities. However, the possibility to degrade the accuracy remains.</li><li>• Imprecision of receiver tracking performance depending on the correlation process.</li><li>• Imprecision of the ionospheric model.</li><li>• Tropospheric effects or models, if used.</li><li>• For time and frequency applications, errors in location, antenna delay, and antenna-cable delay have to be considered. Existence of signal delay variations in the receiver hardware associated with temperature variation near the equipment.</li><li>• Multipath.</li><li>• Signal interference.</li></ul>

### 4.3.5 Time and Frequency Measurement Using Code-Receivers

Many of the receivers that are used for time and frequency applications have an output of 1 pulse per-second (pps) that is related to UTC. These pulses can be used to characterize and calibrate clocks and oscillators. A direct measurement according to this method has the potential to provide an uncertainty of better than 100 ns relative to UTC. The uncertainty for a frequency comparison is approximately  $1 \times 10^{-12}$  for an averaging time of several hours. The uncertainty is limited by the accuracy of the broadcasted satellite position and clocks as well as the signal delay in the atmosphere.

Sometimes this uncertainty is insufficient and there could be a need for comparison of clocks and oscillators against a national reference. A method called common-view (CV), which is illustrated in Fig. 4.3, could be used. CV measurements involve at least two locations that observe the same satellite simultaneously. It is important that the observations are done for one satellite at a time. A subtraction of the data collected at each location and an estimate of the time difference between the clocks in the different locations is obtained. Since the measurements are subtracted from each other most of the common errors such as satellite position and clocks as well as the signal delay in the atmosphere are partly cancelled and dependent on the distance between the locations. The inaccuracy of the satellite's clock is cancelled since it is common for the two locations. Measurement using this method has the potential to provide an uncertainty of better than 5 ns relative to each clock. The uncertainty for a frequency comparison is approximately  $5 \times 10^{-14}$  for averaging times of several hours.

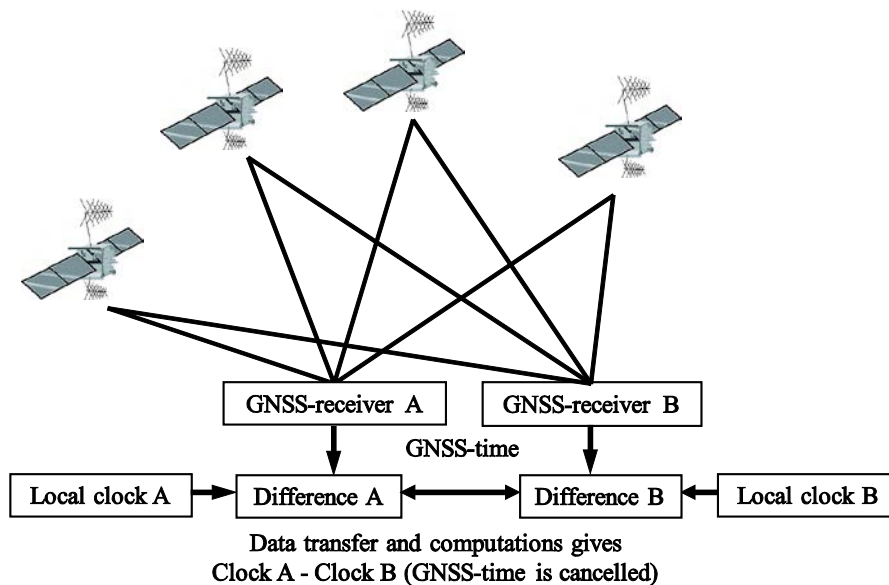


Figure 4.3: Common-view GNSS using carrier phase and C/A code data is one of several methods of using GNSS systems for accurate and precise time transfer. In some processing methods, more than two receivers are normally involved in a network solution.

### 4.3.6 Time and Frequency Measurement Using Carrier Phase-Receivers

Methods that use observable code are not precise enough to characterize the most stable and accurate clocks and oscillators. To improve uncertainty for time comparison with GNSS we need to use more sophisticated receivers that can measure phase changes in the carrier transmitted from the satellites.

This method can provide a precision below 100 ps and a frequency comparison of  $1 \times 10^{-15}$  if the measurements are averaged for several hours up to 24 hours. To obtain this precision, calculation of accurate of the satellites' positions and clocks, as well as the signal delay in the atmosphere, is also required.

One source of error comes from environmental temperature variations that affect the signal delay in the equipment. Absolute time measurements also require an accurate calibration of the constant time delay in the receiver.

## 4.4 Time and Frequency Transfer Utilizing Optical Fiber

The initial parts of section 4.4 manage time and frequency modulated on an optical wave carrier.

The unique characteristic of time, which also complicates its transmission, is that it is ever-changing, and the required information contains both the current time-of-day, (TOD), and how much time has passed since this information was created. For many applications it is sufficient to estimate an approximate delay and accept any variations, but for accuracy that exceeds  $\mu$ s, the transmission time must be constantly estimated or measured and taken into account. The output time  $t_{out}(t)$  from an uncompensated fiber can be described by Eq. (4.6)

$$t_{out}(t) = t_{in}(t) + \tau_{fiber}(t), \quad (4.6)$$

where  $t_{in}$  is the time information from the transmitter clock, and  $\tau_{fiber}(t)$  is the variable delay through the fiber. For increased accuracy, the equation can be elaborated to:

$$t_{out}(t) = t_{in}(t) + \tau_{fiber,0} + \tau_{fiber,det}(t) + \tau_{fiber,rand}(t), \quad (4.7)$$

where  $\tau_{fiber,0}$  is the delay through the fiber at  $t=0$ ,  $\tau_{fiber,det}(t)$  includes any delay variations that can be determined, and  $\tau_{fiber,rand}(t)$  are the remaining, random variations in transfer delay. The main effort in any time transfer is to minimize the undetermined variations in the delay, through complementary measurements to the actual signal transfer.

### 4.4.1 Transfer of Microwave Frequency in an Optical Fiber

While time transfer accuracy is compensated for the actual difference in optical path lengths, stability in both time and frequency transfers is sensitive to how rapidly the delay changes. The output frequency of an uncompensated fiber is described by the equation:

$$f_{out}(t) = f_{in}(t) + \frac{d\varphi(t)}{dt} \quad (4.8)$$

where  $f_{in}(t)$  and  $f_{out}(t)$  are the momentaneous input and output frequencies, respectively, and  $\tau(t)$  is the varying time-delay through the fiber. The derivative  $d\varphi(t)/dt$  arises from the change in  $\tau(t)$  with respect to the period of the microwave frequency, such that

$$\frac{d\varphi(t)}{dt} = 2\pi f_{in}(t) \frac{d\tau(t)}{dt}. \quad (4.9)$$

When a fiber link is used to transfer a microwave frequency modulated on top of an optical carrier, this variation will be more notable over long distances or if the fiber is installed in a harsh environment (open air, sunlit roof, etc.). A two-way frequency transfer will then be implemented schematically as shown in Fig. 4.4. The control equipment adjusts the input signal to the transmitted and returned signals' phase modulator to cancel out the total phase variation after a round-trip in the fiber link.

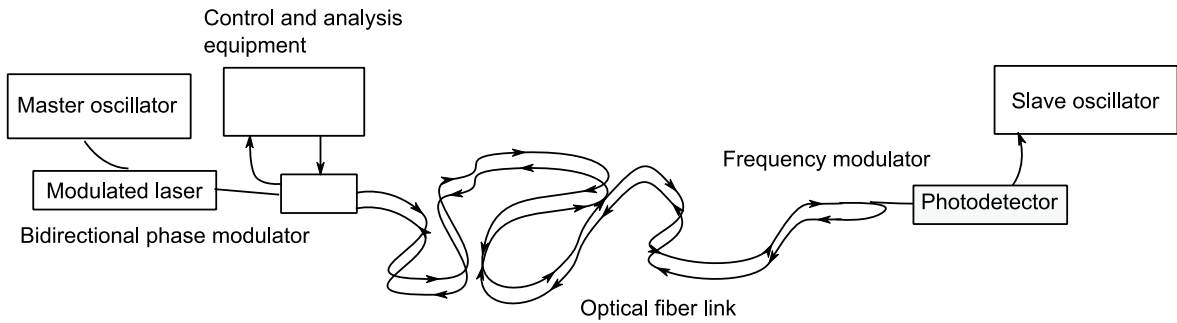


Figure 4.4: Schematic diagram of frequency transfer in microwave domain. A two-way frequency transfer will be implemented schematically as shown. The control equipment adjusts the input signal to the transmitted and returned signals' phase modulator to cancel out the total phase variation after a round-trip in the fiber link.

#### 4.4.2 Time Transfer Using Insertion Technique

Research regarding time and frequency transfer that actively influences existing data transmissions, or inserting specific timing data, has been presented earlier [22-23] and is still a research area with vast potential regarding Institute of Electrical and Electronics Engineers 1588 (IEEE1588) [35], White rabbit [36-37], NTP [28] and other internet protocols.

During the past decade, many timing laboratories have invested money and research into optical clocks and frequency combs. The most common high-performance time and frequency transfer methods use TWSTFT and GPS, but fiber based methods are the ones that can compare optical clocks with each other with sufficient accuracy and stability. A major drawback with fiber based methods is that they often require dedicated fiber in order to achieve the best performance, they are expensive to maintain and several locations with optical clocks are not connected to each other via fiber.

Since the performance of TWSTF and GPS is not sufficient to be utilized for time and frequency transfer between optical clocks, the time and frequency community has been researching fiber optical connections and methods.

The greater part of research into active fiber time transfer has followed two major directions: the first one uses existing networks with active influences, while the second one uses the transfer of coherent light and makes measurements on the optical phase. The results

from optical phase measurements have shown that this technique produces solid performance in relation to optical clocks. The best performance using active techniques is achieved when the fiber path that is used between the sites is known. Since these sites can be far apart (hundreds of km) operating using a duplex fiber path over such a distance would be expensive. Due to the cost and inaccessibility of these networks, research has been carried out on how to implement such time and frequency transfer systems in commercial, fiber based WDM networks [24].

### 4.4.3 Optical Comb

One key innovation for optical frequency transfer, as well as for other techniques, is the optical comb. By generating short optical pulses with a constant repetition rate, the corresponding spectrum will form a comb of equidistant peaks. T. Hänsch and J. Hall managed to broaden this spectrum to exceed one octave of optical tones, thus enabling new measurements [38-39].

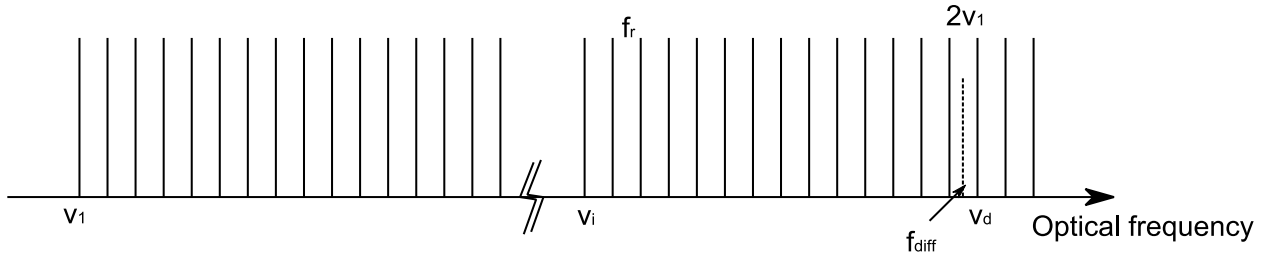


Figure 4.5: Schematic diagram of optical comb spectrum spanning one octave. If one of the lowest frequencies in the spectrum,  $\nu_1$ , is doubled, it will create a new frequency,  $2\nu_1$ , close to one of the highest frequencies in the comb,  $\nu_d$ . Since the difference between these two frequencies is measurable, every optical frequency in the comb can be determined with the comparable accuracy of a microwave frequency. With the parameters  $f_r$  and  $f_{diff}$  describing the repetition frequency of the pulses that create the comb, and the measured frequency difference between  $2\nu_1$  and  $\nu_d$ , respectively can be used to determine an arbitrary optical frequency,  $\nu_i$ .

If one of the lowest frequencies in the spectrum,  $\nu_1$ , is doubled, it will create a new frequency,  $2\nu_1$ , close to one of the highest frequencies in the comb,  $\nu_d$ . Since the difference between these two frequencies is measurable, every optical frequency in the comb can be determined with the comparable accuracy of a microwave frequency. Using the parameters  $f_r$  and  $f_{diff}$  that describe the repetition frequency of the pulses that create the comb, and the measured frequency difference between  $2\nu_1$  and  $\nu_d$ , respectively, Eq. (4.10) and (4.11) can be used to determine an arbitrary optical frequency,  $\nu_i$ . This is illustrated in Fig. 4.5 that presents a comb structure of the optical spectrum.

$$\nu_i = \nu_1 + N_i f_r \cdot \quad (4.10)$$

$$\nu_1 = N_d f_r + f_{diff} \cdot \quad (4.11)$$

#### 4.4.4 Optical Frequency Transfer

For comparisons of two optical clocks at different locations, optical frequency transfer over fiber is an option. Figure 4.6 shows the basic technique, but does not cover all the details. The technique can be described as follows: The optical clock *A* emits a wavelength that corresponds to the atom or ion in use, usually not within the telecommunication bands. Therefore, an ultra-stable wavelength at approximately 1550 nm is also created in lab *A*. Through an optical comb, the frequency relationship between these two wavelengths can be determined.

Light from an ultra-stable laser is launched through an optical frequency modulator (usually an acousto-optical modulator) and transferred through the fiber to lab *B*, where another frequency modulator is passed. A semi-reflecting mirror (the Fresnel reflection of the glass-air interface is often sufficient) lets the light return along the same path. After its return to lab *A*, the received signal is compared with the transmitted one and the modulation is adjusted to counteract any fiber-induced phase variations. The modulator in lab *B* is used to offset the return signal, since scattering effects in the fiber will deteriorate the signal if it is sent at the same wavelength in both directions.

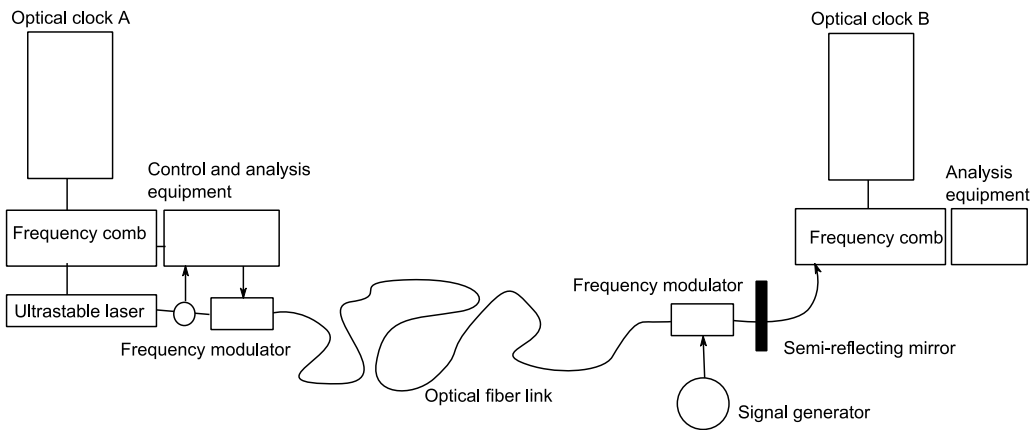


Figure 4.6: Schematic setup for optical frequency transfer. The optical clock *A* emits a wavelength that corresponds to the atom or ion in use. An ultra-stable wavelength at approximately 1550 nm is created at lab *A*. Through an optical comb, the frequency relationship between these two wavelengths can be determined. Light from an ultra-stable laser is launched through an optical frequency modulator and transferred through the fiber to lab *B*, where another frequency modulator is passed. A semi-reflecting mirror lets the light return along the same path. After its return, the received signal is compared with the transmitted one and the modulation is adjusted to counteract any fiber-induced phase variations. The modulator in lab *B* is used to offset the return signal, since scattering effects in the fiber will deteriorate the signal if it is sent at the same wavelength in both directions.

Finally, the light arriving at lab *B* is stable with respect to variations in the fiber, and can, by using another optical comb, be compared with the light emitted from Optical clock *B*. Since all of these comparisons must be performed through analog signal interference in the optical domain, the ultra-stable frequency transfer must be performed in real-time and any perturbations in the fiber must be corrected on the fly. It is also significant that where a microwave frequency can be transferred between two labs through a fiber pair, with the

addition of an increased uncertainty, optical frequency transfer can be performed through a bi-directional two-way transfer in a single fiber and gain performance.

Several groups have reported successful experiments connecting labs with optical clocks via optical frequency transfers over distances of up to 920 km [40-46].

## Chapter 5

# Evaluated Techniques for Time and Frequency Transfers

The work presented in this thesis is based on two kinds of optical time and frequency transmissions. The first technique that is presented in this chapter is a non-insertion method, utilizing existing commercial synchronous optical network/synchronous digital hierarchy (SONET/SDH) transmission lines in a passive sense, while the second technique that was developed utilizes the transmission of two modulated wavelengths in one direction, after which they are comparatively evaluated in order to define a correction algorithm.

The previous chapters in this thesis have provided background information about the theories or equipment used in either fiber based time and frequency transfer techniques or GNSS used as a reference system. This chapter's objectives are to explain the non-insertion time and frequency transfer technology and the one-way technique that was developed during this research.

### 5.1 Applied Two-Way Time and Frequency Transfer

A method for time and frequency transfer by monitoring the bit data that is being transmitted in an optical fiber has been the subject of research and development by the SP since 2004. This method is applicable to any synchronous transmission network, but has so far only been studied in a network based on SDH transmission using packets via SONET/SDH STM-64. Unlike active fiber based methods, this method is based on a non-insertion technology that listens to existing data frames in a fiber optical network in a passive sense and does not require any particular bandwidth. As described later in this thesis, this method only needs an indirect connection to divert a limited amount of the optical signal to the measuring equipment.

The objective of the presented work was to use existing infrastructure, find an alternative and complementary method to already established satellite-based methods such as GNSS, including, among others, GPS and TWSTFT, with the aim of achieving methods with comparable accuracy and stability.

#### 5.1.1 Non-Insertion Technique

Alternative technologies to the non-insertion technique are found in section 4.4.2.

The developed fiber based time transfer technique that is presented in this section is [A-E, 47], with minor adjustments, applicable to any packet-based data transmission network. It utilizes the data bits in standardized protocols, without inserting any additional data. Due to conditions in the supporting network, the technique was developed for use with SDH as the physical layer, using an synchronous transport module 64 (STM-64) bit-rate corresponding to 9,953 Mbit/s. SDH defines the transmission of data packets in nominally 125  $\mu$ s long frames, where each frame starts with the identical sequence of A1 and A2 bytes that defines the beginning of a new frame (A1=11110110, A2=00101000). The A1A2 sequence was chosen since its occurrence elsewhere in the bit stream is unlikely; therefore, it can be used as a reference marker to detect the start of a new frame. At STM-64, this sequence is 192 A1 bytes followed by 192 A2 bytes. In the time transfer setup, the reference marker is an electrical pulse generated at detection of a full A1A2 sequence. For successful time and frequency transfer, this operation must be performed both at the bit stream leaving the connection as well as the bit stream arriving at the connection, i.e. in a two-way sense. The fundamental concept is the registration of the time when this frame-start sequence is transmitted from a connection

in the network, together with the time when the same sequence arrives at the receiving connection. Both time stamps are relative to the local clock at each node, and an initial calibration of the transit time in both directions is required for a time transfer.

### **5.1.1.1 Backbone Fiber Network used for Non-Insertion Two-Way Technique**

Sweden has geographically widespread backbone fiber networks and they were a natural choice to use as a test bed for the purposes of this research. Several experiments were performed in OptoSUNET which is operated by the SUNET. OptoSUNET is configured with a star topology, with a hub in Stockholm and supports the use of SDH. The next sub-section contains an introduction to the SDH/SONET frame structure that is used by the non-insertion time transfer technique. Appendix D provides more information about OptoSUNET and its configuration.

In the beginning of fiber optic communication systems, there was no underlying digital format that supported transfers with high bit rates. All previous standards were developed with the lower bit rate requirements of copper transmissions in mind.

American National Standards Institute (ANSI) and Bellcore began to develop a new digital format standard specially designed for high bit rates in fiber optic networks. They named this standard synchronous optical network (SONET).

This standardization work resulted in two standards: SONET and the synchronous digital hierarchy (SDH) [48]. These formats are optimized for voice operation with 125  $\mu$ s frames and were developed to replace the plesiochronous digital hierarchy (PDH) system for transporting large numbers of telephone calls and data traffic over the same fiber connection without synchronization problems. Both SONET and SDH commonly carry PDH formats such as DS1 (Digital system 1) and E1 (European format for digital transmission), as well as ATM (Asynchronous transfer mode) cells [49].

#### **5.1.1.1.1 SONET**

The SONET standard defines the features and functionality of a transport system based on the principles of synchronous multiplexing. This means that individual participating signals may be multiplexed directly into a higher-rate SONET signal, without intermediate stages of multiplexing. SONET's signal structure allocates 5% to supporting such management and maintenance procedures and practices. This means that SONET can be deployed on top of existing networks and, where appropriate, provide enhanced network flexibility by transporting existing signal types. SONET can carry any octet-based binary format such as transmission control protocol/internet protocol (TCP/IP) [49].

##### **5.1.1.1.1.1 Synchronous Signal Structure**

SONET is based on a synchronous signal comprised of an octet-sequence, which is organized into a frame structure. One way to represent this frame is with a two-dimensional map containing  $N$  rows and  $M$  columns. Each box in this map contains one octet, or byte. The upper left corner of each frame contains an identification marker which has the task of telling the receiver the start of the frame. SONET consists of a first-level structure called synchronous transport signal 1 (STS-1). The STS-1 definition supports 51.84 Mbps and also defines the entire hierarchy of SONET signals, since higher-level SONET signals are obtained by synchronously multiplexing the lower-level modules. Lower-level modules that have been multiplexed together are denoted STS- $N$ , where  $N$  is an integer. The resulting format can then

be converted into an optical carrier  $N$  (OC- $N$ ) or STS- $N$  electrical signal. There is an integer multiple of relationships between the rate of the basic module STS-1 and OC- $N$  electrical signals. Only OC-1, -3, -12, -24, -48 and -192 are presently supported by SONET [49].

#### 5.1.1.1.2 SONET Building Block Structure

Synchronous Transport Signal one (STS-1) is SONET’s basic module and building block. It is a specific sequence of 810 octets (6,480 bits), which includes overhead octets and an envelope capacity for transporting payloads. STS-1, which is illustrated in Fig. 5.1, is depicted as a 90-column, 9-row structure, with a frame period of 125 $\mu$ s (i.e. 8,000 frames per second). The order of transmission is row by row, from left to right [49].

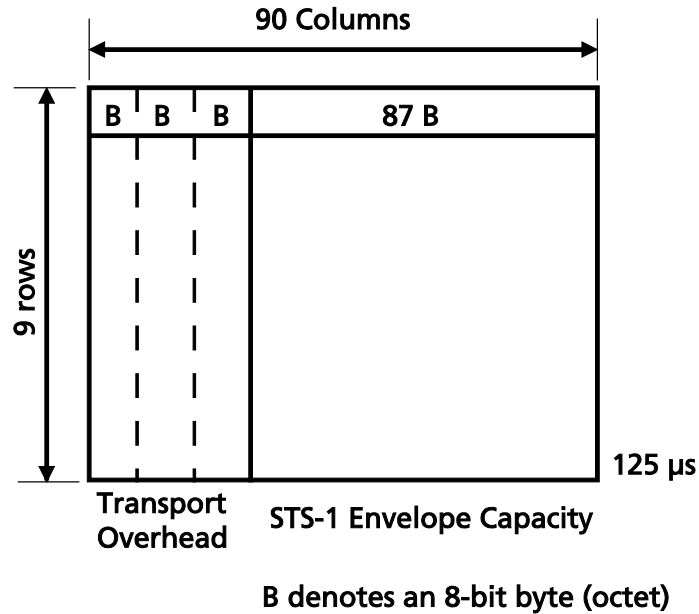


Figure 5.1: STS-1 is depicted as a 90-column, 9-row structure, with a frame period of 125 $\mu$ s. The order of transmission is row by row, from left to right [49].

#### 5.1.1.1.2 SDH

SDH was developed in Europe, whereas SONET was developed in North America. They are quite similar, but one difference is their initial line rate. STS-1/OC-1 (optical carrier one) has an initial line rate of 51.84 Mbps, whereas SDH level 1 has a line rate of 155.520 Mbps. These rates are the building blocks of each system. SONET STS-3/OC-3 is equal to SDH STM-1 (Table 5.1).

Table 5.1 shows SDH standard bit rates. ITU-T Rec. G.707 states that “the first level digital hierarchy shall be 155,520 kbps” and “higher synchronous digital hierarchy bit rates shall be obtained as integer multiples of the first level bit rate...”[48].

Table 5.1: SDH Bit Rates with SONET equivalents

SDH Level	SDH Bit Rate (kbps)	SONET Equivalent Line Rates
1	155,520	STS-3/OC-3
4	622,080	STS-12/OC-12
16	2,488,320	STS-48/OC-48

#### 5.1.1.1.2.1 Synchronous Transport Module (STM)

STM is the information structure used to support section layer connections in SDH. It is analogous to STS in SONET. STM consists of information payload and section overhead (SOH) information fields organized in a block frame structure (Fig. 5.2).

Section 5.1.1 Non-Insertion Technique describes how the SDH frame is used for time stamping. This same information is partly repeated below in order to place it in context with the rest of the frame.

SDH defines the transmission of data packets in nominally 125  $\mu$ s long frames, where each frame starts with the identical sequence of A1 and A2 bytes that defines the beginning of a new frame (A1=11110110, A2=00101000) [49].

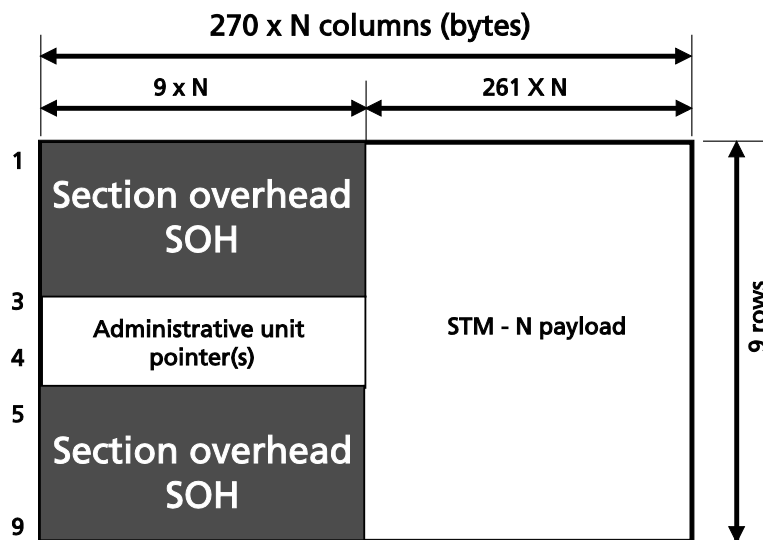


Figure 5.2: An STM-N frame structure. STM is the information structure used to support section layer connections in SDH. STM consists of information payload and section overhead (SOH) information fields, organized in a block frame structure [49].

### 5.1.1.2 Proposed Procedure for Non-Insertion Technique

Figure 5.3 illustrates the time transfer method utilizing a non-insertion technology between two nodes, *A* and *B*, in a network.

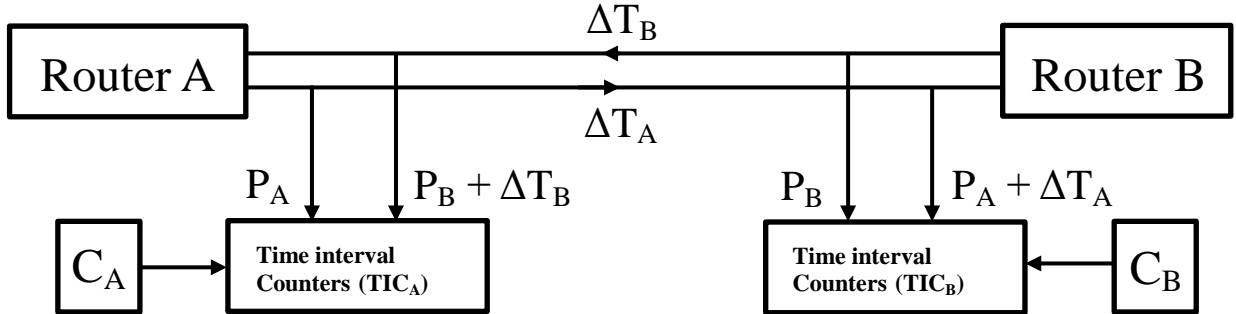


Figure 5.3: Schematic diagram of a one-way time and frequency transfer from node *A* to node *B*.  $\Delta C_{AA}$  is a time interval that is established through a comparison between pulse  $C_A$ , which is generated at clock *A*, and pulse  $P_A$ , which is generated from the frame. The frame generation is referenced in time and frequency to the local oscillator in router *A*.  $\Delta C_{BA}$  is the time interval between  $P_A$  arriving at node *B* compared to  $C_B$  generated at clock *B*, plus the propagation time from node *A* to node *B* ( $\Delta T_A$ ). The influence of  $\Delta T_A$  is minimized by performing a one-way time transfer from node *B* to node *A*, and introducing  $\Delta T_B$ .

$$\Delta C_{AA} = C_A - P_A. \quad (5.1)$$

$$\Delta C_{BA} = C_B - (P_A + \Delta T_A). \quad (5.2)$$

$$\Delta C_{AB} = C_A - (P_B + \Delta T_B). \quad (5.3)$$

$$\Delta C_{BB} = C_B - P_B. \quad (5.4)$$

One-way time and frequency transfer from node *A* to node *B* is described in Eq. (5.1) and (5.2).  $\Delta C_{AA}$  is a time interval that is established through a comparison between pulse  $C_A$ , which is generated at clock *A*, and pulse  $P_A$ , which is generated from the frame. The frame generation is referenced in time and frequency to the local oscillator in router *A*.  $\Delta C_{BA}$  is the time interval between  $P_A$  arriving at node *B* compared to  $C_B$  generated at clock *B*, plus the propagation time from node *A* to node *B* ( $\Delta T_A$ ). The influence of  $\Delta T_A$  is minimized by performing a one-way time transfer from node *B* to node *A* (5.3), (5.4).  $\Delta C_{BB}$  is a time interval that is established through a comparison between pulse  $C_B$ , which is generated at clock *B*, and pulse  $P_B$ , which is generated from the frame. In this path, the frame generation is accordingly referenced to the local oscillator in router *B*.  $\Delta C_{AB}$  is the time interval between  $P_B$  when it arrives at node *A* compared to  $C_A$ , which is generated at clock *A*, plus the propagation time from node *A* to node *B* ( $\Delta T_B$ ).

$$(C_A - C_B) = ((\Delta C_{AA} - \Delta C_{BA}) + (\Delta C_{AB} - \Delta C_{BB}) - F(t)) / 2. \quad (5.5)$$

The clock comparison in Eq. (5.5) is the result of combining Eq. (5.1) to (5.4), including an asymmetry factor,  $F(t)$ , that takes parameters such as differential path delay and local equipment delays into account. As in all two-way methods, this method relies on the stability of  $F(t)$  over time, and that a constant part of  $F(t)$  can be calibrated and compensated.

The method illustrated in Fig. 5.3 is very similar to the simple method illustrated in Fig. 4.2. The difference is that all measurements are carried out relative to the router oscillators, which is mandatory for this non-insertion mode. These router clocks are used as reference “beacons”, not very different from the satellite clocks in GNSS-based time transfer methods.

### 5.1.1.3 Experimental Implementation

In an implementation of the non-insertion technique, each fiber is equipped with two passive fiber-optic power splitters. At the transmitter, where the power level is high, 1% of the light is connected to the time analysis circuits and measurement system, while at the receiving end, where the power level is low, 10% is diverted to the circuits and measurement system. This additional  $-0.5$  dB loss from the fiber transmission will decrease the system’s power margin, but it is made using the assumption that all systems are implemented with a far higher margin. Several experiments performed during the progress of this research have validated that assumption.

In the case of a two-way time transfer, equipment is connected to all fiber ends of the incoming and outgoing traffic in order to generate measurable pulses. All pulses are compared to local clocks using a TIC, and the measured time-interval data exchange will be used to evaluate the two-way time transfer. The experiment setup is illustrated in detail in Fig. 5.4. Each clock is connected to two distribution circuits at 5 MHz and 1 pps. The 5 MHz frequency is used as the time base for the TICs, while 1 pps is used for the reference pulse from the clock that starts the time interval measurement. The set of boxes connected to both ends of each fiber consists of a photo-receiver that transforms the signal to the electrical domain, a Header Recognizer (HR) that analyzes the bit stream and emits a pulse once a frame-start is detected, and a TIC to measure the time interval between the pulses and the local reference clock.

In the beginning of the research with the non-insertion technique, the equipment was set up as in Fig. 5.4. The most recent experiments include the same components as in Fig. 5.4, but have been adapted to fit in a 19-inch rack that is 2 units high and named TTU (Time Transfer Unit).

The photo-receiver is a 10 GHz avalanche photodiode (APD) with an integrated trans-impedance amplifier (TIA). Its sensitivity is as good as, or up to 10 times better than, the sensitivity of the receivers in the router. Since the system can operate at very low power margins, the available 10% power is sufficient. The HR is the device that continuously analyzes the bit stream transmitted via the fiber. At 10 Gbit/s, it searches for the previously described bit sequence that defines the start of a new frame. Every time this sequence is detected, the HR emits a 25 ns pulse with a sharp slope (25 ps rise-time). The HR is based on a Field Programmable Gate Array (FPGA) platform in combination with 10 Gbit/s input and output circuits. For the described system, commercial TICs with a resolution of 100 ps are used. In order to evaluate system performance, a GPS link based on the carrier phase observables is used. Figure 5.4 illustrates an example setup between two nodes for an experiment with the fiber time transfer link, with a GPS carrier phase (GPSCP) link for comparison and evaluation.

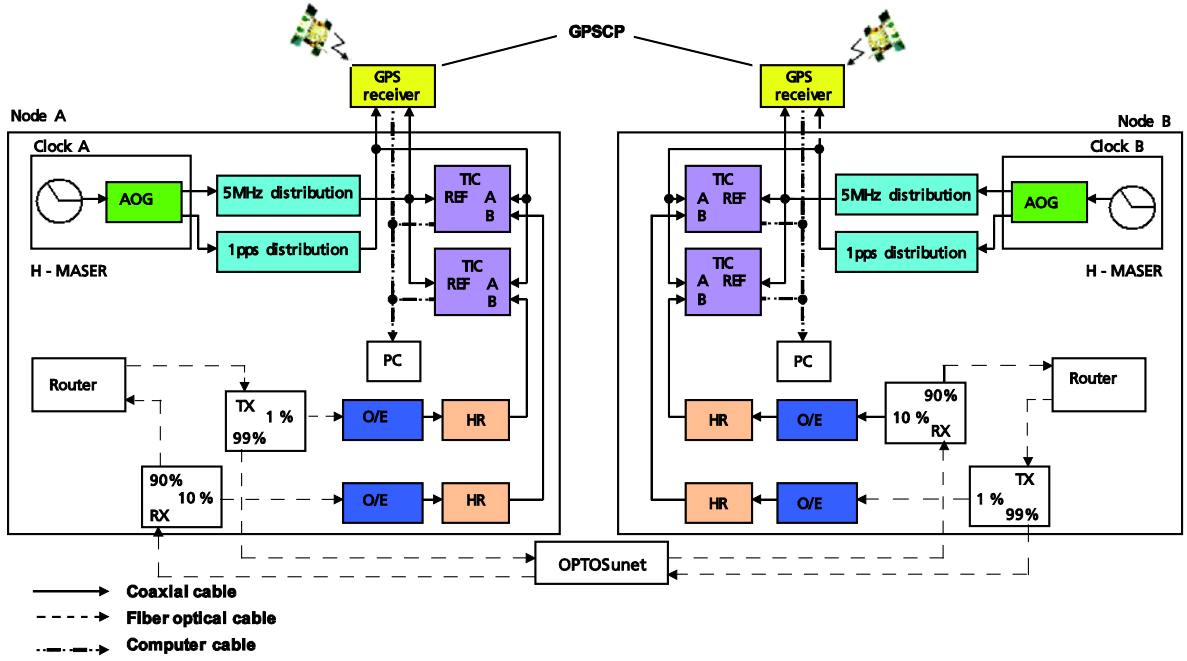


Figure 5.4: Example setup between two nodes for an experiment with the fiber time transfer link, with a GPS carrier phase link for comparison and evaluation. Several more nodes can be introduced. Also bridging nodes are recommended for comparisons over several paths.

### 5.1.1.4 Error and Degradation Modeling

In order to model the error sources, a time transfer between two nodes  $A$  and  $B$  must be carried out and the results collected by the four TICs:  $\Delta C_{AA}$ ,  $\Delta C_{BA}$ ,  $\Delta C_{AB}$ , and  $\Delta C_{BB}$ . This can be expressed as:

$$\Delta C_{AA} = C_A - (P_A + r_1). \quad (5.6)$$

$$\Delta C_{BA} = C_B - (P_A + T_1 + r_2). \quad (5.7)$$

$$\Delta C_{AB} = C_A - (P_B + T_2 + r_3). \quad (5.8)$$

$$\Delta C_{BB} = C_B - (P_B + r_4). \quad (5.9)$$

where  $C_A - C_B$  is the sought time difference between the clocks. Equations (5.6) through (5.9) are expansions of Eq. (5.1) to (5.4), where the term  $r_x$  [ $x=1,2,3,4$ ] represents the limitations in the resolution of the TICs at each node [50].  $P_A$  and  $P_B$  are the pulses that are generated at the respective nodes when a frame is detected.  $T_1$  and  $T_2$  represent the path delays, i.e. the propagation time from node  $A$  to node  $B$  and from node  $B$  to node  $A$ , respectively. The time difference between the clocks can now be written as

$$\alpha = (C_A - C_B) = ((\Delta C_{AA} - \Delta C_{BA}) + (\Delta C_{AB} - \Delta C_{BB}) - (r_1 + r_3) + (r_2 + r_4) + (T_1 - T_2)) / 2. \quad (5.10)$$

The variance of the error in the estimate is then

$$\sigma_{\hat{\alpha}}^2 = \text{Var}[\alpha - \hat{\alpha}] = \text{Var}\left[\frac{1}{2}(r_2 + r_4 - r_1 - r_3) + \frac{1}{2}(T_1 - T_2)\right]. \quad (5.11)$$

An assumption is made that the four TIC measurements are uncorrelated and with identical variance,  $\sigma_r^2$ . It is also assumed that they are uncorrelated with the path delays  $\sigma_F^2$ . Hence, this can be written as

$$\sigma_{\hat{\alpha}}^2 = \sigma_r^2 + \frac{1}{4}\sigma_F^2. \quad (5.12)$$

where

$$\sigma_F^2 = \text{Var}[T_1 - T_2]. \quad (5.13)$$

For time transfer with several nodes, the fact that every specific fiber link is asynchronous to all the other links must be taken into consideration. Because of this, bridge nodes must be used when connecting two or more links. Bridge nodes use the same clock for two links and can therefore “bridge” two asynchronous links.  $N$  represents the total sum of nodes in the link between two clocks, i.e.  $N = 2$  when no bridge routers are present. By assuming that the error contributions are uncorrelated we obtain

$$\sigma_{\alpha_n} = \sqrt{N-1} \cdot \sigma_{\hat{\alpha}} \quad N \geq 2. \quad (5.14)$$

$$\sigma_{\alpha_n}^2 = (N-1) \left( \frac{\sigma_r^2}{R} + \frac{1}{4}\sigma_F^2 \right) \quad (5.15)$$

From the previous equations, we note that the variance of the measured time difference between two clocks separated by  $N$  nodes can be written as Eq. (5.15).

Factors that contribute to the measurement’s uncertainty can be divided into two major categories: short-term variations,  $\sigma_r$ , due to measurement noise, and environmental long-term variations,  $\sigma_F$ . The environmental long-term variations can be divided into fiber path variations,  $\sigma_{Ff}$ , and system component variations,  $\sigma_{Fc}$ . The total length difference is fixed and can be eliminated through calibration, but any local variations, such as temperature in individual stations, can have a notable influence on the time transfer. Variations due to polarization mode dispersion (PMD) will also be introduced, as an asymmetry in the fiber path  $\sigma_{Fpath}$ . Hence, the final version of Eq. (5.15) is written as

$$\sigma_{\alpha_n}^2 = (N-1) \left( \frac{\sigma_r^2}{R} + \frac{1}{4}(\sigma_{Ff}^2 + \sigma_{Fpath}^2 + \sigma_{Fc}^2) \right). \quad (5.16)$$

#### 5.1.1.4.1 The Router Oscillator and its Influence on the Non-Insertion Technique

The transmission from a router is synchronized to a local oscillator, which is an oven-controlled crystal oscillator (OCXO). The jitter introduced by the oscillator's frequency offset and stability used for SONET/SDH framing affect the performance of the time and frequency transfer. This jitter is not significant in the present measurements; however, router oscillators could become a limiting component in systems with better time resolution as well as in the other equipment such as the TIC.

SDH/SONET was designed so that all clocks are synchronized and traceable to UTC in accordance with ITU-T G.821. When operating IP routers over fiber optic systems, no synchronization is required since the entire payload is terminated and the payload data, i.e. IP packets, is transferred to the next link using a store-and-forward model.

The frequency stability requirement is set by the lock range of the WDM transponders that operate down to SDH Stratum 4, (20 ppm), and the jitter is specified up to 30 ps. Stratum is a layer hierarchy, where lower numbers within the hierarchy are more accurate than higher Stratum numbers. Most high-end IP routers implement the clock by using a local SDH Stratum 3E OCXO. Stratum 3E is a standard that was created to meet SONET equipment requirements. Stratum 3E tracks input signals to within 7.1 Hz of 1.544 MHz from a Stratum 3 or better source. The relative frequency drift with no input reference is less than  $1 \times 10^{-8}$  in 24 hours. This equals less than four frame slips in 24 hours, compared to 255 slips for Stratum 3 [51]. The local clock of each router is used to clock the transmitter.

The frequency and stability of the clock source for the SDH/SONET framing do not significantly affect time transfer performance due to the short measurement time in the system.

#### 5.1.1.4.2 Influence of Fiber Nonlinearities

Since the two-way transfer is performed using two parallel fibers, the asymmetry error must be determined. Constant asymmetries, e.g. different fiber lengths and different transmission wavelengths, can be compensated for in the implementation algorithm. Dynamic changes, however, must be minimized due to the difficulty of including their absolute influence in the model. The main dynamic changes that have been identified are the influences from PMD and cross phase modulation (XPM).

PMD is the differential dispersion between two polarizations. PMD will mainly be an influence if its values are high, and the transmitted signal goes from one polarization to the orthogonal state (or, alternatively, the PMD induces a similar change in velocity). The influence of PMD in the present system is estimated in Paper D to be less than 20 ps.

XPM will cause a phase change due to the power in adjacent channels, and this asymmetry occurs when the WDM system transmits the maximum number of channels in one direction, but only one in the returning direction. Assuming a maximum channel power of 100mW exiting each amplifier, and a maximum of 100 channels (resulting in the high, but not impossible, power level 10W). Furthermore, the system contains 10 sections, each of which exceeds the effective length  $L_{eff}$ . In Eq. (5.17), the length  $L$  is set to be equal to  $L_A$ , the amplifier spacing.

$$L_{eff} = L[1 - e(-\alpha L_A)]/(\alpha L_A) = (1 - e(-\alpha L_A))/\alpha \quad (5.17)$$

In Eq. (5.17) and Eq. (5.18) are various nonlinear effects occurring within the fiber included in the  $\gamma$  parameter.

$$\gamma = \frac{2\pi n_2}{\lambda_0 A_{eff}} \quad (5.18)$$

The maximum phase shift is [52]

$$\tau_j = N\gamma L_{eff} (P_j + 2\sum_{m \neq j}^M P_m) \quad (5.19)$$

Using the values of  $n_2 = 3.2 \times 10^{-16} \text{ cm}^2 / \text{W}$ ,  $\alpha = 0.2 \text{ dB / km}$  and  $A_{eff}$  for G.652 this phase shift will induce a time delay of less than 100 ps. This will also be the asymmetry when nothing is induced in the opposite direction.

The XPM-induced phase shift arises from the average power of 99 channels in a dispersive fiber that is not fully compensated. The crosstalk and chirp that occurs when few channels co-propagate will be blurred from averaging and not visible. Any frequency shift, which would cause a changed group velocity due to dispersion, is therefore neglected.

### 5.1.2 Results and Conclusions of the Two-Way Non-Insertion Technique

The feasibility of performing a two-way time and frequency transfer by exploiting a repetitive design of the well-established optical network communication structure has been experimentally verified.

The structure utilized to extract data for time and frequency transfer in a non-insertive and passive sense is called synchronous digital hierarchy, SDH.

Development has evolved from theory and modeling to prototypes and demonstration units and has included several experiments using varying baselines, from a few kilometers to 1,100 km.

The initial experiment compared two clocks, a Cesium clock and a Rubidium clock, and the results are presented in Paper A.

Common for all evaluations of the proposed technology is that the GPS carrier phase has been the only available option for validation of the technique, as several baselines have been extensive.

After a successful first verification of the theory, the length of the baseline was increased to over 500 km, including several km of airborne fiber transmission. This raised some new questions about the error sources in the technique. The evaluations of these error sources have been carried out in several stages and are presented in Papers B, C and D. A major conclusion from these evaluations is that most of the components in the amplifier stations along the transmission paths are temperature-sensitive and produce asymmetries. These phenomena are uncorrelated, which indicates that the temperature should be monitored at these sites and be included in a mathematical correction algorithm to achieve the best accuracy.

The conclusions from the most recent evaluation are presented in Paper E which describes a 1,129 km long fiber connection between two national time scales UTC(SP) and UTC(MIKE). An interesting fact about this connection is that about half of the fiber distance is located in a stable temperature environment (water), as can be seen in the time transfer results. The rest of the connection shows previously proven sensitivity to daily temperature variations. These variations are not corrected by any mathematical algorithm mentioned in Paper D.

Regardless of any evaluation or configuration for this technique, all results present an RMS precision relative to the GPS carrier phase of <1 ns.

## 5.2 Applied One-Way Fiber Based Frequency Transfer

In the beginning of Chapter 4 the basic theories for one-way time and frequency transfer are discussed, including a simple schematic diagram (Fig. 4.1). This section presents how these theories can be applied to the performance of a one-way time and frequency transfer.

When the fiber's surrounding temperature varies, it affects both transit times and the dispersion, which can be measured at the receiving end of the fiber. Since there is an unambiguous relationship between these two parameters, the correlation between them can be used to deduce one from the other. The measurement technique for fiber dispersion is well known [53] and the variation with respect to temperature has been studied previously [54-55]. These attributes are utilized in the one-way time and frequency transfer, while the scale coefficient for a specific fiber link must be individually characterized.

In a fully operational solution, the time from the Master oscillator is distributed to a Slave oscillator with a precision that exceeds what it would be in the case of a single transmitted signal. The system is described schematically in Fig. 5.5.

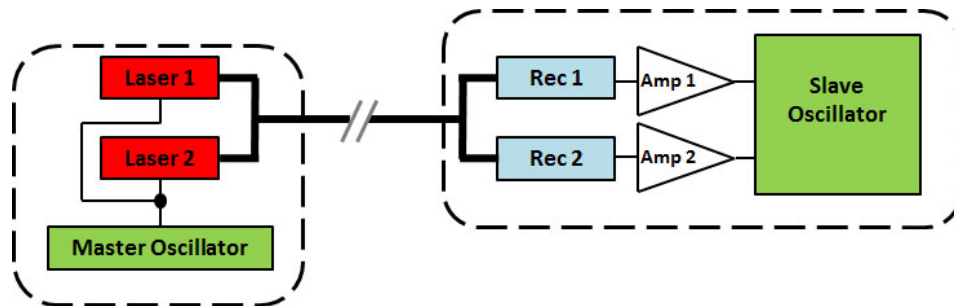


Figure 5.5: Schematic system diagram of one-way fiber based time and frequency transfer setup. The transmitter includes a master oscillator and two lasers connected through a fiber to the receiver side. The receiver side includes “filters” for wavelength separation, detectors and amplifiers before a connection to the slave oscillator.

At the transmitting end, a master oscillator controls two lasers and a slave oscillator interprets the two signals at the receiving end. To enhance precision, these signals are transmitted over two wavelengths. The thin and thick lines are electrical cables and optical fibers, respectively, while the open line on top symbolizes the outdoor transmission fiber of arbitrary length and the dash-encompassed regions indicate indoor environments.

### 5.2.1 Dispersion Theory

The one-way dual wavelength frequency transfer technique is based on dispersion in optical single-mode fiber and how it relates to a signal's transit time through that fiber. The intention with this technique is to create a compensation algorithm for variable propagation delays.

Dispersion in SMF is divided into two main quantities: chromatic and polarization mode dispersion (PMD).

### 5.2.1.1 Chromatic Dispersion

Chromatic dispersion,  $D_C$ , is the sum of material dispersion,  $D_M$ , and waveguide dispersion,  $D_W$ . Material dispersion arises out of the variation of refractive index with wavelength, while waveguide dispersion arises out of the fiber's waveguide properties' dependence on wavelength. A similar analysis has been presented previously [56] and assumes the dispersion slope is not dependent on temperature and that all variations can be linearly scaled from the change in zero-dispersion wavelength. Our model, however, is based on the simplified Sellmeier equations for material dispersion and a step-index fiber's waveguide properties for waveguide dispersion, as well as the influence of temperature on these.

#### 5.2.1.1.1 Material Dispersion

The group delay is the time delay per unit length  $L$  of a medium, which is the basis of the technique that uses two wavelengths in an optical fiber to determine changes in the dispersion along the medium's length. It is possible to determine the group delay as a function of wavelength and refractive index in an arbitrary optical medium where the refractive index itself is a function of wavelength. When applied on an optical fiber core with the refractive index  $n_l$ , the group delay, in terms of measurable physical quantities, is given in Eq. (5.20) where  $c$  is the speed of light in vacuum and the result,  $\tau_m$ , is the time it takes for a pulse to propagate a distance  $L$ .

$$\tau_m = \frac{L}{c} \left( n_l - \lambda \frac{dn_l}{d\lambda} \right). \quad (5.20)$$

The first derivative of  $\tau_m$  with respect to  $\lambda$  is obtained through the derivative of Eq. (5.20), i.e.

$$\frac{d\tau_m}{d\lambda} = -\frac{L\lambda}{c} \left( \frac{d^2n_l}{d\lambda^2} \right). \quad (5.21)$$

The phase shift, due to material dispersion after a distance  $L$ , between two optical signals that were in phase at the transmitter is obtained by

$$\Delta_m \cong \Delta_\lambda \frac{L}{c} \left| -\lambda \frac{d^2n_l}{d\lambda^2} \right| = \Delta_\lambda L \cdot |D_M|. \quad (5.22)$$

Finally, the material dispersion,  $D_M$ , is defined by Eq. (5.23) and is usually presented in ps / (nm × km),

$$D_M = \frac{-\lambda}{c} \left( \frac{d^2n_l}{d\lambda^2} \right). \quad (5.23)$$

### 5.2.1.1.2 Waveguide Dispersion

Evaluation of waveguide dispersion assumes that the cabling or mounting will stretch the fiber as the temperature increases. Its volume, however, remains intact. The variations in the material dimensions are assumed to be negligible. If the core of the fiber is modeled as a glass cylinder, with the length  $L$  and diameter  $d$ , a geometrical approach gives that the variation in temperature will change the length by  $\Delta L (T - T_0)$  and the diameter with  $\Delta d (T - T_0)$ , such that

$$\frac{\Delta d(T - T_0)}{d} = -\frac{\Delta L(T - T_0)}{2L}, \quad (5.24)$$

where  $T$  is the temperature and  $T_0$  is the temperature at the starting point. This variation in diameter will change the dispersion according to the variation in waveguide dispersion [57-58], described as

$$D_w(\lambda) = -\frac{n_2 \Delta}{c\lambda} V \frac{d^2(Vb)}{dV^2}, \quad (5.25)$$

where  $n_2$  is the refractive index of the cladding and  $\Delta$  is the relative difference in refractive index between the core and the cladding.  $V$  and  $b$  are the normalized frequency and the normalized propagation constant, respectively, and can be found through

$$V = ka\sqrt{n_1^2 - n_2^2} \cong kan\sqrt{2\Delta}, \quad (5.26)$$

$$b = \frac{(\beta/k)^2 - n_2^2}{n_1^2 - n_2^2}, \quad (5.27)$$

where  $a = d/2$  is the fiber core radius. From these equations it is apparent that fiber with notable waveguide dispersion, e.g. dispersion-shifted fiber, dispersion-compensating fiber, etc., will respond differently to changes in the diameter  $d$  compared to standard fiber where material dispersion is dominant. However, this response must be evaluated for each fiber design, since the term  $V(d^2(Vb)/dV^2)$  lies between 0 and 1.2, with a maximum at  $V \approx 1.2$ . For a standard single-mode fiber, the operating range is  $V=2.0 - 2.4$  and results in  $V(d^2(Vb)/dV^2)$  of 0.1 to 0.2 with  $\Delta = 0.01$  and  $n_2 = 1.5$  [58].

According to ITU-T Rec.G.652 for single-mode fiber, the chromatic dispersion in the 1550 nm range should be less than 17 ps / (nm × km). It is important to note that both the material and waveguide dispersion are included in this value, and whereas waveguide dispersion is relatively linear, material dispersion behaves nonlinearly [58].

### 5.2.1.2 Polarization Mode Dispersion

The polarization state changes randomly along the fiber since it is not a perfectly uniform, cylindrical medium, and also due to mechanical stress called birefringence. The group delay will be different for different polarizations, which leads to pulse broadening due to PMD. A statistical analysis of the random differential group delay (DGD) results in Eq. (5.28), [12]

$$\Delta\tau_{RMS} \equiv D_p \sqrt{z}. \quad (5.28)$$

$D_P$  is the PMD parameter and typical values in modern fibers are in the range 0.05 to 1 ps /  $\sqrt{\text{km}}$ ,  $z$  is the fiber length from start and  $L$  is the total fiber length, both expressed in km. The average value of PMD is easily characterized, but instantaneous PMD varies unpredictably and consequently is difficult to compensate.

## 5.2.2 Theory Evaluation

This section is intended to provide a brief introduction of the theories used as a basis for the one-way two-color technology. A more detailed theoretical evaluation is found in the appended Paper K.

The theoretical basis for the presented one-way dual wavelength optical fiber frequency transfer technique is the transit time  $\tau_m$  for propagation of a single mode in a fiber due to different kinds of dispersions. The transit time  $\tau_m$  in a fiber is dependent on the refractive index and the wavelength, as expressed in Eq. (5.20). The magnitude of single mode fiber's temperature dependence has been shown in previous studies [55], and the property is utilized in this technique. The dispersion causes two different wavelengths to propagate at different velocities in the same fiber and since the material dispersion is concluded to be dominant, the analysis focuses on this. By calculating the derivative of Eq. (5.20) with respect to temperature, variations in both wavelength and refractive index will be taken into account as

$$\left. \frac{d\tau_m}{dT} \right|_{\lambda_N} = \frac{1}{c} \left( \frac{dL}{dT} \left( n_1 - \lambda \frac{dn_1}{d\lambda} \right) + L \left( \frac{dn_1}{dT} - \lambda \frac{d^2 n_1}{d\lambda dT} \right) \right) \quad N = 1, 2. \quad (5.29)$$

The variation in transit time as a function of temperature can thus be calculated where  $\lambda_N$  with  $N = 1, 2$  represents the two wavelengths. The equations for the two wavelengths are subtracted from each other, resulting in

$$\left. \frac{d\tau_m}{dT} \right|_{\lambda_1 - \lambda_2} = \frac{1}{c} \left( \frac{dL}{dT} \left( n_{\lambda_1} - n_{\lambda_2} \right) + \lambda_2 \frac{dn_{\lambda_2}}{d\lambda_2} - \lambda_1 \frac{dn_{\lambda_1}}{d\lambda_1} \right) + L \frac{d}{dT} \left( \left( n_{\lambda_1} - n_{\lambda_2} \right) + \lambda_2 \frac{dn_{\lambda_2}}{d\lambda_2} - \lambda_1 \frac{dn_{\lambda_1}}{d\lambda_1} \right). \quad (5.30)$$

This expression shows how the refractive indices of the two wavelengths are influenced by temperature, and, based on this, the variations in the transit time delay can be calculated. The frequency transfer technique uses the fact that the variations are different, but correlated, which is also supported by the experimental results shown further on.

The difference in transit time through the fiber will, as shown in Eq. (5.30), depend on the variation of length,  $L$ , and the variation in refractive index,  $n$ . Both of these effects will influence the chromatic dispersion of the fiber, but through different properties.

### 5.2.2.1 Experimental Setup for Theory Evaluation

The theory was evaluated in a laboratory experiment with the setup shown in Fig. 5.6. The aim of the experiment was to verify the equations for material dispersion, and the results are presented as time-resolved transit time variations compared with arrival time difference. The same oscillator was used both at the transmitter and as the reference at the TIC at the receiver. This isolates the variations to the transmission of the fiber, with no significant errors from a reference system.

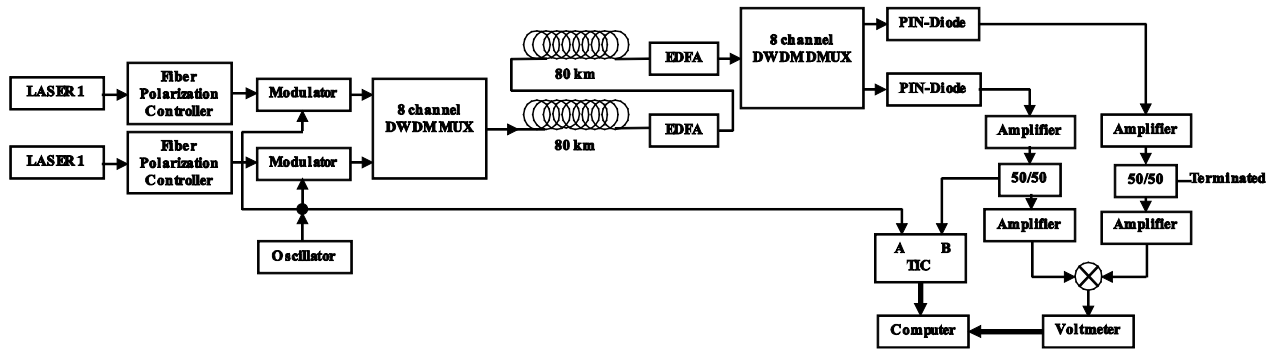


Figure 5.6: Experimental setup of the two-color one-way technique. The modulators are telecom Mach Zehnder modulators, the EDFAs are Erbium-Doped Fiber Amplifiers, and the p-i-n diode includes an electrical trans-impedance amplifier. Amplifiers are electrical amplifiers and TIC is a time interval counter.

A setup for verification of the proposed time and frequency transfer technique is shown in Fig. 5.6. Two continuous-wave lasers at wavelengths 1551 nm and 1559 nm are, after polarization controllers, modulated by separate Mach-Zehnder modulators using a 10 MHz reference oscillator, after which the modulated light is launched into the G.652 through an 8-channel dense wavelength-division multiplexing multiplexer (DWDM MUX). For evaluation of the method, the reference oscillator is also used as a time base for the TIC. The total sum of the two spools of fiber that were used was measured with an OTDR (optical time-domain reflectometer) to be  $2 \times 80$  km. Added to this length is 188 m of fiber between the lab and the outdoor fiber spools. The fiber path starts and ends in the laboratory for evaluation. The use of several fiber spools instead of one creates a case similar to a commercial link, which is an assembly of multiple fibers spliced by connectors, and where there is no possibility to determine the ageing of all optical fiber along the path.

At the receiving end, the two wavelengths are separated by an 8-channel dense wavelength-division multiplexing demultiplexer (DWDM DMUX), and detected in two 10 Gbit/s p-i-n receivers. The signals are amplified and connected to the radio frequency (RF) ports of a double balanced mixer. One of the signals passes a power splitter that is connected to the TIC, which measures the total transit time as a reference for the evaluation. The output of the TIC is interpreted as the result of an uncompensated one-way frequency transmission.

By measuring the voltage changes from a mixer, a correction signal is achieved and can be used for a real-time delay control of the uncompensated signal. Most of the equipment is housed in a laboratory with a controlled environment, except the spools of G.652-fiber which are placed outdoors inside a box for simulation of actual environmental conditions.

The 8-channel DWDM DMUX has a built-in optical filter function that is used to separate the two wavelengths. Measurement equipment detects the two 10 MHz sine waves after propagation through the fiber link, amplifies and compares them with a reference signal. The results are extracted from a data set of approximately eight days and are displayed in Fig. 5.7.

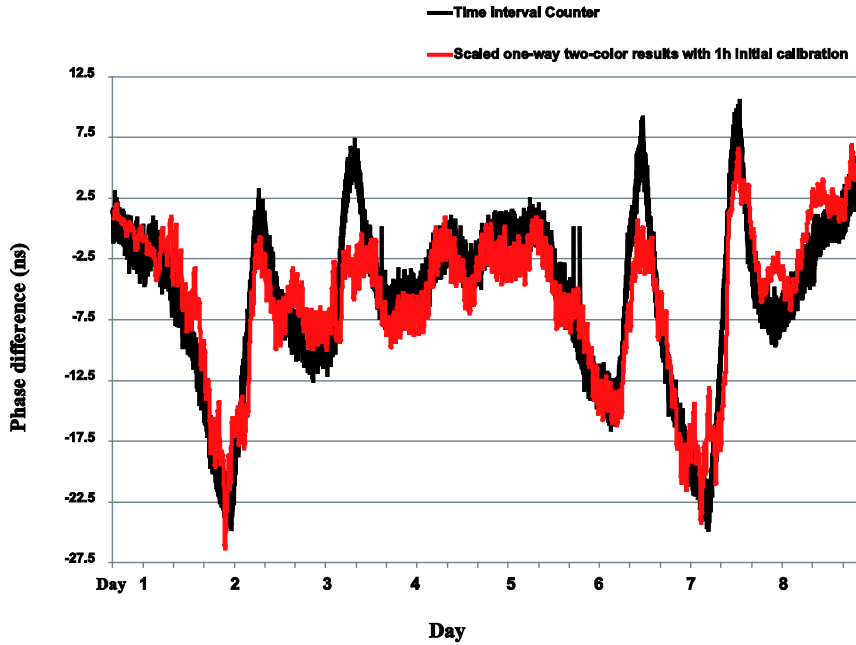


Figure 5.7: The red graph presents data collected for the one-way two-color technique including a 1h initial calibration. The black graph presents the time interval data used as reference. Their phase difference is represented on the y axis and the x axis represents the amount of days that measurement was carried out.

The mixer is set to run an initial calibration at the start to enable a calculation of fiber path parameters that would not be possible to measure in a system spread over a large distance. This calibration is presumed necessary for every individual system. The results from the mixer in this experiment are also set to have an initial startup period of 1 hour, which is used to create a running average with the aim of reducing noise. Furthermore, the mixer solution is scaled to enable an evaluation versus the TIC measurements and a graph displaying this data is shown in Fig. 5.7.

The standard deviation of the difference between the TIC data and the scaled one-way two-color technique results is 3.12 ns and the data showed a temperature dependence in transit time of 6 ns / °C.

This experimental analysis demonstrates the main contributing effects of the difference in transit time and how it relates to the variations in transit time induced by temperature variations. In addition to the temperature dependence of group velocity and chromatic dispersion in the fiber, there are other effects that may influence the signal's transit time. If these additional variations also vary linearly with temperature, they will be taken into account in the compensation calculated by empirical parameters.

The analysis enables a model for post-processing of data to compensate for transit time variations.

### 5.2.3 Two-Color One-Way Limitation

The main limitation of the two color one-way technique is noise, and since it is based on detecting a small delay signal and magnifying it to correct the output delay, any noise will be amplified by the same amount. In the setup where the two 10 MHz signals are 8 nm apart, multiplication is approximately 5000x, and at the same time as a measured 10 ps arrival time difference will correct the total delay by 50 ns, 0.2  $\mu$ rad of noise (or the equivalent at the output of the phase detector) will cause 5 ns of noise in the output.

The noise that appears in the measurements will be a combination of transmission noise and detection noise. To some extent, this will limit the maximum practical transmission distance, but the gain of an optimized receiver is of utmost importance.

### 5.2.4 Results and Conclusions of the Two-Color One-Way Technique

The theory has been experimentally verified and the results show that it is possible to perform a one-way frequency transfer in optical, single-mode fiber with a continuous real-time estimate of transit time variations. The technique is based on transmission utilizing two wavelengths, 8 nm apart and both residing in the conventional band (C-band) of optical communication. By evaluating the phase difference between the two signals' transit time delays, corrections can be applied to compensate for any unwanted delay variations along the transmission path.

The improvement that real-time compensation contributed to the one-way fiber frequency transfer method was substantial in lab experiments [G, H, I and J], but small in an urban network installation [K]. This latter fiber is more stable, because it is located below ground and the duration of the measurements was too short to include large temporal variations in the transit time delay. The advantage gained over longer periods is presumably larger, but remains to be characterized. Furthermore, evaluation of the technique requires more stable clocks on both ends, since both links are fiber based and GPS seems to be limited by the instability of Cesium frequency standards.

In conclusion, the experiment was a practical success and has shown that a compensated one-way fiber solution can be implemented in an existing metropolitan data network. The results show the feasibility of transferring the frequency from a Cesium-beam frequency standard over distances less than 10 km via underground fiber with an accuracy that is comparable to GPS PPP, even without delay compensation. For distances exceeding 10 km, some compensation will be necessary.

Future improvements are related to size-reduction of the hardware and increased reliability of the transmitter and receiver. The setup is expected to work unsupervised during continuous long-term operation and to complement GPS frequency transfer.



## Chapter 6

### Summary of Appended Papers

Papers A to E present the technique that was developed to utilize the repetitive framing of the well-established optical network communication structure synchronous digital hierarchy, SDH, to extract data for time and frequency transfer. This development progressed from theory and modeling, over prototypes to a demonstration unit, which was implemented in the first fiber based time comparison between two UTC realizations in different countries. The time and frequency transfer in these links is achieved through post-processing of measured data.

Paper F describes the first work performed by author on real-time stabilized phase over optical fiber. This is more engineering than physics, but acts as a link between the first Papers of post-processed timing information and the later Papers aiming for real-time adjustments.

Papers G to K describe the progress on a novel one-way technique, utilizing dispersion as a marker for transit time variations.

#### **Paper A: Time Transfer by Passive Listening Over a 10 Gb/s Optical Fiber**

This Paper presents the first time transfer with the non-insertion technique that is based non-insertion technology that utilizes passive listening to existing data frames in a fiber optical network with data traffic at 10 Gbit/s. Two clocks are compared: a Cesium clock at SP in Borås and a Rubidium clock in downtown Borås. The time difference between these two clocks was estimated using a proposed technique for listening to independent data traffic and a GPS link, based on carrier phase measurements as a reference. The RMS difference between the two techniques was approximately 300 ps.

#### **Paper B: Time Transfer Using an Asynchronous Computer Network: Results From a 500 km Baseline Experiment**

Previous time transfer experiments have been configured for baselines shorter than 70 km, with and without intermediate nodes, as described in Paper A. The experiment presented in Paper B is the first that uses a baseline distance greater than 500 km. The transfer between Borås and Stockholm is a time-transfer experiment that spans more than 500 km of transmission fiber, of which several km are airborne lines.

By comparing the results with a GPS carrier phase link, an RMS precision better than 1 ns is achieved during several months of measurements between two Hydrogen-MASERS. The experiment indicates that there is no obvious linear degradation of precision with distance, compared to the results presented in Paper A. It is a known fact that optical fiber is sensitive to temperature, as shown by the results in Paper B. The results also indicate a temperature sensitivity in the equipment, which gives rise to varying asymmetries. The equipment's temperature sensitivity is further evaluated in Paper C.

## **Paper C: Time Transfer over a 560 Km Fiber Link**

This Paper is a further study of the results in Paper B, which indicated that the equipment is sensitive to temperature, which may give rise to varying asymmetries. The distance and equipment are the same as in the previous Paper, but the distance was more accurately determined to 560 km to enable temperature evaluations. The measurement period was increased from 4 to 6 months and now includes temperature data from a number of amplification stations.

Some conclusions from the experiment are that the system can serve as a permanent link for distances above 560 km with an precision relative to the GPS carrier phase of  $<1$  ns, but would work even better with more detailed information about temperatures along the way.

## **Paper D: Measurements and Error Sources in Time Transfer Using Asynchronous Fiber Network**

Several time transfer experiments with varying complexity and distance have been performed and all of these experiments used the non-insertion technique described in Papers A to C. A precision compared to the GPS carrier phase of  $<1$  ns was obtained in all the experiments, regardless of the configuration.

This Paper used the same distance and equipment as in Papers B and C, but the amount of data was increased to almost a year.

The purpose of this Paper was to evaluate the error sources of the technique that is presented in Papers A to C. One objective was to calculate a value for each error source for future implementation of a mathematical model to achieve better accuracy.

## **Paper E: Time Transfer Between UTC(SP) and UTC(MIKE) Using Frame Detection in Fiber-Optical Communication Networks**

This Paper presents an experiment that utilizes the technology presented in Papers A to D. The difference in this experiment is that the distance was increased to 1,129 km and connected two national time and frequency laboratories with each other, i.e. SP in Sweden and National metrology institute of Finland (MIKES), including an intermediate time and frequency laboratory (STUPI). The results show a time transfer stability of less than 10 picoseconds for an average time of a few hundred seconds.

As previously shown in Papers B and C, the method is sensitive to daily variations. However, the mathematical algorithm mentioned in Paper D was not implemented in this experiment.

Interestingly, approximately half of the fiber distance is located in a temperature-stable ambient environment which can be seen in the results.

A comparison with GPS carrier phase time transfer over three months shows an RMS agreement of less than 1 nanosecond.

## **Paper F: A Fiber Based Frequency Distribution System with Enhanced Output Phase Stability**

This Paper describes the first work within this thesis regarding real-time stabilized phase over optical fiber. This is more engineering than physics, but functions as a link between the first Papers [A to E] of post-processed timing information and the later Papers [G to K] that aim for real-time adjustments without exchanging data.

An experimental evaluation using a laser-based transmitter with an 850 nm wavelength and 625 meters of multi-mode fiber detected a temperature dependence of 100 ps / °C. To compensate for these slow variations in real-time, a setup using two-way transmission, in conjunction with an adjustable optical delay, was constructed.

In conclusion, activating a dynamically controlled pre-delay in a fiber based frequency transmission system will induce a small penalty on faster variations of the output phase, but will result in a remarkable improvement on slower variations.

## **Paper G: Fiber Based One-Way Time Transfer with Enhanced Accuracy**

There are several fiber based techniques for time and frequency transfer, and most of them rely on two-way transmission in which asymmetry variations in transmission time should be compensated. One of these techniques are presented in Papers A to F and as an alternative, a one-way transmission via a fiber optical WDM network is proposed. It estimates variations in the transmission time based on detection of the differences in transit time between two co-propagated light waves of different wavelengths. This Paper presented the results of an experiment where both wavelengths are in the optical C-band.

## **Paper H: Active Detection of Propagation Delay Variations in One-Way Time Transfer Utilizing Dual Wavelengths in an Optical Fiber Network.**

This Paper is a further development of the technique presented in Paper G. The distance between wavelengths was reduced from 18 nm to 8 nm and the propagation distance was increased from 38 km to 160 km. The quality of the measurements was improved compared to before by performing an analysis of the receiver component, which resulted in minimization of errors.

## **Paper I: One-Way Time Transfer Utilizing Active Detection of Propagation Delay Variations of Dual Wavelengths in an Optical Fiber Network**

This Paper is a further development of Papers G and H in an effort to minimize errors and increase accuracy. It introduced some new components such as a real WDM network, unlike earlier work where only the receiver side had a DWDM and the transmitter used an optic combiner. An evaluation of the receiver linearity was performed and new algorithms as well as a demonstration of real-time compensation for delay variations were introduced.

## **Paper J: Real-Time Phase Stabilization Utilizing Two-Color, One-Way Frequency Transfer**

Paper J was based on Papers G to I and presented progress in the determination of the sources of error introduced by the equipment used for phase comparisons. To improve the technology, the frequency modulation was increased and a third frequency modulation, superimposed on a wavelength between the other wavelengths, was inserted.

An evaluation of the receiver was performed, resulting in reduced measurement noise.

## **Paper K: Two-Color, One-Way Frequency Transfer in a Metropolitan Optical Fiber Data Network**

This Paper was the most comprehensive Paper in terms of the technology presented in Papers G to J. Earlier Papers have been carried out in the laboratory, while this Paper presented the results of a comparison between the two Cesium beam frequency standards located about 3 km apart and connected via an urban optical fiber network. The Cesium standards were simultaneously compared to each other with a GPS link, so that the optical fiber technique could be comparatively evaluated with respect to the GPS technique. The results show a frequency stability comparison in the order of  $3 \times 10^{-15}$  at  $1 \times 10^4$  s between the fiber based and GPS methods. The equipment was adapted in size and a new type of real-time compensation was introduced.

This Paper also presented a properly detailed theory section that forms the foundation for this technology.

## References

- [1] G. V. Rosenbaum, “Determination of GPS RF Signal Strengths”, Position, Location and Navigation Symposium, *IEEE/ION*, pp. 449–458, 2008.
- [2] “NSTAC Report to the President on Commercial Communications Reliance on the Global Positioning System (GPS)”, National Security Telecommunications Advisory Committee (NSTAC) Publications, 2008.
- [3] Svensk Författningssamling, SFS 2001:127, 2001.
- [4] C. Audoin, B. Guinot, “The Measurement of Time: Time, frequency and the Atomic Clock”, University Press, 2001.
- [5] J. Robb, D. Miner, “From Sundials to Atomic Clocks Understanding Time and Frequency”, U.S. Government Printing Office, 1999.
- [6] C. W. Chou, D. B. Hume, J. C. J. Koelemeij, D. J. Wineland, and T. Rosenband, “Frequency Comparison of Two High-Accuracy  $Al^+$  Optical Clocks”, *Phys. Rev. Lett.* *104*, 2010.
- [7] N. F. Ramsey, “A Molecular Beam Resonance Method with Separated Oscillating Fields”, *Phys. Rev.*, vol. 78, pp. 695–699, 1950.
- [8] N. F. Ramsey, "Experiments With Separated Oscillatory Fields and Hydrogen Masers", *Frequency Control Symposium (FCS)*, pp. 3–11, 1990.
- [9] M. Lombardi, T. Heavner, S. Jefferts, “NIST Primary Frequency Standards and the Realization of the SI second” *The Journal of Measurement Science*, vol. 2, no. 4, pp 74–89, 2007.
- [10] R. Paschotta, “Encyclopedia of Laser Physics and Technology Volume 1 and 2”, Wiley-VCH Verlag GmbH &Co, 2008.
- [11] G. Agrawal, *Lightwave Technology Component and Devices*, Wiley-Interscience, 2004.
- [12] G. Agrawal, *Lightwave Technology: Telecommunication Systems*, Wiley-Interscience, 2005.
- [13] Telecommunication standardization Sector of ITU “Characteristics of a Single-Mode Optical Fibre and Cable”, ITU-T Recommendation G.652, 11/2009.
- [14] Telecommunication standardization Sector of ITU “Spectral Grids for WDM Applications: DWDM Frequency Grid” ITU-T Recommendation G.694.1 , 06/2002.
- [15] Telecommunication standardization Sector of ITU “Spectral Grids for WDM Applications: CWDM Wavelength Grid” ITU-T Recommendation G.694.2, 12/2003.
- [16] J. Bromage, “Raman Amplification for Fiber Communications Systems”, *J. Lightwave Technol.*, vol. 22, pp. 79–93, 2004.
- [17] F. L. Pedrotti, L. S. Pedrotti, “Introduction To Optics, Second Edition”, Prentice-Hall, Inc., 1993.

- [18] B. E. A. Saleh, M. C. Teich, “Fundamentals Of Photonics, Second Edition”, John Wiley & Sons, Inc., 2007.
- [19] D. W. Allan, N. Ashby, C. C. Hodge, “The Science of Timekeeping”, Hewlett Packard application Note 1289, 1997.
- [20] P. Defraigne and G. Petit, “Time Transfer to TAI Using Geodetic Receivers”, *Metrologia*, vol. 40, pp. 184–188, 2003.
- [21] G. Petit and Z. Jiang, “GPS All in View Time Transfer for TAI Computation”, *Metrologia*, vol. 45, pp. 35–45, 2008.
- [22] S. Jefferts, M. Weiss, J. Levine, S. Dilla, and T. Parker, “Two Way Time Transfer Through SDH and Sonet Systems”, *European Frequency and Time Forum (EFTF)*, pp. 461–464, 1996.
- [23] M. Kihara, A. Imaoka, M. Imae, and K. Imamura, “Two Way Time Transfer Through 2.4 Gb/s Optical SDH Systems”, *IEEE T. Instrum. Meas.*, vol. 50, no. 3, pp. 709–715, 2001.
- [24] F. Kefelian, O. Lopez, H. Jiang, C. Chardonnet, G. Santarelli and A. Amy-Klein, “Ultra-Stable Optical Frequency Transfer over an Optical Telecommunications Network With Live Data Traffic”, *CLEO Europe - EQEC*, 2009.
- [25] S. Yang, C. Lee, Y. Lee, J. Lee, Y. Kim and S. Lee, “Accuracy Improvement Technique for Timing Application of LORAN-C Signal”, *IEEE T. Instrum. Meas.*, vol. 60, no. 7, pp. 2648–2654, 2011.
- [26] D. Engeler, “Performance Analysis and Receiver Architectures of DCF77 Radio-Controlled Clocks”, *IEEE T. Ultrason. Ferr.*, vol. 59, no. 5, pp. 869–884, 2012.
- [27] J. Levine, “A Review of Time and Frequency Transfer Methods”, *Metrologia*, vol. 45, no. 6, pp. 162–174, 2008.
- [28] D. L. Mills, “Internet Time Synchronization: The Network Time Protocol”, *IEEE Trans. Communications COM-39*, pp. 1482–1493, 1991.
- [29] Hoffman-Wellenhof B, Lichtenegger, H, Collins J, “GPS Theory and Practice, Fifth edition”, Springer Wien NewYork, 2001.
- [30] G. Seeber, “Satellite Geodesy 2nd edition”, Walter de Gruyter Berlin NewYork, 2003.
- [31] B. Hoffman-Wellenhof, H. Lichtenegger, E. Wasle E, “GNSS Global Navigation Satellite Systems: GPS, GLONASS, Galileo and more”, Springer Wien NewYork, 2008.
- [32] D.E. Wells, N. Beck, D. Delikaraoglou, A. Kleusberg, E.J Krakiwsky, G. Lachapelle, R.B Langley, M. Nakiboglu. K.P Schwartz, J.M Tranquilla and P Vanicek, “Guide to GPS Positioning”, Canadian GPS Associates, Fredericton, N.B, 1986.
- [33] C. Rieck, P. Jarlemark, and K. Jaldehag, “The Use of Ambiguity Resolution for Continuous Real-Time Frequency Transfer by Filtering GNSS Carrier Phase Observations”, *European Frequency and Time Forum (EFTF)*, 2006.

- [34] C. Rieck, P. Jarlemark and K. Jaldehag, “Thermal Influence on The Receiver Chain of GPS Carrier Phase Equipment for Time And Frequency Transfer”, *Frequency Control Symposium (FCS) and the European Frequency and Time Forum (EFTF) joint Conference of the IEEE International*, pp. 326–331, 2003.
- [35] IEEE Instrumentation and Measurement Society, “IEEE Standard for a Precision Clock Synchronization Protocol for Networked Measurement and Control Systems” IEEE Std 1588 2008 (Revision of IEEE Std 1588–2002), 2008.
- [36] G. Daniluk and T. Wloostowski, “White Rabbit: Sub-Nanosecond Synchronization for Embedded Systems”, *Precise Time and Time Interval (PTTI) Systems and Applications Meeting*, pp. 45–60, 2011.
- [37] M. Lipinski, T. Wloostowski, J. Serrano, P. Alvarez, “White Rabbit: A PTP Application for Robust Sub-Nanosecond Synchronization”, *International IEEE Symposium on Precision Clock Synchronization for Measurement Control and Communication (ISPCS)*, pp. 25–30, 2011.
- [38] J. Hall, J. Ye, S. Diddams, L. Ma, S. Cundiff and D. Jones, “Ultrasensitive Spectroscopy, The Ultrastable Lasers, The Ultrafast Lasers, and The Seriously Nonlinear Fiber: A New Alliance for Physics and Metrology”, *IEEE. J. Quant. Electr.*, vol. 37, no 12, pp. 1482–1492, 2001.
- [39] R. Holzwarth, M. Zimmermann, T. Udem and T. Hänsch, “Optical Clockworks and the Measurement of Laser Frequencies With A Mode-Locked Frequency Comb”, *IEEE J. Quant. Electr.*, vol. 37, no. 12, pp. 1493–1501, 2001.
- [40] H. Jiang, F. Kéfélian, S. Crane, O. Lopez, M. Lours, J. Millo, D. Holleville, P. Lemonde, C. Chardonnet, A. Amy-Klein, and G. Santarelli, “Long-Distance Frequency Transfer over an Urban Fiber Link Using Optical Phase Stabilization”, *J. OSA B*, vol. 25, no 12, pp. 2029–2035, 2008.
- [41] S. Foreman, A. Ludlow, M. de Miranda, J. Stalnaker, S. Diddams and J. Ye, J, ”Coherent Optical Phase Transfer over a 32-Km Fiber with 1 s instability  $<10^{-17}$ ” *Physical Review Letters*, 2007.
- [42] O. Terra, G. Grosche and H. Schnatz, “Brillouin Amplification in Phase Coherent Transfer of Optical Frequencies over 480 Km Fiber”, *Opt. Express.*, vol. 18, pp. 16102–16111, 2010.
- [43] S. Droste, K. Predehl, J. Alnis, T. W. Hansch, T. Udem, R. Holzwarth, S. Raupach, O. Terra, T. Legero, H. Schnatz, G. Grosche, “Optical Frequency Transfer via 920 Km Fiber Link with  $10^{-19}$  Relative Accuracy”, *Conference on Lasers and Electro-Optics (CLEO)*, 2012.
- [44] K. Predehl, C.G. Parthey, A. Matveev, A. Beyer, J. Alnis, N. Kolachevsky, R. Pohl, S. Droste, T. Udem, T. W. Hansch, R. Holzwarth, H. Schnatz, T. Legero, B. Lipphardt, O. Terra, G. Grosche, S. Weyers, “Highly Stable Remote Clock Comparisons via 920 Km Optical Fiber For Precision Spectroscopy Of Atomic Hydrogen”, *Conference on Lasers and Electro-Optics (CLEO)*, 2012.

- [45] H. Schnatz, O. Terra, K. Predehl, T. Feldmann, T. Legero, B. Lipphardt, U. Sterr, G. Grosche, R. Holzwarth, T. W. Hansch, T. Udem, Z. H. Lu, L. J. Wang, W. Ertmer, J. Friebe, A. Pape, E. M. Rasel, M. Riedmann, T. Wubbena, “Phase-Coherent Frequency Comparison of Optical Clocks Using a Telecommunication Fiber Link”, *IEEE Transactions on Ultrasonics, Ferroelectrics and Frequency Control*, vol. 57, no. 1, pp. 175–181, 2010.
- [46] K. Predehl, R. Holzwarth, T. Udem, T. W. Hansch, O. Terra, G. Grosche, B. Lipphardt, H. Schnatz, “Ultra Precise Frequency Dissemination Across Germany - Towards a 900 Km Optical Fiber Link From PTB to MPQ”, *Conference on Lasers and Electro-Optics and Conference on Quantum electronics and Laser Science CLEO/QELS*, 2009.
- [47] R. Emardson, P.O. Hedekvist, M. Nilsson, S.C. Ebenhag, K. Jaldehag, P. Jarlemark, J. Johansson, L. Pendrill, C. Rieck, P. Löthberg and H. Nilsson, “Time and Frequency Transfer in an Asynchronous TCP/IP over SDH-network Utilizing Passive Listening”, *IEEE International Frequency Control Symposium (FCS) and Precise Time and Time Interval (PTTI) Systems and Applications Meeting*, 2005.
- [48] Telecommunication standardization Sector of ITU “Network node interface for the synchronous digital hierarchy (SDH)”, ITU-T Recommendation G.707/Y.1322, 01/2007.
- [49] R. L. Freeman, “Fundamentals of Telecommunications”, John Wiley & Sons, 1999.
- [50] Pendulum Instruments, “Start-up Measurements on Oscillators: Using the CNT-90/CNT-91 to measure oscillator start-up”, Whitepaper Pendulum Instruments, 2007.
- [51] American National Standards Institute (ANSI), “Synchronization Interface Standards for Digital Networks”, (ANSI/T1.101 – 1987), 1987.
- [52] G. Agrawal, “Nonlinear Fiber Optics”, Academic press limited, 1989.
- [53] P. Vella, P. Garrel-Jones, and R. Lowe, “Measuring Chromatic Dispersion of Fibers”, *United States Patent 4551019*, 1985.
- [54] W. Hatton and M. Nishimura, “Temperature Dependence of Chromatic Dispersion in Single Mode Fiber”, *J. Lightwave Technol.*, vol. LT-4, no. 10, pp. 1552–1555, 1986.
- [55] A. Walter and G. Schaefer, “Chromatic Dispersion Variations in Ultra-Long-haul Transmission Systems Arising from Seasonal Soil Temperature Variations”, *Proceedings of Optical Fiber Communication OFC02*, pp. 332–333, 2002.
- [56] A. Imaoka and M. Kihara, “Accurate Time/Frequency Transfer Method Using Bidirectional WDM Transmission”, *IEEE T. Instrum. Meas.*, vol. 47, no. 2, pp. 537–542, 1998.
- [57] D. Gloge, “Dispersion in Weakly Guided Fibers”, *Appl. Opt.*, vol. 10, no. 11, pp 2442–2445, 1971.
- [58] G. Keiser, “Optical Fiber Communication, McGraw-Hill”, 2<sup>nd</sup> Edition, 1991.

# Appendix A Optics

## A1 Optical Fiber

An optical fiber is a dielectric waveguide made of a low loss material such as silica glass. It has a central core through which the light is guided, surrounded by a cladding with a lower refractive index. Light rays that incident on the core-cladding boundary at angles larger than the critical angle undergo total internal reflection and are guided through the core without being refracted into the cladding [A1].

Two parameters characterize the design of a step-index fiber: the core radius  $a$  and the refractive index difference,  $\Delta n$ , between core and cladding. Typical values for the core radius are a few microns for single-mode fibers, and tens of microns or more for multi-mode fibers. Instead of the refractive index difference, the numerical aperture (NA) is often used and is defined as Eq. (A1)

$$NA = \sqrt{n_{core}^2 - n_{cladding}^2} \quad (A1)$$

which is the sine of the maximum acceptable angle of an incident beam with respect to the fiber axis. NA also quantifies the strength of guidance. Typical values are in the order of 0.1 for single-mode fibers and around 0.3 are typical for multi-mode fibers. A fiber's sensitivity to bending losses decreases strongly as NA increases.

The principles of light transmission are essentially the same as those applicable to planar dielectric waveguides and the most distinguishing characteristic is the fiber's cylindrical geometry. Both types of waveguides propagate the signal in different modes. Each mode travels along the axis of the waveguide with a distinct propagation constant and group velocity, maintaining its transverse spatial distribution and a varying polarization. Each mode is described as the sum of the multiple reflections of a TEM wave bouncing within the core [A2].

### A1.1 Fiber Modes

Optical fibers can support one or several guided modes. Most of the intensity distributions are located at or immediately around the fiber core, although some of the intensity may propagate within the fiber cladding which also provides a multitude of cladding modes. Cladding modes' optical power is usually lost after some moderate distance of propagation, but can in some cases propagate over longer distances.

Outside the cladding there is a protective polymer coating. This coating improves the fiber's mechanical strength and protects it against moisture, as well as determines the losses for cladding modes. Table A1.1 presents the difference between single-mode and multi-mode fiber (MMF).

Table A1.1: Important difference between single-mode and multi-mode

<b>Difference between SMF and MMF [A1-A2]</b>
<ul style="list-style-type: none"> <li>• Single-mode fibers usually have a relatively small core with a diameter of only a few micrometers and will guide only a single spatial mode, irrespective of the fact that there are two different polarization directions. Changing the launch conditions only affects the power launched into the guided mode, whereas the spatial distribution of the light exiting the fiber is fixed. The mode radius of a single-mode fiber is often in the order of 5 <math>\mu\text{m}</math>, but large mode area fibers with single-mode guidance also exist.</li> <li>• Multi-mode fibers have a larger core and/or a larger index difference between core and cladding, so that they support multiple modes with different intensity distributions.</li> </ul>

Long-range optical fiber communication systems mostly use single-mode fibers, because of the different group velocities of different modes (intermodal dispersion) that distort signals at high data rates. Multi-mode fibers are convenient for some shorter distances reducing the demands on light sources and component alignment.

Single-mode fibers are also used as a base for fiber-lasers and amplifiers [A1-A2].

One way of determining the number of wavelengths for a specific fiber is to examine the cutoff conditions, which is referred to as being the mode when it is no longer bound to the core of the fiber. An important parameter connected with the cutoff condition is the normalized frequency  $V$ , which is defined as

$$V^2 = \left( \frac{2\pi a}{\lambda} \right)^2 (n_{core}^2 - n_{cladding}^2), \quad (\text{A2})$$

and is a dimensionless number that determines how many modes a fiber can support. The term  $a$  represents the core radius,  $\lambda$  is the wavelength in vacuum,  $n_{core}$  is the maximum refractive index of the core and  $n_{cladding}$  is the refractive index of the homogeneous cladding.

Single-mode operations require that  $V < 2.4456$ , but multi-mode fibers can have large  $V$  values, which allows the number of modes to be estimated using  $V^2$  [A1]. Figure A1.1 presents a simple illustration of supported modes in the relationship between normalized propagation constant  $b$  and normalized frequency  $V$ . It is apparent from Eq. (A2) that the single-mode relationship is wavelength-dependent, which means that a single-mode fiber is defined for one wavelength interval and is able to act as a multi-mode for different wavelengths.

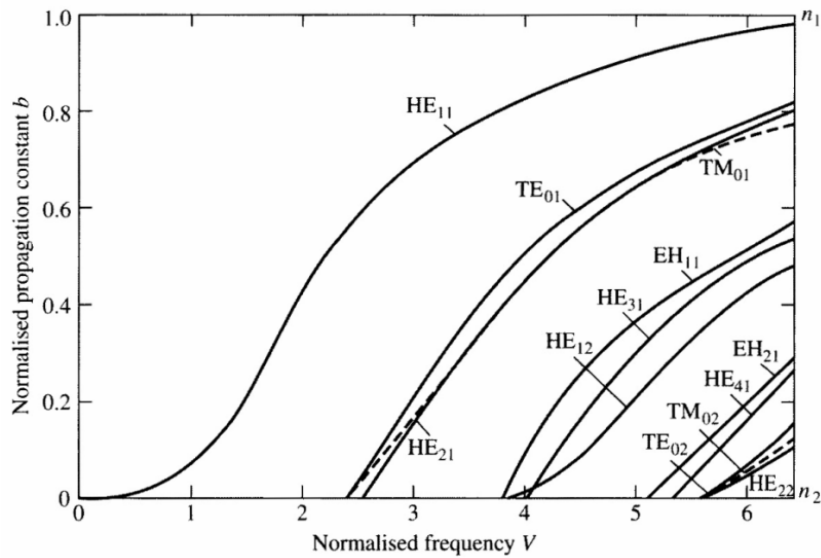


Figure A1.1: An illustration of supported modes in the relationship between normalized propagation constant  $b$  and normalized frequency  $V$  [A3].

## A1.2 Refractive Index Profiles

A refractive index profile of a fiber often deviates substantially from that of a step-index profile that has a constant refractive index within the core. Some common profiles are presented in Table A1.2.

Table A1.2: Refractive index profile of different fibers

<b>Refractive index profiles</b>
<ul style="list-style-type: none"> <li>• In graded-index fibers, the refractive index gradually decreases as you move away from the center, e.g. with a parabolic shape. Parabolic index profiles are useful for example in multi-mode fibers because they minimize intermodal dispersion.</li> <li>• There are also “W profiles”, where the core is surrounded by a region with a refractive index that is lower than that of the cladding. There can even be additional index steps, or combinations with smooth refractive index variations.</li> <li>• Triangular, trapezoidal and Gaussian index profiles are used for dispersion-shifted fibers.</li> <li>• Index profiles do not need to be cylindrical. An elliptical core shape can provide increased birefringence, for example polarization-maintaining fibers or even single-polarization guidance</li> </ul>

### **A1.3 Propagation Losses**

Power losses for light being propagated in a fiber can be extremely small, particularly in single-mode silica fibers. The resulting attenuation is typically dominated by Rayleigh scattering, which is the elastic scattering of light by particles much smaller than the wavelength. Other loss contributions comes from inelastic scattering, i.e. spontaneous Brillouin scattering [A4] and Raman scattering [A5] from absorbed impurities and from fluctuations in the core diameter.

For silica fibers the minimum loss that occurs is in the region of 1.5–1.6  $\mu\text{m}$  and can be below 0.15 dB / km, which is close to the theoretical limit based on Rayleigh scattering in an amorphous glass material [A1-A2].

### **A1.4 Dispersion Properties**

Dispersion is the linear effects that describe how the different frequencies within a signal travel at different speeds and thereby cause the data bits to smear out. Dispersion is a major limiting factor for any long-haul intensity-modulated light system with high data rates.

By carefully designing a fiber's waveguide properties, its chromatic dispersion can deviate considerably from its material dispersion. This makes it possible to achieve unusual dispersion properties by engineering the fiber's waveguide properties.

Birefringence makes the group delay polarization-dependent; this is often referred to as polarization mode dispersion. Multi-mode fibers also have intermodal dispersion, i.e. a dependence of the group velocity on the fiber mode, which can be minimized by choosing a suitable refractive index profile, but is typically larger than the dispersion in single-mode fibers [A1-A2].

#### **A1.4.1 Dispersion Compensation Fiber (DCF)**

There is a solution for minimizing the total dispersion and the basic idea consists of periodically compensating dispersion along the fiber link. This is performed using fibers or devices with inverse dispersion characteristics. The parameter  $\beta_2$  is known as the second order dispersion parameter, and it is a measure of the pulse broadening in a fiber. In common communication fiber, the  $\beta_2$  constant is highly negative. The use of DCF provides an all-optic technique that is capable of overcoming the detrimental effects of chromatic dispersion in optical fibers, provided the average signal power is low enough that the nonlinear effects remain negligible [A2]. Dispersion compensation can be achieved in three different ways: pre-compensation, periodic compensation and post-compensation. In theory, for a linear system any of these three should fully compensate for dispersion. Nonlinear effects are however always present, which result in dispersion management adopted for each specific case according to components and power [A1-A2].

### **A1.5 Polarization Properties**

Despite their typically cylindrical symmetry, fibers usually exhibit some amount of birefringence, which can cause light's polarization state to evolve in an uncontrolled way [A1-A2].

## **A1.6 Transmission Capacity of Optical Fibers**

A fiber's transmission capacity depends on the fiber's length. The longer a fiber is, the more detrimental certain effects such as intermodal or chromatic dispersion are there, and the lower will the achievable transmission rate be.

Over short distances of a few hundred meters or less, it is often more convenient to use multi-mode fiber. Depending on the transmitter technology and fiber length, data rates between a few hundred Mbit/s and  $\approx 10$  Gbit/s can be achieved.

Single-mode fiber is typically used for longer distances, such as a few kilometers or more. Current commercial telecom systems typically transmit 2.5 Gbit/s, 10 Gbit/s or 40 Gbit/s per data channel. Future systems may use higher data rates per channel, but currently the required total capacity is normally obtained by transmitting many channels at slightly different wavelengths through the fibers; this is called wavelength division multiplexing (WDM). Total data rates can be several terabits per second. Even this capacity is far from the physical limit of an optical fiber.

### **A1.6.1 Wavelength-Division Multiplexing (WDM)**

Signals can be multiplexed in the spectral domain through frequency-division multiplexing (FDM). This technology is routinely used for radio waves and microwaves. Its extension to the optical domain enables high bit-rate capacity in light wave systems through the large frequency associated with the optical carrier. Wavelength-division multiplexing is a technology that multiplexes multiple optical carrier signals in a single optical fiber by using different wavelengths (colors) of laser light to carry different signals. This allows for a multiplication of capacity, in addition to enabling bidirectional communications over a single strand of fiber. This is a form of FDM, but is commonly called WDM. This technique was first used in the 1980's when the capacity of existing fiber links operating at  $1.3 \mu\text{m}$  was doubled by adding another channel operating near  $1.55 \mu\text{m}$ . The designs of such systems require attention to many details related to the generation and propagation of multiple bit streams that overlap in the time domain. Especially interchannel, nonlinear effects such as XPM (Cross-phase modulation), Raman and FWM (Four-way multiplexing) must be evaluated to ensure that they do not induce crosstalk, which limits system performance [A2].

#### **A1.6.1.1 Basic WDM Scheme**

The basics of the WDM technique follow a scheme in which the capacity of one lightwave system is expanded by employing multiple optical carriers at different wavelengths simultaneously. Each carrier is modulated separately and independently using different electrical bit streams and is transmitted utilizing the same fiber.

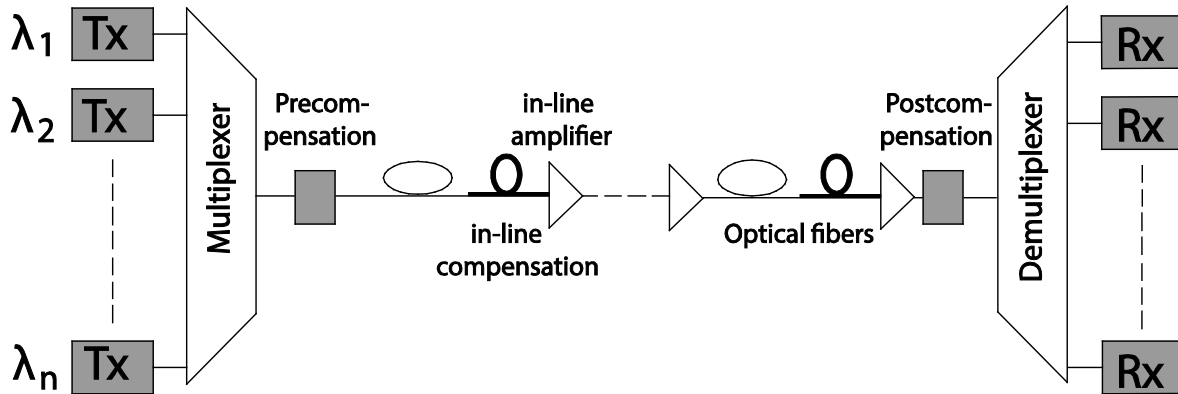


Figure A1.2: Schematic diagram of a WDM link. Each channel operates at its own wavelength through its own transmitter. Pre, post, and in-line compensators are used to manage the dispersion of the fiber link [A2].

Fig. A1.2 shows the schematic layout of an ordinary dispersion compensated one-way WDM-link. All wavelengths are gathered into one output through the multiplexer. The multiplexed signal is then launched into the fiber link for transmission to its destination, where a demultiplexer separates the signal into individual channels for detection in each receiver [A2].

#### A1.6.1.2 Capacity and Spectral Efficiency of WDM

WDM can increase a system's capacity through transmission of simultaneous multiple bit streams in the same fiber. When  $N$  channels at bit rates  $B_1, B_2, \dots,$  and  $B_N$  are transmitted simultaneously through a fiber of length  $L$ , the total bit rate of the WDM link becomes

$$B_T = B_1 + B_2 + \dots + B_N. \quad (\text{A3})$$

For equal bit rates, system capacity is enhanced by a factor of  $N$ . The most important parameters for WDM systems are the number of channels,  $N$ , the bit rate,  $B$ , at each channel, and the frequency spacing,  $\Delta\nu_{ch}$ , between two neighboring channels. To represent the total optical bandwidth of a WDM system, we need to know  $N\Delta\nu_{ch}$ .  $NB$  represents the system capacity.

WDM systems are often classified as being coarse or dense, depending on their channel spacing. However, there is no precise definition that distinguishes between the two. Coarse channel spacing often exceeds 5 nm, whereas dense is often less than 1 nm [A2]. A common measure of a WDM system is its spectral efficiency, which is defined as

$$\eta_s = \frac{B}{V_{ch}}. \quad (\text{A4})$$

For a given system bandwidth, the link's capacity depends on how closely the channels can be compressed in the wavelength domain. The minimum channel spacing is limited by

interchannel crosstalk. Channel spacing  $\Delta\nu_{ch}$  in commercial systems often exceeds the bit rate by a factor of two or more. The channel frequencies or wavelengths in WDM systems have been standardized by the ITU on a 100 GHz grid in the frequency range of 186-196 THz [A6]. The current steps in channel spacing for the fixed grids have historically evolved by subdividing the initial 100 GHz grid by successive factors of two.

WDM, DWDM (dense WDM) [A6] and CWDM (coarse WDM) [A7] are summarized in Table A1.3 and are based on the same concept of using multiple wavelengths of light in a single fiber, but differ in the spacing between these wavelengths and the number of channels.

Table A1.3: Different WDM systems: conventional, coarse and dense

<b>Type</b>	<b>Description</b>
Original WDM	Provides up to 16 channels in C-band, 1,530 to 1,565 nm of silica fibers.
Dense WDM (DWDM)	Uses C-band, but with denser channel spacing. Channel plans vary, but a typical system would use 40 channels at 100 GHz spacing or 80 channels at 50 GHz spacing. Some technologies are capable of 12,5 GHz spacing (sometimes called ultra-dense WDM) [A6].
Coarse WDM (CWDM)	In contrast to conventional WDM and DWDM, it uses increased channel spacing. CWDM uses wavelengths from 1,270 nm through 1,610 nm with a channel spacing of 20 nm [A7].

### A1.6.1.3 Telecom Windows

Typical operations in optical fiber communications fall into one of the telecom windows presented in Table A1.4.

Table A1.4: Typical telecom windows

<b>Three telecom windows</b>
<ul style="list-style-type: none"> <li>• The first window at 800–900 nm was originally used. Fiber losses are relatively high in this region and fiber amplifiers are not very well-developed for this spectral region. Therefore, this first telecom window is suitable for short-distance transmissions in MMF.</li> <li>• The second telecom window (see Table A1.5) utilizes wavelengths in the region of 1.3 <math>\mu\text{m}</math>, where losses in silica fibers are much lower and the fibers' chromatic dispersion is very weak, thus minimizing dispersive broadening. This window was originally used for long-haul transmission. Fiber amplifiers for 1.3 <math>\mu\text{m}</math> are not as good as their 1.5 <math>\mu\text{m}</math> based counterparts. Low dispersion is not necessarily ideal for long-haul transmission, as the effect of optical nonlinearities can increase.</li> <li>• The third telecom window (see Table A1.5), which is most widespread at present writing, utilizes wavelengths around 1.5 <math>\mu\text{m}</math>. Losses in silica fibers are at their lowest in this region, and Erbium-doped fiber amplifiers with very high performance are available. Fiber dispersion is usually anomalous, but can be tailored with great flexibility.</li> </ul>

Table A.1.5 shows the different frequency bands of the second and the third telecom windows.

Table A1.5: Second and third telecom windows

<b>Band</b>	<b>Description</b>	<b>Wavelength range</b>
O	Original	1260–1360 nm
E	Extended	1360–1460 nm
S	Short wavelengths	1460–1530 nm
C	Conventional (“Erbium window”)	1530–1565 nm
L	Long wavelengths	1565–1625 nm
U	Ultra-long wavelengths	1625–1675 nm

#### **A1.6.1.4 WDM Transmitter and Receivers**

The spacing between assigned channels in WDM systems can be narrow and the precision of the emitted wavelength is important. A fully equipped system can require a high number of lasers.

The transmitters are usually equipped with distributed feedback lasers (DFB) or tunable lasers. A DFB is manufactured for a specific wavelength, but is slightly tunable to operate at the assigned channel. Even though the cost of a DFB is relatively low, the number of spare parts that need to be kept in stock for repairs is high. A tunable laser for communication is usually designed to cover a full communication band (see Table A1.5), but is generally a more expensive solution. A tunable laser emits a continuous flow of light and data is modulated onto the light using external modulators. These modulators are sometimes integrated with the laser chip, but are not part of the laser cavity.

Receivers are optimized for high responsivity, low noise and sufficient bandwidth. If the received power level is sufficiently high, a p-i-n detector can be used, which is a less expensive solution than the avalanche photo-diode (APD) with internal optical magnification. In either case, the detector is followed by a matched trans-impedance amplifier, increasing the signal strength and harmonizing it to the succeeding electronics. Multichannel receivers were developed because their use simplifies system design and reduces the overall cost. Before WDM receivers were introduced, a separate receiver was used for each channel. A WDM receiver consists of monolithic receivers that comprise a demultiplexer for separation of wavelengths, followed by an array of photodiodes. Instead of a demultiplexer, an amplified waveguide grating (AWG) can be used before the photodiode array.

### **A1.7 Fiber Applications**

Optical fibers have many applications, but some of the more important ones are summarized in Table A1.6.

Table A1.6: Important fiber applications

---

**Fiber applications**

---

- Optical fiber communications that utilize optical fibers for data transmission. A large amount of data can be sent through a single fiber, which is immune to external influences such as electric and magnetic fields.
  - Different kinds of active fiber-optic devices that contain rare earth-doped fiber, for instance fiber lasers that can generate laser light at various wavelengths, and fiber amplifiers that can be used to boost the optical power of, i.e. amplify, some weak signals.
  - Different kinds of fiber-optic sensors that can be used for distributed temperature and stress measurements in buildings and oil pipelines.
  - Passive fibers can be used to transport light from a source to another point for such purposes as illumination, diode pumping of lasers and power over fiber. They are also used to connect components in fiber-optic devices, such as interferometers and fiber lasers. They then play a role that is similar to that of electrical wires in electronic devices.
- 
- 

## A2 Loss Compensation

Fiber losses must be compensated for in lightwave systems with reaches longer than 100 km, due to the cumulative effects eventually making the signal so weak that the information cannot be recovered at the receiver. Until 1990, one common method was to insert an optoelectrical regenerator, also known as a repeater. This technique would be quite expensive in WDM systems, since each channel would require a separate regenerator. Several kinds of optical amplifiers were developed to solve the problem of loss management. These new amplifiers can amplify multiple WDM channels simultaneously in the optical domain and are much more cost-effective.

Optical amplifiers can be divided into two categories known as lumped and distributed amplifiers. Most systems employ lumped, Erbium-doped fiber amplifiers in which losses accumulated over 60 to 80 km of fiber lengths are compensated by using short lengths (~10 m) of Erbium doped fibers. In distributed amplification, the transmission fiber itself is used for signal amplification, e.g. by exploiting the nonlinear phenomena of stimulated Raman scattering (SRS). Using them for loss compensation requires the periodical injection of optical power from one or more pump lasers through fiber couplers.

Any loss management technique based on optical amplification degrades the signal-to-noise ratio (SNR) of the optical bit stream, since all optical amplifiers add noise to the signal through amplified spontaneous emission [A1-A2, A8-A9].

## A2.1 Erbium-Doped Fiber Amplifier

Erbium-doped fiber amplifiers are the by far most important fiber amplifiers in the context of long-range optical fiber communications, since they can efficiently amplify light in the 1.5  $\mu\text{m}$  wavelength region, where telecom fibers have their loss minimum [A1-A2, A8-A9].

### A2.1.1 Operation Principle and Setup

An example of a simple EDFA is shown in Fig. A2.1 with an Erbium-doped optical fiber based core. In this example, the active fiber is pumped with light from two laser diodes (bidirectional pumping), although unidirectional pumping is also common. The pump light, which often has a wavelength around 980 nm or 1480 nm, excites the Erbium ions ( $\text{Er}^{3+}$ ) into the  $^4\text{I}_{13/2}$  state, from where they can amplify light in the 1.5  $\mu\text{m}$  wavelength region via stimulated emission back to the ground-state manifold.

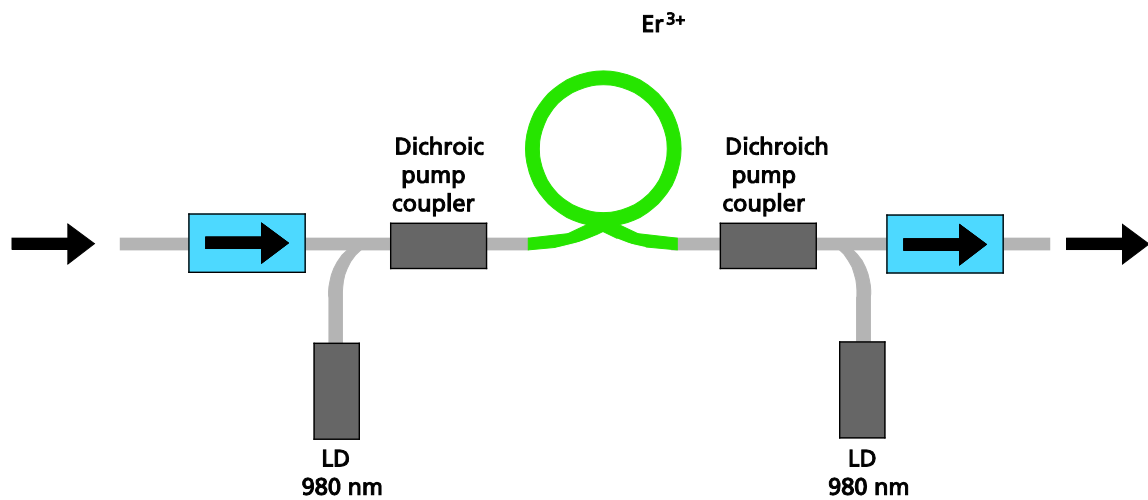


Figure A2.1: Schematic setup of a simple Erbium-doped fiber amplifier. The Erbium-doped fiber is pumped by two laser diodes (LDs). Dichroic fiber couplers inject the pumped light, while pig-tailed optical isolators before and after the pumping mechanisms reduce the device's sensitivity to back-reflections [A10].

The illustrated setup also contains two fiber-coupled optical isolators. The isolator at the input prevents light originating from amplified spontaneous emissions from disturbing any previous stages, whereas the isolator at the output suppresses lasing in case output light is reflected back to the amplifier. Without isolators, fiber amplifiers are sensitive to back-reflections.

## A2.1.2 Erbium-Doped Amplifiers in Telecom Systems

EDFAs are very important in optical fiber communication systems and serve various functions. Some of their most important applications are summarized in Table A2.1. These features are realized in the telecom C- and L-bands (conventional- and long wavelengths-band).

Table A2.1: Important fiber amplifier applications

---

<b>EDFA in telecom systems</b>
<ul style="list-style-type: none"><li>• The power of a data transmitter can be boosted with a high-power EDFA before entering a long fiber span or a device with large losses.</li><li>• A fiber amplifier can be used in front of a data receiver if the arriving signal is weak. Despite the introduction of amplifier noise, this application can improve the signal-to-noise ratio and thereby the achievable data transmission.</li><li>• In-line EDFAs are used between long spans of passive transmission fiber. Using multiple amplifiers in a long fiber-optic link has the advantage of compensating for large transmission losses without letting the optical power drop to levels that are too low and which would spoil the signal-to-noise ratio. Another advantage is the ability to transmit without using excessive optical power at other locations, which would cause detrimental nonlinear effects due to unavoidable fiber nonlinearities.</li></ul>

---

EDFAs are particularly attractive because of their large gain bandwidth, typically in the tens of nanometers, which is more than enough to amplify data channels with the highest data rates without introducing any gain-narrowing effects. A single EDFA can be used to simultaneously amplify several data channels at different wavelengths within a gain region. The only competitors to Erbium-doped fiber amplifiers in the 1.5  $\mu\text{m}$  region are Raman amplifiers. These have gained from the development of higher power pump lasers. Raman amplification can also be carried out in the transmission fiber [A5]. Nevertheless, EDFAs remain very dominant [A1-A2, A8-A9].

## References

- [A1] G. Agrawal, “Lightwave Technology Component and Devices”, Wiley-Interscience, 2004.
- [A2] G. Agrawal, “Lightwave Technology: Telecommunication Systems”, Wiley-Interscience, 2005.
- [A3] D. Gloge, “Dispersion in Weakly Guided Fibers”, *Appl. Opt.*, vol. 10, no. 11, pp 2442–2445, 1971.
- [A4] E.P. Ippen and R.H. Stolen, “Stimulated Brillouin Scattering In Optical Fibers”, *Appl.Phys. Lett.*, vol. 21, pp. 539–541, 1972.
- [A5] J. Bromage, “Raman Amplification for Fiber Communications Systems”, *J. Lightwave Technol*, vol. 22, pp. 79–93, 2004.
- [A6] Telecommunication standardization Sector of ITU “Spectral Grids for WDM Applications: DWDM Frequency Grid”, ITU-T Recommendation G.694.1, 06/2002.
- [A7] Telecommunication standardization Sector of ITU “Spectral Grids for WDM Applications: CWDM Wavelength Grid”, ITU-T Recommendation G.694.2, 12/2003.
- [A8] B. E. A. Saleh, M. C. Teich, “Fundamentals Of Photonics, Second Edition”, John Wiley & Sons, Inc, 2007.
- [A9] F. L. Pedrotti, L. S. Pedrotti, “Introduction To Optics, Second Edition”, Prentice-Hall, Inc., 1993.
- [A10] R. Paschotta, “Encyclopedia of Laser Physics and Technology Volume 1 and 2”, Wiley - VCH Verlag GmbH &Co, 2008.



## Appendix B Sources for Precise Time and Frequency Transfer

This appendix provides reference information for some techniques used for precise time and frequency transfer. It is extracted from, “The Science of Timekeeping” by David W. Allan, Neil Ashby, Clifford C. Hodge, Hewlett Packard Application Note 1289, 1997.

Table B1.1: Characteristics of some potential sources and dissemination techniques for precise time-and-frequency reference information.

Type	Typical time transfer accuracy capability	Typical Frequency accuracy capability	Example system
LF broadcast	1 ms	$10^{-10}$ to $10^{-11}$	DCF 77
Television broadcast (terrestrial links)	10 ns for CV	$10^{-12}$ to $10^{-13}$	
Television broadcast satellite	0.5 – 10 $\mu$ s 10 – 100 ns	$10^{-10}$ to $10^{-11}$ $10^{-12}$ to $10^{-13}$	DBS satellites
Navigation Satellite, broadcast	20 – 500 ns	$10^{-9}$ to $10^{-13}$	GPS and GLONASS
Navigation satellite common view	5 – 20 ns	$10^{-13}$ to $10^{-15}$ ( $\approx$ 24 h)	GPS and GLONASS
Communication satellite two-way	1 – 10 ns	$10^{-14}$ to $10^{-15}$	
Telephone time code	1 – 10 ms	$10^{-8}$ ( $\approx$ 24 h)	Europe and North America
Optical fiber < 50 km	10 – 50 ps	$10^{-16}$ to $10^{-17}$	Dedicated to frequency transfer
$\approx$ 2000 km	100 ns	$10^{-13}$ to $10^{-14}$ ( $\approx$ 24 h)	SDH network
Microwave link	1 – 10 ns	$10^{-14}$ to $10^{-15}$	
Coaxial Cable	1 – 10 ns	$10^{-14}$ to $10^{-15}$	



## Appendix C Variance

Variance is used to characterize the fluctuations of frequency sources. This is a second-moment measure of scattering, much as standard variance is used to quantify variations. The variations from the mean are squared, summed, and divided by one less than the number of measurements; this number is called the “degrees of freedom”. Frequency stability analysts have several statistical variance measures at their disposal, for example Hadamard variance and Allan variance. Allan variance is the most common variance in time-domain measurement of frequency stability, since there are several versions of this measure that provide better statistical confidence [C1]. Hadamard variance is more suitable for handling frequency drift and other divergence noise types. Several versions of this variance also exist. The newer Total and Thêo1 variances provide better confidence at longer averaging factors. Table C1.1 shows several types of variances and their characteristics [C1].

Table C1:1 Variance types

Type	Characteristics
Standard	Non-convergent for some clock noise – don’t use
Allan	Classic – use only if required – relatively poor confidence
Overlapping Allan	General purpose – most widely used – first choice
Modified Allan	Used to distinguish W and F PM
Time	Based on modified Allan variance
Hadamard	Rejects frequency drift, and handles divergent noise
Overlapping Hadamard	Better confidence than normal Hadamard
Total	Better confidence at longer averages for Allan
Modified Total	Better confidence at longer averages for modified Allan
Time Total	Better confidence at longer averages for time
Hadamard Total	Better confidence at longer averages for Hadamard
Thêo1	Provides information over nearly full record length
ThêoH	Hybrid of Allan and ThêoBR (bias removed Thêo1) variances

## C1.1 Standard Variance

Standard  $N$ -sample variance is defined as

$$s^2 = \frac{1}{N-1} \sum_{i=1}^N (y_i - \bar{y})^2, \quad (\text{C1})$$

where  $y_i$  stands for the  $N$  fractional frequency values, and  $\bar{y}$  is the average frequency Eq. (C2).

$$\bar{y} = \frac{1}{N} \sum_{i=1}^N y_i. \quad (\text{C2})$$

Standard variance is usually expressed as its square root, otherwise standard deviation,  $s$  is expressed. It is not recommended as a measure of frequency stability, since it is non-convergent for some types of noise that are commonly found in frequency sources [C1].

## C1.2 Allan Variance

Allan variance is the most common time-domain measure of frequency stability. Some of its greatest advantages are that it is convergent for most types of clock noise. There are several versions of Allan variance that provide better statistical confidence and that are able to distinguish between different kinds of noise as well as describe time stability.

The two sample non-overlapping, or original, Allan variance (AVAR), i.e. time-domain measure of frequency stability, is calculated as

$$\sigma_y^2(\tau) = \frac{1}{2(M-1)} \sum_{i=1}^{M-1} [y_{i+1} - y_i]^2. \quad (\text{C3})$$

Where  $y_i$  is the  $i$ th of  $M$  fractional frequency values averaged over the measurement (sampling) interval,  $\tau$ .

In terms of phase data, the Allan variance can be calculated as

$$\sigma_y^2(\tau) = \frac{1}{2(N-2)\tau^2} \sum_{i=1}^{N-2} [x_{i+2} - 2x_{i+1} + x_i]^2. \quad (\text{C4})$$

where  $x_i$  is the  $i$ th of the  $N=M+1$  phase values spaced by the measurement interval  $\tau$ .

The result is usually expressed as a square root value,  $\sigma_y(\tau)$ , the Allan deviation, ADEV [C1].

### C1.3 Overlapping Allan Variance

The fully overlapping Allan variance, or AVAR, is a form of normal Allan variance,  $\sigma_y(\tau)$ , that makes maximum use of data by forming all possible overlapping samples at each averaging time  $\tau$ . It can be estimated from a set of  $M$  frequency measurements for averaging time,  $\tau=m\tau_0$ , where  $m$  is the averaging factor and  $\tau_0$  is the basic measurement interval, using the formula

$$\sigma_y^2(\tau) = \frac{1}{2m^2(M-2m+1)} \sum_{j=1}^{M-2m+1} \left\{ \sum_{i=j}^{j+m-1} [y_{i+m} - y_i] \right\}^2. \quad (C5)$$

This formula is not used for large data sets because of the computationally intense inner summation. In terms of phase data, the Allan variance can be estimated from a set of  $N=M+1$  time measurement as

$$\sigma_y^2(\tau) = \frac{1}{2(N-2m)\tau^2} \sum_{i=1}^{N-2m} [x_{i+2m} - 2x_{i+m} + x_i]^2. \quad (C6)$$

Overlapping Allan deviation is the most common measure of time domain frequency stability. The term AVAR has come to be used mainly for this form of the Allan variance, while ADEV is used for its square root [C1].

### C1.4 Modified Allan Variance

The modified Allan variance,  $\text{Mod } \sigma_y^2(\tau)$ , or MVAR, is another common time domain measure of frequency stability. It is estimated from a set of  $M$  frequency measurements for averaging time  $\tau=m\tau_0$ , where  $m$  is the averaging factor and  $\tau_0$  is the measurement interval in the following formula

$$\text{Mod}\sigma_y^2(\tau) = \frac{1}{2m^4(M-3m+2)} \sum_{j=1}^{M-3m+2} \left\{ \sum_{i=j}^{j+m-1} \left( \sum_{k=i}^{i+m-1} [y_{k+m} - y_k] \right) \right\}^2. \quad (C7)$$

In terms of phase data, the modified Allan variance is estimated from a set of  $N=M+1$  time measurements as

$$\text{Mod}\sigma_y^2(\tau) = \frac{1}{2m^2\tau^2(N-3m+1)} \sum_{j=1}^{N-3m+1} \left\{ \sum_{i=j}^{j+m-1} [x_{i+2m} - 2x_{i+m} + x_i] \right\}^2. \quad (C8)$$

The result is usually expressed as a square root value,  $\text{Mod}\sigma_y(\tau)$ , the modified Allan deviation. The modified Allan variance is the same as the normal Allan variance for  $m=1$ . Modified Allan deviation is used to distinguish between white noise and flicker noise [C1].

Figure C1.1 shows two graphs that illustrate frequency stability between two Hydrogen-MASERS, one calculated with overlapping Allan Deviation (Sigma) and the other with Modified Allan Deviation (Mod Sigma).

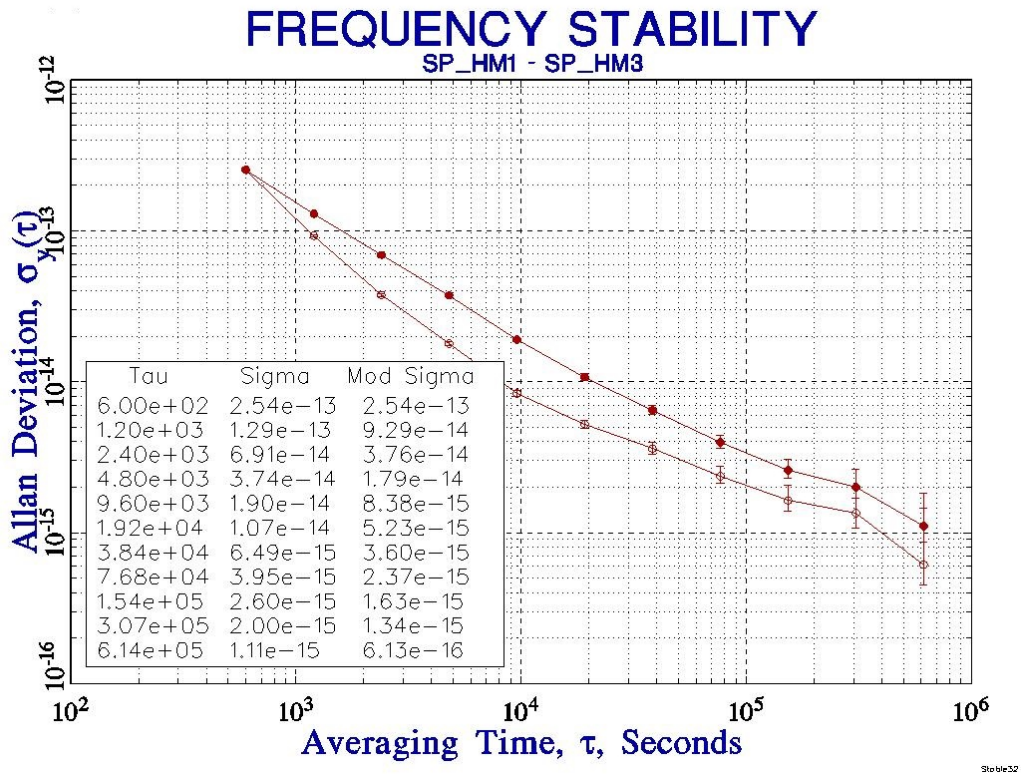


Figure C1.1: Example of two graphs illustrating frequency stability between two Hydrogen-MASERS, one calculated with overlapping Allan Deviaton (Sigma) and the other with Modified Allan Deviation (Mod Sigma).

## C1.5 Time Allan Variance

The Time Allan Variance, TVAR, with its square root TDEV, is a measure of time stability based on the Modified Allan Variance. It is defined as

$$\sigma_x^2(\tau) = \left(\frac{\tau^2}{3}\right) \cdot \text{Mod}\sigma_y^2(\tau). \quad (\text{C9})$$

TDEV is MDEV, but its slope is transposed by +1 and normalized by  $\sqrt{3}$  on a log-log plot. The time Allan variance is equal to the standard variance of the time deviations for white PM noise. It is particularly useful for measuring the stability of time-distributed networks. Time deviation is used to characterize the time error of a time source or distribution system [C1].

## Reference

- [C1] W. J Riley, "Handbook of Frequency Stability Analysis", Time and Frequency division Physics Laboratory National Institute of Standards and Technology, 2008.

## Appendix D OptoSUNET

OptoSUNET is the Swedish University Network and covers most of Sweden, as illustrated in Fig. D1.1.

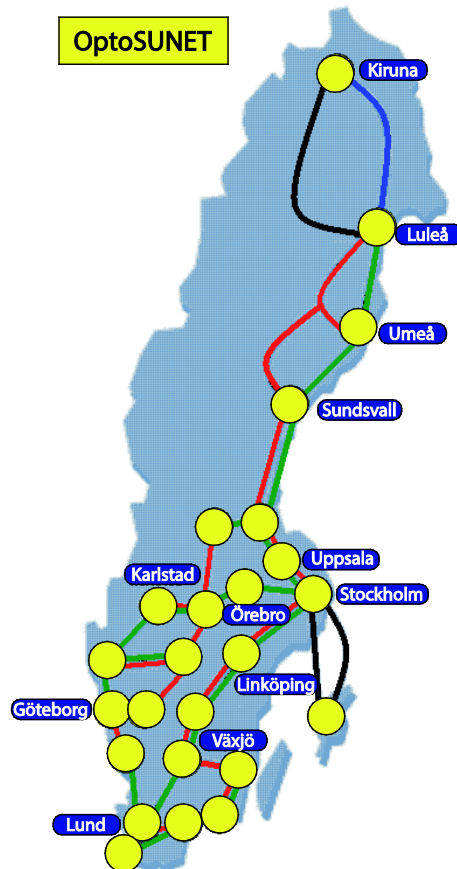


Figure D1.1: OptoSUNET the Swedish University Network

OptoSUNET is a WDM network with a star topology [D1], implemented so that every user is connected on a dedicated wavelength, and communication runs without routing between the user-node and the network hub. Thus, data between two users communicating will always be routed by the network hub. Up to 80 wavelengths with 50 GHz spacing can be launched on each fiber link in the network, with a specified maximum data rate/channel of 10 Gbit/s. Practical tests have shown that the network also can handle a channel with a data rate of 40 Gbit/s [D1]. At present, only a fraction of the available wavelengths are equipped with transponders and the additional capacity is reserved for future needs and research activities. One of the advantages of the star topology WDM network is the transparency of data formats, enabling different users to communicate using different data formats, only requiring format-specific equipment at the user site and the central hub. Furthermore, adjacent channels are unaffected by the data format used on other channels.

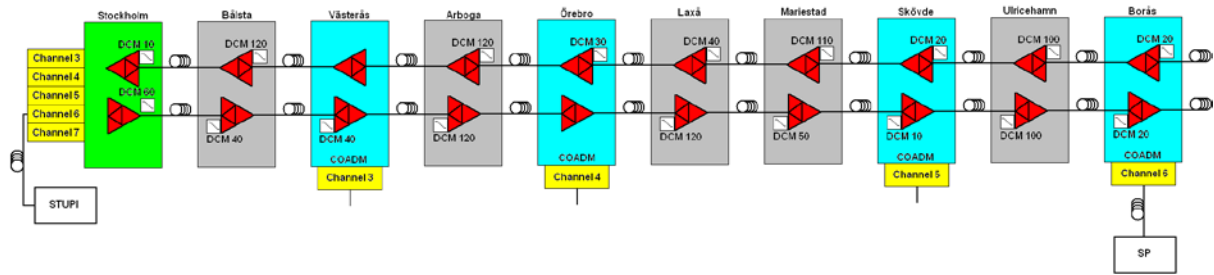


Figure D1.2: The WDM network between Stockholm and Borås used as a testbed. The amplifier stations are located along the route, at distances of 60–120 km apart. At every station the light is amplified in an optical limiting amplifier (OLA), and the effects of chromatic dispersion are compensated in a DCM (dispersion compensating module). In some stations additional users are connected through the Compact Optical Add Drop Module (COADM).

Figure D1.2 is a schematic illustration of the path between the two laboratories in the non-insertion time transfer experiment. In the upper left, STUPI is connected via a 5 km long dedicated fiber to the Fredhäll WDM node. In the lower right, SP is connected in the same way to the Borås node through 7 km of dedicated fiber. Between Fredhäll and Borås, communication runs on a dedicated wavelength, on the same fiber as a multitude of other users' wavelengths.

The amplifier stations are located along the route, at distances of 60–120 km apart. At each station, as Fig. D1.2 shows, the light is amplified in an optical limiting amplifier (OLA), and the effects of chromatic dispersion are compensated in a DCM (dispersion compensating module). Furthermore, in some stations additional users are connected through the Compact Optical Add Drop Module (COADM). Most of the fiber between stations is placed underground, but a few fiber segments also run above ground, following the power lines of the electrical power grid.

The total DCF compensation lengths for both directions are similar. However, for most stations, there is a difference in DCF length in the two directions, which leads to an asymmetry in the two-way transfer.

## Reference

- [D1] Imtech Telecom and SUNET, “High Level Design: Description for SUNET”, document Rev: 10.0, 2008.

# Appendix E GPS, GLONASS and Galileo

## E1 GPS

In 1978, the first prototype satellite for use in what would later become the global positioning system, GPS, was launched. Since then, GPS has developed into a well-known and highly utilized system. GPS continuously provides accurate three-dimensional position (latitude, longitude, and altitude), velocity, and precise time, traceable to UTC to all users worldwide [E1-E3].

### E1.2 GPS Structure and Operation

GPS consists of three segments: the control segment (CS), the Space Segment (SS) and the user segment (US).

#### E1.2.1 Space Segment

The Space Segment is mainly comprised of the orbiting GPS satellites. The original GPS design called for 24 satellites in three circular, orbiting planes, but was later modified to six planes with minimum four satellites each. The six planes have an inclination of approximately  $55^\circ$  and are separated by  $60^\circ$  along the equator.

Orbiting at an altitude of approximately 20,200 kilometers, their orbits are arranged so that, most of the time, at least 6 of the 30 (April, 2013) satellites are within line of sight from almost anywhere on Earth (following an orbital radius of 26,600 km from the Earth's center). Each satellite makes two complete orbits each sidereal day, and the ground track of each satellite is repeated simultaneously. In comparison, geostationary satellites, such as communications satellites, have an altitude of 35,800 km. Figure E1.1 shows a sky plot of the GPS satellite constellation in 2009.

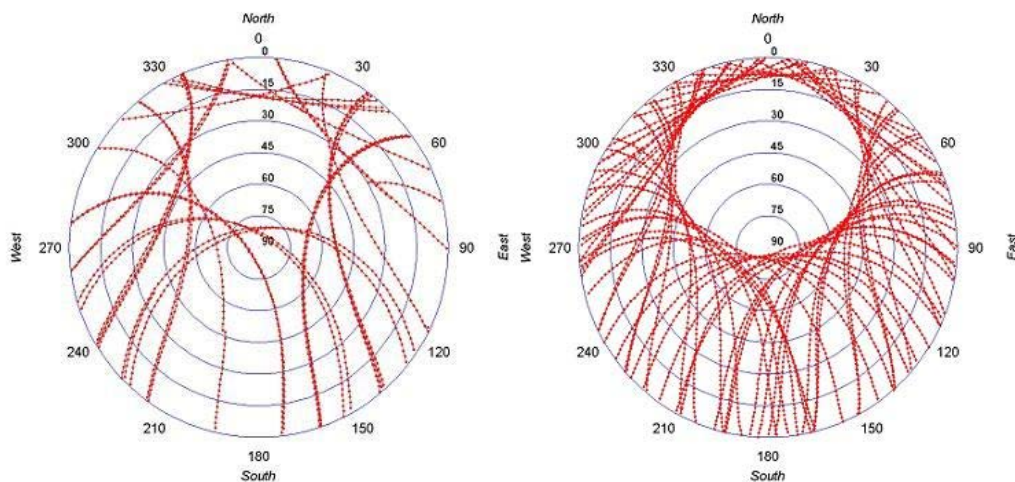


Figure E1.1: GLONASS (left) and GPS (right) at the Borås site in Sweden. As shown in the two plots, there is an area (circle) in which no satellites are ever visible. The position of this area varies depending on the latitude of the observing receiver.

## **E1.2.2 Control Segment**

The original control segment was operated by the US Air Force (USAF) and tracks the satellites' paths from monitoring stations on the ground, together with monitoring stations operated by the National Geospatial-Intelligence Agency (NGA). The monitoring station system is currently in a phase of extension to the initial stations that are located near the equator. These new stations will increase the spread in latitude, resulting in better tracking geometry and better orbital estimations.

Each GPS satellite is regularly updated with navigational data, the atomic clocks onboard the satellites are synchronized to within a few nanoseconds of each other and the ephemeris of each satellite's internal orbital model is adjusted. These updates use inputs from the ground monitoring stations, space weather information and various other inputs.

In order to change the orbit of a satellite, the satellite must be marked 'unhealthy' so that receivers will not use it in calculations. The satellite can be put back in use when the new ephemeris has been uploaded and the satellite is marked as 'healthy' again [E1-E3].

## **E1.2.3 User Segment**

GPS receivers come in a variety of formats ranging from devices integrated into cars, phones, and watches.

In general, GPS receivers are composed of an antenna tuned to the frequencies transmitted by the satellites, receiver-processors, and a highly-stable clock, often a crystal oscillator. They may also include a display for providing location and speed information to the user. A receiver is often described by its number of channels, which signifies how many satellites it can monitor simultaneously.

By using EGNOS (European Geostationary Navigation Overlay Service) as a supplementary system to GPS in Europe, precision can be increased. Ground stations estimate the error in the regular signal and send corrective information to three geostationary satellites. With this information, a receiver can increase its precision. The American equivalent is called WAAS and stands for Wide Area Augmentation System [E1-E3].

## **E1.3 GPS Signals**

The GPS satellites transmit two digitally modulated carrier signals (L1=1575.42 MHz and L2=1227.60 MHz) using Binary Phase Shift Keying (BPSK). GPS utilizes the Code Division Multiple Access (CDMA) technique, and the satellites' radio signals consist of pseudorandom noise modulated L-band carriers (spread spectrum technique).

The coarse codes are called C/A (coarse/acquisition) codes and are available for civilian use, while precision codes with higher chip rates, which allow more accurate positioning, are called P(Y)-codes and are primarily intended for military use. Both the C/A-code and the P-code are pseudorandom noise codes consisting of a predetermined digital sequence with a chip rate generated by an onboard atomic clock. This clock provides the transmit time of the broadcast signals. The chip rates of the C/A-code and P-code are approximately 1.023 Mbit/s and 10.23 Mbit/s, respectively. The C/A-code is only available on the L1 carrier while the P-code is available on both the L1 and L2 carriers. All satellites broadcast using the same carrier frequencies. Each satellite has a different code sequence that identifies the satellite. The new generation of satellites also transmits L2C, a new improved C/A code, on the L2 carrier.

The U.S. authorities have mainly degraded the performance of GPS in two different ways, namely SA and AS.

The intentional degradation Selective Availability (SA) was the most significant error source in many real-time low-accuracy GPS applications. It is associated with the insertion of false satellite ephemeris, or dithering of the clock and signal. Since May 2, 2000, SA has been inactivated.

Anti-Spoofing (AS) is the encoding of the Precise (Military) Code broadcast on both the L1 and L2 carrier frequencies. In GPS carrier phase-based positioning, the availability of both frequencies is essential for ensuring access to more data and to correct for the signal propagation path delay caused by the Earth's ionosphere. Access to the digital codes also makes it easier to track the carrier phase of the signal. Under AS conditions, receiver performance is degraded because the P-code is encrypted and the C/A-code is not available on L2.

Several sophisticated methods have been developed by different receiver manufacturers to gain access to the L2 carrier for civilian receiver equipment. The encrypted P-code, often called P(Y) code, is only fully available to military equipment with a proper decryption key [E1-E3].

### **E1.3.1 Navigation Message**

Each GPS satellite continuously broadcasts a Navigation Message that contains the time-of-week, GPS week number and satellite health information, an ephemeris and an almanac. The messages are sent in frames, each taking 30 seconds to transmit. Transmission of each 30 second frame begins precisely on the minute and half minute, as indicated by the satellite's atomic clock according to satellite message format.

The ephemeris could be updated as often as every 2 hours. The time needed to acquire the ephemeris is becoming a significant element of the delay in first position establishment. The reason for this is that, as hardware capability increases, the time needed to lock on to the satellite signals decreases, but due to the low data transmission rate, reception of the ephemeris data still requires 30 seconds.

The almanac consists of coarse orbit and status information for each satellite in the constellation, an ionosphere model, and information to relate GPS-derived time to Coordinated Universal Time. Each frame contains 1/25th of the almanac, so receiving the entire almanac from a single satellite requires 12.5 minutes. One purpose of the almanac is to relate time derived from the GPS (called GPS time) to the international UTC time standard. The almanac allows a single-frequency receiver to correct for ionosphere error by using a global ionosphere model [E1-E3].

### **E1.4 Time Keeping in GPS**

While most clocks are synchronized to UTC, the atomic clocks onboard the GPS satellites are set to GPS time. The difference is that GPS time is not corrected to be equal to the rotation of the Earth, so it does not contain leap seconds or other corrections that are periodically added to UTC. GPS time was set to be equal to UTC in 1980, but has since diverged. The GPS navigation message includes the difference between GPS time and UTC, which as of 2013 is 16 seconds. Receivers subtract this offset from GPS time to calculate UTC. The timing in the GPS system is very precise, and this is accomplished in several different ways. Every satellite is equipped with three or more atomic references; one is in use and the other two are backups. In order to keep the correct time, all satellites must send their codes at the same moment. This is achieved through synchronization with a master ground clock every 12 hours.

In GPS receivers, a quartz oscillator is used for time measurement. These are quite decent for short periods of time (a couple of minutes) and are therefore synchronized regularly using the satellites' atomic references. When the receiver oscillator is synchronized, time codes for both the receiver and the satellite are created. By comparing these in the receiver, the distance between them can be calculated.

The GPS date is expressed as a week number plus a day-of-week number. The week number is transmitted as a navigation message, which only repeats every 8,192 weeks [E4-E6].

## **E1.5 Sources of Degradation in GPS**

There are several effects on GPS that degrade its performance, such as atmospheric and multipath effects, orbit estimations of the satellites, and disturbances such as jamming and spoofing.

### **E1.5.1 Satellite Orbits**

One source of degradation within GPS is satellite orbit estimation. The orbit determination for GPS satellites is based on observations at monitoring stations. Global networks provide higher accuracy and reliability of the orbit calculations than those that are determined from regional networks. The distribution of these sites is essential to achieve the highest accuracy.

Several global networks have been established for orbit determination. One global network is the International GNSS service (IGS). The main purpose of this service is orbit determination for geodynamic applications that require the greatest accuracy.

The IGS stations collect code ranges and carrier phases from all GNSS satellites (GPS, GLONASS and Galileo as a complement to the USAF) in view using civilian dual-frequency receivers and broadcast orbits. The data is analyzed independently by seven agencies and is archived daily in receiver and software-independent exchange formats.

Predicted orbits with an accuracy of about 10 cm are available in near real-time, whereas post-processed orbits have a delay of about 1 day (rapid solution) and 2 weeks (final solution). The accuracy of the final solution is estimated to be better than 5 cm.

Raw tracking data, satellite clock parameters, Earth rotation parameters and other data such as ionospheric and tropospheric information are also available through IGS [E3].

### **E1.5.2 Atmospheric Effects**

Inconsistencies in atmospheric conditions affect the speed of the GPS signals as they pass through the Earth's atmosphere, especially the ionosphere. These effects are smallest when the satellite is directly overhead and increase as the satellite approaches the horizon, since the signal's path through the atmosphere is longer. Once the receiver's approximate location is known, that information can, in combination with a mathematical model, be used to estimate and compensate for these errors.

Because ionosphere delays affect the speed of microwave signals differently depending on their frequency, dispersion delays measured on two or more frequency bands can be used to estimate dispersion, and this estimate can then be used to estimate the delay at each frequency. Many military and survey-grade civilian receivers measure the different delays in the L1 and L2 frequencies in order to measure atmospheric dispersion, and apply a more precise

correction. This can be achieved in civilian receivers without the need to decrypt the P(Y) signal carried on L2 by tracking the carrier wave instead of the modulated code.

In general, ionospheric effects change slowly and can be averaged over time. The effects for any particular geographical area can easily be calculated by comparing the GPS-measured position to a known surveyed location. This correction is also valid for other receivers in the same general location. Several systems send this information over radio or other links to allow L1-only receivers to make ionosphere corrections. Ionosphere data is transmitted via satellite in Satellite Based Augmentation Systems (SBAS) such as WAAS, EGNOS (Europe and Asia) or MSAS (Japan), which transmit it on the GPS frequency using a special pseudorandom noise sequence (PRN), so only a GPS receiver and antenna are required.

The lower atmosphere, often referred to as the troposphere, has a major impact on satellite signals. The delay there is caused by electrically neutral gases. The size of the tropospheric delay is the same for the two signal frequencies. Some weather conditions have an effect that can cause variable delay, resulting in errors similar to ionosphere delay, but occurring in the troposphere. This effect is more local, changes more quickly than ionosphere effects and is not frequency-dependent.

Changes in receiver altitude also change the amount of delay due to the signal having to pass through less of the atmosphere at higher elevations. Since the GPS receiver computes its approximate altitude, this error is relatively simple to correct, either by applying a function regression or correlating margin of atmospheric error to ambient pressure using a barometric altimeter [E1-E3].

#### **E1.5.2.1 Multipath Effects**

GPS signals can also be affected by multipath issues, where the radio signals are reflected by the surrounding terrain: buildings, canyon walls, hard ground, etc. These delayed signals can cause inaccuracy. For long-delay multipath, the receiver itself can recognize the wayward signal and discard it. To address shorter delay multipath specialized antennas can be used to reduce the signal power that the antennas receive. Short-delay reflections are more difficult to filter out, since they interfere with the true signal, causing effects that are almost indistinguishable from routine fluctuations in atmospheric delay [E7-E8].

#### **E1.5.3 Disturbance**

There are two categories of GPS signal disturbance: jamming and spoofing. Jamming means broadcasting noise at the transmission frequencies that are used by GPS, saturating receivers and thereby disabling their ability to detect and isolate the navigation signals. Several systems have been developed to jam the system and those could presumably result in serious problems for GPS users.

Spoofing means using the GPS signal code to send out false information, impersonating a real satellite but broadcasting adjusted data. Due to its encryption, the P code is harder to disrupt than the C/A code.

GPS is, in general, an easy way of obtaining synchronization between systems. Since it was launched, the GPS system has never failed, which makes it difficult predict the potential results of a total breakdown [E2].

## **E2 GLONASS**

The first satellite of the Russian satellite navigation system GLONASS was launched in 1982. GLONASS was declared operational in 1993, enabling free use of its signals. GLONASS is under the operative control of the Russian Ministry of Defense. The satellite constellation encompasses more or less 24 satellites (Jan, 2010) and is considered fully operational. The GLONASS satellite orbits are slightly more advantageous for users at higher latitudes, compared to GPS, as indicated by Fig. E1.1. The signal package is similar to GPS.

GLONASS is interesting for positioning and timing, since the intentional degradation in clock and orbit information (SA) and the encrypted P-code (AS) cannot be employed as it is in GPS. In the present situation with SA turned off, GPS is slightly more accurate than GLONASS due to GPS's better coding (CDMA vs. FDMA), greater bandwidth (chip rate), and signal quality (stability of frequency standards).

Unfortunately, so far, the GLONASS satellites have experienced shorter lifetimes than the GPS satellites. This is most likely due to the fact that GLONASS satellites only carry two frequency standards. New generations of GLONASS satellites will have three onboard clocks and extended lifetimes [E3].

### **E2.1 GPS/GLONASS Comparison**

When comparing GPS and GLONASS one can find many similarities; both systems consist of a nominal number of 24 satellites in near-circular inclined orbits about 20,000 km above the Earth's surface. The orbital period is approximately half a day. GLONASS has three orbital planes, 19,100 km above the Earth and a  $64.8^\circ$  inclination, with eight satellites in each. In GLONASS the size of the "hole" in Fig. E1.1 (the part of the sky above the user that is not accessible for the satellites) is smaller and located further North, resulting in more favorable satellite geometry at high latitudes.

Each satellite in these two systems transmits pseudorandom codes that are modulated (BPSK) onto two L-band carriers. Whereas GPS uses one frequency for L1 and another for L2, the same for all satellites, each GLONASS satellite has its own unique frequencies for both L1 and L2.

GLONASS uses spread-spectrum codes for range determinations. However, unlike GPS, GLONASS satellites transmit the same codes, i.e., one C/A and one P-code that is identical for all satellites. GLONASS is a frequency-division multiplex system, while GPS utilizes Code-division multiplex (CDM). There is also a difference in the chip-rate of the codes [E3].

## **E3 Galileo**

The European Commission is currently developing a separate Global Navigation Satellite System, Galileo, in co-operation with the European Space Agency (ESA), which will be under civilian control. It will consist of 30 satellites, including 3 active spares, and be based on international co-operation through a global ground infrastructure and regional/local augmentations. Most of the satellites will be located in circular Medium-altitude Earth Orbits (MEO), complemented by EGNOS. GalileoSat is ESA's complementary development initiative for the space and associated ground-control segments. Galileo's performance will be equal to the current GPS standard positioning service and has two kinds of prototype satellites, GIOVE A and GIOVE B. As of 2013, four working satellites are in orbit validation.

## References

- [E1] B. Hoffman – Wellenhopf, H. Lichtenegger, J. Collins, “GPS Theory and Practice, Fifth Edition”, Springer Wien NewYork, 2001.
- [E2] G. Seeber, “Satellite Geodesy 2nd Edition”, Walter de Gruyter Berlin NewYork, 2003.
- [E3] B. Hoffman – Wellenhopf, H. Lichtenegger, E. Wasle, “GNSS Global Navigation Satellite Systems: GPS, GLONASS, Galileo and more”, Springer Wien NewYork, 2008.
- [E4] P. Defraigne and G. Petit, “Time Transfer to TAI Using Geodetic Receivers”, *Metrologia*, vol. 40, pp. 184–188, 2003.
- [E5] B. Guinot and E.F. Arias, “Atomic Time Keeping from 1955 to the Present”, *Metrologia*, vol. 42, pp. 20–30, 2005.
- [E6] G. Petit and Z. Jiang, “GPS All in View Time Transfer for TAI Computation”, *Metrologia*, vol. 45, pp. 35–45, 2008.
- [E7] P. Elósegui, J.L. Davis, R.T.K. Jaldehag, J.M. Johansson, A.E. Niell and I.I. Shapiro, “Geodesy Using the Global Positioning System: The Effects of Signal Scattering on Estimates of its Positioning”, *Journal of geophysical research*, vol. 100, no. B7, pp. 9921–9934, 1995.
- [E8] R.T.K. Jaldehag, J.M. Johansson, B.O. Rönnäng, P.Elósegui, J.L. Davis, I.I. Shapiro and A.E. Niell, “Geodesy Using the Swedish Permanent GPS Network: Effects of Signal Scattering on Estimates of Relative Site Positions”, *Journal of geophysical research*, vol. 101, no. B8, pp. 17,841–17,860, 1996.